5-2016

Rhizosphere Interactions Between Copper Oxide Nanoparticles and Wheat Root Exudate in a Sand Matrix; Influences on Bioavailability and Uptake

Paul McManus
Utah State University

RHIZOSPHERE INTERACTIONS BETWEEN COPPER OXIDE NANOPARTICLES AND WHEAT ROOT EXUDATES IN A SAND MATRIX; INFLUENCES ON BIOAVAILABILITY AND UPTAKE

by

Paul McManus

A thesis submitted in partial fulfillment
of the requirements for the degree

of

MASTER OF SCIENCE

In

Civil and Environmental Engineering

(Environmental)

Approved:

_____	_____
Joan E. McLean Major Professor	Anne J. Anderson Committee Member
_____	_____
David W. Britt Committee Member	David K. Stevens Committee Member

_____
Mark. R. McLellan
Vice President for Research and
Dean of the School of Graduate Studies

UTAH STATE UNIVERSITY
Logan, Utah

2016

ABSTRACT

Rhizosphere Interactions Between Copper Oxide Nanoparticles and Wheat Root Exudates in a Sand Matrix; Influences on Bioavailability and Uptake

by

Paul McManus, Master of Science

Utah State University, 2016

Major Professor: Joan E. Mclean
Department: Civil and Environmental Engineering

Copper oxide nanoparticles (NPs) are used in an expanding range of industries including a potential for agricultural applications as a fungicide. Accidental spills or misapplication of CuO NPs may lead to soil contamination. Plant roots exude a wide range of organic chemicals for bioprotection and to enhance bioavailability of nutrients. Many of these chemicals are metal chelators that may increase the solubility of CuO NPs, thus enhancing the impact of these NPs on plants. This work was directed towards understanding which plant exudates force increased solubility of CuO NPs and to determine if the level of NP in the growth matrix drives a feedback effect, regarding composition and quantity of exudates.

Wheat seedlings (*Triticum aestivum* cv Deloris) were grown in a sand matrix

for 10 days after 3 days of germination. The sand was amended with sublethal doses of CuO NPs from 0 to 300 mg Cu/kg dry sand. Sand was selected as the solid growth matrix as a proxy for soil in terms of plant root morphology, mechanical impedance and water stress, while providing a low background of dissolved organic carbon for the isolation of root exudates. After plant growth, the pore water was collected from the sand by vacuum filtration and analyzed.

By coupling analytic techniques including Triple Quad Mass Spectroscopy and ion chromatography with geochemical modeling, we have identified citrate and the phytosiderophore, deoxymugineic acid (DMA) as chelators that drove the majority of dissolution of CuO NPs, especially DMA at higher CuO NP doses. Altered biogeochemistry within the rhizosphere was correlated with increased plant uptake of Cu and bio-response via exudate type, quantity and metal uptake. Exposure of wheat to CuO NPs lead to dose-dependent reduction in Fe, Ca, Mg, Mn and K in roots and shoots. This work is relevant to growth of commercially important crop wheat in the presence of CuO NPs as a fertilizer, fungicide or a pollutant.

(164 pages)

PUBLIC ABSTRACT

Rhizosphere Interactions Between Copper Oxide Nanoparticles and Wheat Root Exudates in a Sand Matrix; Influences on Bioavailability and Uptake

Copper oxide nanoparticles (CuO NPs) are extremely small particles (less than 1 nm in one or more dimension, or one billionth (10^{-9}) of a meter) used in a diverse range of industries. They have been shown to travel through water systems, and like pharmaceuticals, can end up in wastewater treatment plants and then be land applied as biosolids, where crops are grown for animal consumption, potentially leading to food chain accumulation.

Cu is an essential micronutrient for plants, but is phytotoxic at higher concentrations. CuO NPs present an increasingly real environmental threat to agriculture in soils treated with biosolids, in addition to aquatic systems.

To understand this interaction, wheat was grown in sand amended with various levels of CuO NPs for 10 days. Compared to the control, roots of wheat grown with nanoparticles were dose-dependently shorter. Analysis of the shoot tissue showed that micronutrients, calcium, magnesium, manganese and iron (Fe) as well as potassium were lower, while Cu was higher in CuO NP-treated wheat.

Additionally, higher levels of root exudates, citrate and Fe uptake molecule

deoxymugineic acid, were found at higher CuO NP doses. These negatively charged molecules at neutral pH bind to Cu^{2+}, dissolving more Cu into solution compared to a solution without plants. Our studies show that increasing amounts of Cu in solution, driven by complexes formed by root exudates, may be in part responsible for the toxicity of CuO NPs.

ACKNOWLEDGMENTS

The United States Department of Agriculture and the Utah Water Research Laboratory funded this work. It was a privilege to be challenged and led by a multidisciplinary team comprised of my major Professor Joan McLean, alongside Dr. Anne Anderson and Dr. David Britt. Professor McLean's keen eye for detail and extremely hard work ethic challenged me to higher levels. The statistical and experimental design expertise of Dr. David Stevens was also crucial to the project's success.

Without the technical skill and wise consultation of Joe Stewart and Tessa Guy, this work would have been far less fun, and much less productive. Additionally, the laboratory assistance from Josh Hortin, Rashelle Wegelin, Jeremy Jensen and Will Fulmer was vital in successfully obtaining quality data at harvest time. I appreciate their help, without which the project would not have been possible.

On a personal note, my family and friends have been supportive and kept me accountable to continue, especially when the project underwent challenging phases. Also thank you to Café Ibis for supplying me with all the caffeine a grad student could need.

CONTENTS

Page

LIST OF FIGURES

Figure Page

Figure Page

LIST OF TABLES

Table Page

Table Page

CHAPTER 1

INTRODUCTION

Uses of nanoparticles are gaining momentum in commerce, and their increased production and utilization makes agricultural risk assessment prudent. Nanoparticles (NPs) may enter the environment intentionally through remediation (nano Fe^{o}) (Zhang 2006), as fertilizers or pesticide, or incidentally through waste streams (Rivera Gil et al 2010), accidental spills, misapplication or construction materials (Lee et al 2009). It is of paramount importance to better understand how increased concentrations of NPs in the environment may impact viability of crops, and ultimately the food chain (Chen et al. 2014).

Nanoparticles (NPs) are defined as particles having at least one dimension between 1 and 100 nm (1 nm = 10^{-9} m). An especially large surface area to volume ratio makes their physical properties different from 'bulk' materials, and as a result, the physiochemical, optical, reactive and electrical properties are different. NPs are also more bio-reactive than larger particles and have applications as anti-microbials, especially Ag, CuO and ZnO.

This study focuses on the biogeochemistry of copper oxide (CuO) NPs in the context of bread wheat (*Triticum aestivum* cv Deloris (Hole et al. 2004)) grown in a sand matrix. CuO NPs are primarily used in sensors, but also used as catalysts, in solar energy conversion and electronic printing, surfactants and antimicrobials

(Ahamed and Alhadlaq 2014; Bondarenko et al. 2012; Wang et al. 2013). CuO NPs have been shown to be bacteriostatic to soil microbes (Gajjar et al. 2009) and dose dependently toxic to plants in hydroponic culture (Trujillo-Reyes et al. 2014; Wang et al. 2012). CuO NPs at 300 mg Cu/kg dry sand also show sub-lethal effects on wheat plants in preliminary studies by the author done in sand over 10 days (Dimkpa et al. 2012, 2013). Of pertinence to this system is the solution phase biogeochemistry, particularly the interplay between the increased NP dose and the exudation of organic carbon by the wheat plant since it will affect CuO NP aggregation-dissolution and plant-NP-Cu^{2+} interaction.

Cu has significance as an essential micronutrient for plant growth, but at elevated levels Cu becomes toxic (Michaud et al. 2007, 2008). Plants have developed various mechanisms for regulating Cu uptake, including production of root exudates to increase or decrease bioavailability of Cu. Additionally, specific metallochaperones transport Cu internally, and can sequester Cu in a non-harmful form, or efflux pumps may remove Cu from the plant (Clemens et al. 2002).

The bioavailability of Cu is controlled by solution phase chemistry. pH and dissolved organic matter (DOM) are most influential on Cu mobility and bioavailability (Michaud et al. 2007; Sauve et al. 2000). pH increases dissolution by a factor of 10 with every 0.5 unit decrease in pH (Lindsay 1979), whereas DOM drives dissolution of Cu from CuO via complexation (McBride and MartÍnez 2000), in some cases enhancing uptake. Cu in solution exist as a free ion (Cu^{2+}) or complexed with inorganic or organic ligands. The presence of ligands, including plant and bacterial exudates, changes Cu mineral dissolution, desorption and bioavailability. For

example, citric acid, a bacterial and root exudate, complexes Cu and enhances uptake by a soil bacterium *Pseudomonas putida* (McLean et al. 2013). Additionally, wheat plants grown under Fe deficient conditions will up regulate production of phytosiderophores (Fe–chelating compounds) that have been reported to form Cu-complexes (Michaud et al. 2007). Low molecular weight organic acids (LMWOAs) such as citrate and malate, can solubilize unavailable metals also (Dakora and Phillips 2002). Competing stabilities between complexes make this system non-trivial (Callahan et al. 2006). Thus organic ligands play a crucial role in defining the rhizosphere (rooting zone of plants influenced by plant biochemistry) and controlling Cu uptake.

Comparing the effects *in planta* of the concentration of ions produced by dissolution of CuO NPs, with Cu^{2+} ions from Cu salt, suggest CuO NPs exhibit both soluble Cu and specific NP effects on wheat growth in sand (Dimkpa et al. 2012). In a hydroponic setting, free cupric ions from CuO NPs did not explain the root phytotoxicity in radish, lettuce and cucumber seeds over 3 days of growth, similarly implying a specific NP interactions with the seed/root surface (Wu et al. 2012). The mechanism of toxicity from Cu ions or directly from the CuO NPs is still a matter that requires further investigation (Atha et al. 2012; Shi et al. 2011; Stampoulis et al. 2009; Trujillo-Reyes et al. 2014).

Solution properties will affect NP solubility, through chelation, and ligands can increase bioavailable Cu to plants, but many of these studies are in hydroponic systems, with inherent shortcomings from a morphologic and geochemical perspective. There is a critical need to understand the biogeochemistry of CuO NPs

in a solid phase system. Jones (1998) highlights that roots grown hydroponically will be morphologically and physiologically different from those grown in solid systems, including the lack of root hairs, mechanical impedance and water stress. The outcome of this research has greater relevance to how CuO NPs may impact agricultural processes as compared to hydroponic systems.

This study aims to assess the interaction between root exudates of bread wheat in response to sub-lethal levels of CuO NP in a sand matrix, along with a control without nanoparticles. This interaction will model rhizosphere processes, and isolate plant-NP interactions (in the absence of added microbes) to assess how plant exudates may defend against toxicity, or drive dissolution of the NP into Cu^{2+} ions and complexes, and affect Cu uptake by the wheat plant. The solution phase of this system will be rigorously analyzed to better understand the CuO NP wheat root exudate interplay.

Aims

The current study aimed to examine the influence of root exudates from bread wheat (*Triticum aestivum* cv Deloris) on the dissolution of CuO nanoparticles (NPs), as well as the bioactivity of the NPs on wheat morphology and micronutrient uptake into roots and shoots. A particular focus on Cu chelating compounds, including citrate, malate (Haydon and Cobbett 2007), other LMWOAs, phytosiderophores and other amino acids, provided additional detail to this dynamic system. In essence, what was the composition and role of exudates from

wheat in complexing Cu^{2+} from CuO NPs? Did different concentrations of CuO NPs influence exudate composition?

Hypotheses

1. DOC forming complexes with Cu does not drive dissolution of CuO NPs.

Approach: Total dissolved Cu and predicted Cu complexes from MINTEQ were compared across unplanted and planted treatments. Correlations were defined between soluble Cu and DOC species. Geochemical modeling software (MINTEQ) was employed using known stability constants and concentrations metal and ligands, to create a model of the solution phase to complement analytical techniques.

2. Cu speciation in the rhizosphere is not the driver of Cu uptake into the plant, or root morphological impact.

Approach: Root and shoot Cu levels and solution properties, including total DOC, LMWOA, amino acids and Cu-ligands as determined under hypothesis 2 were statistically compared by ANOVA/Tukey's HSD to NP dose. Root elongation reduction was compared by 1-way ANOVA across NP dose.

3. Metal homeostasis in the plant shoot is unaffected by dose of CuO NP.

Approach: Digestion and analysis of shoots revealed levels of nutrients Ca, Mg, K, Fe, Cu, Zn, Mn and these were statistically compared between doses of CuO NP.

CHAPTER 2

LITERATURE REVIEW

Nanotechnology

Nanoparticles (NPs) are defined as particles having at least one dimension between 1 and 100 nm. Increasingly, NPs are being manufactured for commercial purposes. However, NPs also exist in natural systems from volcanoes to fire and soil erosion (Stampoulis et al. 2009). Plants and bacteria have evolved alongside nano-sized materials. Plants and bacteria have been used to produce NPs in industry (Thakkar et al. 2010).

The advent and expansion of the nano-technology industry is poised to increase both the varieties and quantities of NPs to which natural systems will be subjected (Flynn et al. 2014). The large surface area to volume ratio makes the physical properties of NPs different from 'bulk' material, including altered physiochemical, optical, reactive and electrical properties that are exploited in nano-technological advances.

Ag, CuO and ZnO NPs are among mass produced NPs. Their antimicrobial activity is beneficial in controlling pathogens (Chen et al. 2014) but potentially detrimental to beneficial soil microbes that play essential ecosystem roles in element cycling and plant health (Dimkpa 2014). The focus of this study is CuO NPs. CuO NPs are infrequently studied in an environmental context (Gardea-Torresdey et al. 2014). Their presence in soils may be through contamination, but also

purposeful applications. Regarding industrial application of CuO NPs, Lee et al. (2010) suggested elemental Cu (Cu^0)-based NPs, which readily oxidize to CuO NPs, created better welds, corrosion resistance and formability in steel used in construction. CuO NPs are also used in sensors, as catalysts, in solar energy conversion and electronic printing, surfactants and antimicrobials (Ahamed and Alhadlaq 2014; Bondarenko et al. 2012; Wang et al. 2013). These NPs could be released during crushing, land filling or incineration of the steel. Semiconductor production creates CuO NPs along with a significant amount of wastewater requiring treatment (Otero-González et al. 2014). CuO NPs, due to formulation as antibacterials that are cheaper than nano-size Ag^o, may also enter wastewater systems, and be subsequently land-applied via biosolids/sludge (Kiser et al. 2012). Otero-González et al. (2014) demonstrated negative effects in activated sludge with respect to the microbial-driven process of methanogenesis due to the presence of CuO NPs. These applications may pose risks to plant growth and higher trophic levels through bioaccumulation (Chen et al. 2014).

One intentional use of CuO NPs in agricultural systems may be as fungicides. Such NPs might be more efficient than traditional copper solution fungicides, such as the Bordeaux mixture that is commonly applied to vineyards (Giannousi et al. 2013). NPs have been shown to release ions over time, as opposed to adding discrete treatments of highly concentrated salt solutions. Thus, a possible use for Cu NPs could be as a fertilizer for slow release of Cu to improve Cu uptake into plants, with potential health benefits for humans (Dimkpa 2014). The difference between concentration of Cu affecting plant protection and causing plant damage by copper,

however, is narrow. CuO NPs have been shown to be bacteriostatic to soil microbes (Gajjar et al. 2009) and dose-dependent toxicity to plants in hydroponics (Trujillo-Reyes et al. 2014; Wang et al. 2012).

Chen (2014) stated that more investigation is required between engineered nanomaterials and ecosystem species. Studies of wheat would be valuable because it is a crop of global significance.

This present study examines processes involved in dissolution of CuO NPs in the plant rhizosphere (Fig. 2-1). CuO NPs may influence the type of exudates, or quantity, which may in turn aggregate or dissolve the NPs into Cu ions. These processes may have implications for toxicity, bioavailability and uptake. The rhizosphere was first defined in 1904 by German biologist Lorentz Hiltner as soil influenced by both plant root and bacterial nutrient mobilization (Hartmann et al. 2007). It has a much larger carbon content than bulk soil, as well as a less diverse but many times more concentrated bacterial community, which interacts directly and indirectly with the plant root.

Factors driving dissolution of CuO NP

Dissolution

Both NPs and the ions released through dissolution of NPs may have an impact on the wheat plant. pH strongly affects CuO NP dissolution (Eqn 1), particularly with smaller NPs (Misra et al. 2012; Odzak et al. 2014). In ultrapure water at pH 5.5, 20 nm CuO NPs undergo 95% dissolution, compared to 0.3 % at pH

7 (Misra et al. 2012). Only 1% of 45 nm CuO NPs dissolved at pH 7.7, compared to 3% of 7.5 nm CuO particles (Odzak et al. 2014). At pH 6.1, the trend was the same; 7.5 nm particles underwent 62% dissolution, whereas 45 nm particles only 14% (Odzak et al. 2014).

$$CuO_{(s)} + 2H^+ \rightarrow Cu^{2+} + H_2O \quad \text{(Equation 1)}$$

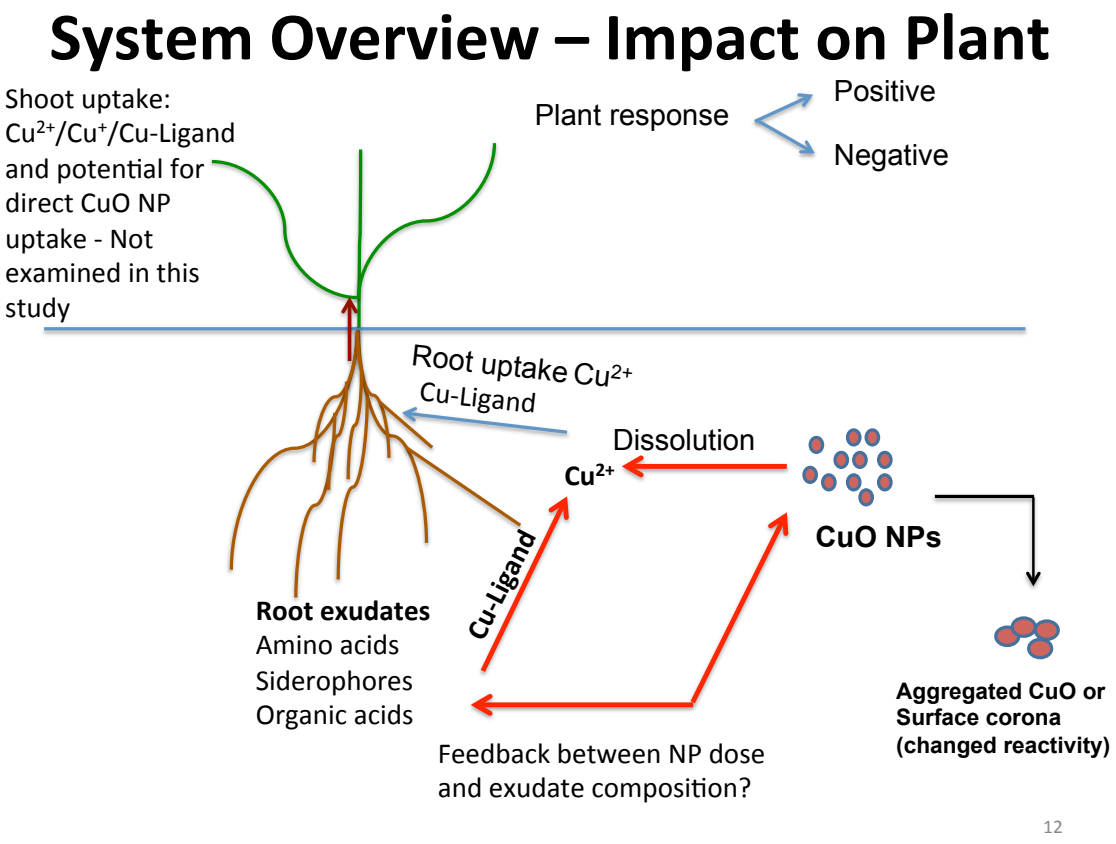

Fig. 2-1. Components involved in the interaction between wheat and CuO NPs in the rhizosphere. CuO NPs interact with plant exudates, altering the NPs' surface chemistry and inducing aggregation and/or dissolution into Cu^{2+} ions or Cu complexes (Cu-ligand), processes that may affect bioavailability, root uptake and translocation.

Gunawan et al. (2011) found that solubility of CuO NPs was additionally driven by the presence of organic ligands (dissolved organic carbon or DOC) in media, usually used for bacterial or plant growth (Table **2**-**1**.) The presence of amino acids increased soluble Cu from the CuO NPs by 2 orders of magnitude, a finding not replicated with micro sized CuO particles (Gunawan et al. 2011). This suggests that DOC in a system will drive dissolution of the NPs.

Table 2-1. CuO NPs dissolution in various media after 48 hours from Gunawan et al. (2011).

NP Size (nm)	NP added (mg/L)	Media	Soluble Cu (mg/L)
20-30	480	DI Water	6.4
20-30	480	NaCl (5g/L) (a)	3.9
20-30	480	Tryptone (10g/L) (b)	338
20-30	480	Yeast Extract (5g/L) (c)	282
20-30	480	Culture Media (a)+(b)+(c) in DI water	366

Metal-organo complexes

In a planted system, root exudates will affect solubility. Plant exudates include sugars, amino acids, LMWOAs, sterols, phenolics, iron-binding phytosiderophores, and enzymes, many of which are quickly consumed and metabolically transformed by bacteria (Dennis et al. 2010). Concentrating exudates washed from 7 day old wheat seedlings grown in vermiculite, Martineau et al. (2014) found DOC at 2,600 mg/L including 137 mg/L proteins, 119 mg/L neutral sugars, 200 mg/L LMWOAs with iso-butyrate, acetate, succinate, malate the highest contributors. Amino acids were not assessed in this study. Root exudation in the presence of CuO NPs was not assessed, but would seem a relevant next step.

In another study, the amount of soluble Cu in the sand matrix with wheat plants was three times that of the treatments without plants (

Table **2-2**.), suggesting Cu was solubilized due to complexation from root exudates (Dimkpa et al. 2013). The plant-NP interaction promoted release of Cu^{2+} ions (Fig. 2-1.). This release was not exclusively due to acidification of the rooting zone since the pH was only reduced by 0.3 units, as measured in the bulk solution, not in the rhizosphere (Dimkpa et al. 2013). Microparticles (MPs – particles between 0.1 and 100 μm in diameter) of CuO showed a ~50% lower solubility compared to NPs in the presence of wheat. Without plants, CuO MPs released only 20% less soluble Cu than the NPs. This suggests root exudates in particular drove much more significant dissolution.

Table 2-2. Soluble Cu released from CuO NPs in sand, and with the addition of wheat plants over 14 days from Dimkpa et al. (2013)

NP Type	Media	Soluble Metal (mg/kg sand)	pH
CuO	Sand (no plants)	0.29 ± 0.07	7.2 ± 0.05
CuO	Sand with wheat	1.02 ± 0.1	6.9 ± 0.03

Conway et al. (2015) studied CuO NPs in water including seawater, lagoon, wastewater and hydroponic media. Hydroponic media and freshwater drove between 3 and 4% of the Cu into solution after 100 days, about double that of other waters tested. The study suggested that 30% (fresh) and 60% (hydroponic media) of the Cu dissolved was present as ionic or complexed Cu (as opposed to nanoparticulate Cu).

Low molecular weight organic acids (LMWOAs)

Organic acids are released from the root due to stressors such as K^+, Ca^{2+} and Zn^{2+} deficiency, the latter two increasing root membrane permeability, driving a release of organic acid efflux (Jones 1998). P and Fe deficiency is also reported to drive release of LMWOAs (Dakora and Phillips 2002). Malate, citrate, succinate, fumarate and aconitate are intermediates of the Krebs Cycle involved in general metabolism (Dakora and Phillips 2002). Cu(II) forms strong complexes with LMWOAs due to their negatively charged carboxylic acid functional groups above pH 6, allowing more Cu to dissolve from the solid phase (Karlsson et al. 2006; Manceau and Matynia 2010). As a practical example, the standard method of determining extractable Cu in soils to estimate soil fertility is with diethylene triamine pentaacetic acid (DTPA), a chelating compound. LMWOAs have been used to successfully assess Cu bioavailability in several soils over acidic and higher pH ranges, highlighting their importance in impacting metal mobility in a more realistic way (the exudates are biologically relevant, whereas DTPA is not a root exudate (Feng et al. 2005)). Using LMWOAs (acetate, lactate, malate, citrate and formate) for Cu extraction in a range of soils had significantly better correlation with root and shoot uptake in wheat compared to DTPA, EDTA (Ethylenediaminetetraacetic acid), $CaCl_2$ and $NaNO_3$ extractions, reiterating it's biological relevance (Feng et al. 2005).

LMWOAs are also used in phytoremediation studies to improve plant metals uptake (Almaroai et al. 2012; Sinhal et al. 2010).

Amino acids including phytosiderophores

Amino acids play a role in increasing nutrient sources, by chelating poorly available nutrients and act as a "chemoattractant" for microbes (Dakora and Phillips 2002). Amino acids have been studied in the presence of CuO NPs, and histidine and asparagine specifically found to leach high levels of Cu from NPs (Gunawan et al. 2011; Wang et al. 2013). Wheat relies on amino acid-based products called phytosiderophores (PSs), in this case deoxymugineic acid (DMA) (von Wiren 2000) (Haydon and Cobbett 2007; Jones 1998) to capture Fe(III) (Fig. 2-2.).

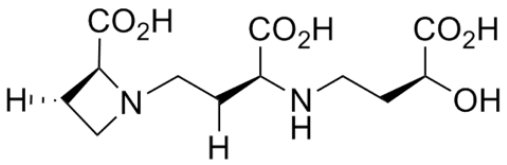

Deoxymugineic acid

Fig. 2-2. Deoxymugeneic acid with full protonation (pKa = 2.35, 2.74, 3.20, (carboxylic groups) 8.25 (OH), 10.00 (NH)) (von Wiren 2000).

Particularly in alkaline soils, the production of these chelating molecules increases the bioavailability of Fe(III), which is low because of low solubility of Fe(III) at high pH. These phytosiderophores also complex Cu, increasing solubility (Treeby et al. 1989). Oburger et al. (2014) indicated that soil grown wheat exuded a

significantly lower concentration of PSs compared to reports in hydroponics, a finding that points to solid phase growth systems being more realistic for wheat growth. Additionally, Oburger et al. (2014) reports a 10-fold increase of PS release compared to Fe uptake, suggesting excess exudation of PS. In the presence of CuO NPs, this may have large implications for dissolution; the excess DMA may dissolve Cu from NPs and have potential implications for Cu and Fe uptake into shoots (Ma et al. 1993; Ma and Nomoto 1993) (Fig. 2-1.) Some uncertainty exists over whether plants can uptake the CuDMA complex intact (Ma et al. 1993; Ryan et al. 2013), but Fe acquisition has been shown to be interrupted in the presence of large rhizosphere Cu concentrations (Michaud et al. 2007).

Stability of complexes

Release of DOC by wheat roots is diverse and dynamic. The interplay between these exudates and CuO NPs, will depend on both quantities of exudates and stability of the complexes (Anjum et al. 2015 b). Of particular importance is how the CuO NPs dissolve into Cu^{2+} ions and their speciation in complexes. Cu-DMA complexes for example are orders of magnitude (log 18.7 to log 10.2) more stable than complexes with amino acids and LMWOAs with Cu (Table 2-3.). Thus, DMA is a strong candidate for favoring Cu complexation against other root exudates. Quantifying this contribution is therefore of importance in understanding what drives dissolution of CuO NPs, and uptake into wheat plant. Histidine, an amino acid,

has a higher affinity for Cu than for Fe(III). Amino acids have been studied alongside CuO NPs and found to have increased their dissolution (Wang et al. 2013).

Table 2-3. Stability constants (log 10) (Molar) for Fe(III), Cu(II) complexes with deoxymugeniec acid (DMA) (Murakami et al. 1989). Fe/Cu-histidine from Callahan et al. (2006). FeGluconate (Bechtold et al. 2002), and CuGluconate (Gajda et al. 1998). Oxalate and arginine from GEOCHEM (Parker et al. 1995) all others taken from MINTEQ+ (Gustafsson 2014) and are 1:1 metal:ligand ratio. All logK are at STP (25 °C, 1 atm). (See supporting information **Table 3-7** for detailed list).

	Siderophore	LMWOAs		
	DMA	Citrate	Malate	Gluconate
Cu(II)	18.7	7.6	4.53	2.51
Fe(III)	18.4	13.13	8.39	10.51

	Amino acids		
	Glycine	Histidine	Arginine
Cu(II)	8.56	10.2	8.4
Fe(III)	9.38	4.7	9.3

Aggregation

Aggregation of NPs involves increasing particle size, and is driven by increasing pH, as well as increasing ionic strength (depending on the charge and the affiliation of the ion with the nanoparticle) due to reduced repulsion between particles (Jośko and Oleszczuk 2013; Navarro et al. 2008). As the charge on the particle is reduced, repulsion between particles drops and the particles may bind together (Navarro et al. 2008). Particles may aggregate past nano size, losing their nano-specific properties. Charge of particles in solution is generally characterized by their zeta potential, which measures the stability of the colloidal dispersion. In a

14 day study, bread wheat was grown in sand containing CuO NPs, and the surface charge of colloids in the sand matrix was reduced in the presence of plants, causing aggregation in the presence of organic root exudates (Dimkpa et al. 2013). A reduction in zeta potential and resulting aggregation may cause suspended particles to settle out of solution. In several different aqueous systems ranging from ocean water to freshwater, however, Keller et al. (2010) reports a reduction in aggregation in the presence of high dissolved organic carbon (DOC) and ionic strength with ZnO, TiO2 and CeO2. In another study, CuO NPs were found to be stabilized by the presence of phosphate (PO_4^{3-}) due to surface charge alteration from positive to negative, and aggregation correlated positively with increasing ionic strength (Conway et al. 2015). Ionic strength and aggregation were also positively correlated for CuO NPs by Odzak et al. (2015) in natural waters, in addition to commenting that DOC could either stabilize NPs, or drive dissolution. Understanding the speciation of DOC is important to understand how CuO NPs will undergo transformation in natural systems.

Changes in surface properties

The exposure media impacts the toxicity from NPs to plants and bacteria due to surface coatings, or coronas. Specifically, organic root exudates can alter the potency and impact of CuO NPs, and have been shown to change toxicity to beneficial soil bacterium *Pseudomonas putida KT2440* (Martineau et al. 2014). Taking into account the specific conditions in the rhizosphere that affect the dissolution and/or uptake of NPs is therefore crucial.

Deng et al. (2009) found that coronas, in this case protein-based shells surrounding the NPs (ZnO, TiO_2), have implications for both bioavailability and dissolution. The sorption of proteins onto the NPs can alter the shape and therefore functionality of the protein (Rivera-Gil et al. 2013). This, in turn, will alter the biochemical context and plant/bacterial response. Lynch and Dawson (2008) indicate that proteins will almost immediately encapsulate the NPs, and the rates of attachment and detachment will provide a signature for the NP. Hence, root and exudates, as well as their interaction with CuO NPs, are vitally important in understanding what mitigates or pronounces their toxicity to wheat plants and/or soil bacterial health. Organic molecules are not the only source of CuO NP coronas. Xu et al. (2012) found that CuO NPs in media can be capped with inorganic ions, irrespective of the presence of proteins.

The presence of DOC can bind to the surfaces of the NPs and prevent formation of aggregates (in the case of ZnO, TiO_2 and CeO) thus stabilizing the NPs (Keller et al. 2010). Bacteria are a key component of soils. Exudates such as exopolysaccharides from beneficial soil bacteria strains, *Pseudomonas,* have been suggested to provide a defense mechanism by capping NPs, thus reducing their potency (Nezhad et al. 2014). The surface chemistry of Ag NPs was altered by humic acid and Ca^{2+} ions from pore water from a loamy soil, driving agglomeration. These processes removed potential toxicity of the Ag NPs to bacteria soil bacterium (Calder et al. 2012).

Thus components from bacteria, plants and soil solution are expected to influence how the CuO NPs are presented to the wheat plant, and vice versa. Studies

of how exudates from wheat affect dissolution of CuO NPs, and which exudates are triggered as a result of exposure to NPs are lacking, to the author's knowledge. While CuO NPs undergo dynamic aggregation and surface coatings, understanding the smaller fraction of NPs (<10 nm and < 1 nm) may be key to understanding their toxicity, as small particles may be more phytotoxic (Mudunkotuwa et al. 2012).

Plants and copper: micronutrient, toxin and strategies for control

Wheat cells require Cu as an essential micronutrient, and have strategies to enhance uptake. As a key component of chloroplasts, Cu is required for photosynthetic electron transport (Maksymiec 1998; Marschner 1995). Cu is also a co-factor in several enzymes and their complexes, including Cu superoxide dismutase (SOD), cytochrome c oxidase, amino oxidase, laccase, plastocyanin and polyphenol oxidase (Marschner 1995). Cu also plays a role in mitochondrial respiration, oxidative stress responses, cell wall metabolism and hormone signaling (Marschner 1995). The concentration difference between required Cu in plants and toxic levels is however narrow. Plants have therefore evolved strategies to prevent excessive uptake (Fig. 2-3.).

Clemens et al. (2002) described the four stages involved in metal homeostasis in plants: mobilization, uptake and sequestration, xylem transport and finally, unloading, trafficking and storage (Fig. 2-3.). To mobilize metals, plants carry out rhizosphere acidification (and to charge balance uptake of cations), as well as exudation of carboxylic acids, to increase bioavailability. Root-colonizing bacteria

and fungi can similarly enhance bioavailability of metals in the rooting zone. Alternatively root exudates enable protection by defensive signaling to neighboring plants (Bais et al. 2006). Parker et al. (2001) found that bread wheat exposed to Cu, supplied as 2mM $CuCl_2$, experienced less toxicity (measured by root elongation) when the Cu was combined with LMWOAs malonate and malate, whereas citrate had no impact in reducing toxicity in a hydroponic system.

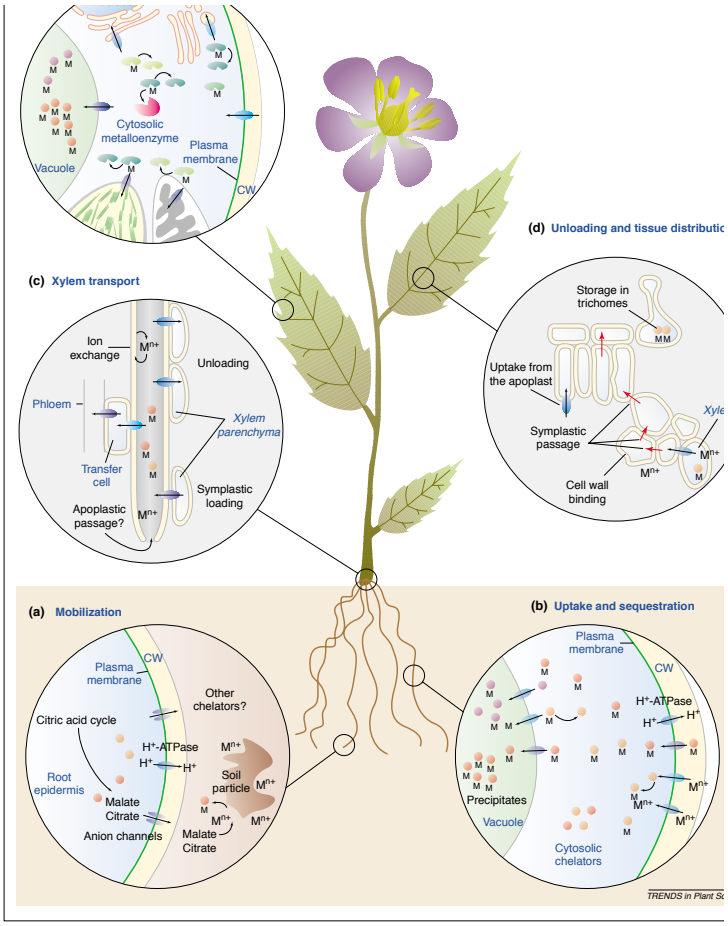

Fig. 2-3. Plant mechanisms to manage metal uptake

Abbreviations and symbols: CW, cell wall; M, metal; filled circles, chelators; filled ovals, transporters; bean-shaped structures, metallochaperones. Taken from (Clemens et al. 2002)

Uptake through the root is initialized by the attachment of the metal to the root cell wall. Transporters then take the metal across the plasma membrane. nRAMP (natural resistance-associated macrophage protein) and ZIP (ZRT, IRT-like protein) genetic families are thought to generate most of the Cu transporters as shown by exposing the plant to micronutrient deficient conditions (Clemens et al. 2002, White and Broadley 2009).

Transport of transition metals within the xylem is tightly controlled; Cu is almost always attached to a ligand, and movement of Cu is done by exchange reactions, substituting one ligand for another. The ligand attached to the Cu will impact bioavailability and toxicity. Cu is unloaded through the xylem sap, where it is required in leaf cells. Excessive Cu is also sequestered into the plant vacuoles cells, which act as a storage for unwanted micronutrients (Clemens et al. 2002).

Cu toxicity

Copper is a necessary micronutrient, but the range of tolerance is narrow. Cu becomes damaging due to its redox potential as an ion and ability to disrupt thiol bonds in proteins, compromising their secondary structure (Ducic and Polle 2005). Marschner (1995) suggests deficient shoot loadings of 1 – 5 mg Cu/kg dry shoot mass, and an upper threshold of 20 – 30 mg Cu/kg dry shoot mass. Wheat plants undergoing Cu phytotoxicity demonstrate oxidative stress (as the Cu^{2+} ion is reduced to Cu^{+}) (Dimkpa et al. 2012) and shoot growth reduction (Dimkpa et al. 2012), as well as chlorosis (yellowing of shoots). Oxidative stress may be

demonstrated by potassium (K^+) efflux (Demidchik 2014) from roots, observed in a matter of hours after the plant is exposed to sufficiently high levels of Cu ions.

The toxicity of metals may be related to their attachment to the root cell wall. Research by Kopittke et al. (2011) showed that in 3 day old cow pea seedling roots (a dicot) exposed to Cu ions, the Cu ions concentrate around the root tip. This concentration may be responsible for the lack of root elongation, due to Cu binding with citric acid and cysteine binding with -SH functional groups on the root surface, restricting cell growth after 3 hours, and the outer cortex (polygalacturonic acid) after 24 hours of Cu exposure. It is possible that Cu ions, in sufficient concentrations, might damage root cells, making ingress of Cu ions, or CuO NPs, more efficient.

Cu rhizotoxicity in wheat is indicated by stunted and thickened root growth, darkening in color, and abnormal root branching, which increases with Cu concentration (Dimkpa et al. 2012; Michaud et al. 2008). The effect may increase with pH, as carboxylic groups on the root surface are deprotonated, (Michaud et al. 2008) enhancing Cu sorption.

Copper and iron homeostasis

Despite Cu levels controlled into the wheat plant, studies have shown in environments with high concentrations of Cu, uptake of Fe is reduced seemingly in place of increasing Cu uptake (Michaud et al. 2007). Whether this is because of increasing phytosiderophores production is unknown from this study (plants here were grown in calcareous soils where Fe is less available, hence increased

phytosiderophores production is likely but unconfirmed). Inside the plant, Grotz and Guerinot (2006) indicate that Cu and Fe have different transport mechanisms, though some transporters may be common to both, implying increased uptake of Cu by phytosiderophores could share common internal pathways with Fe. Metal homeostasis has both plant health implications, as well as importance in staple crops like wheat, as the nutrients Fe and Cu are required for human health.

Plants and Cu/CuO NPs

Various species of edible plants have been studied to understand how CuO NPs may impact agriculture. Phytotoxicity, defined as a distinct response to abiotic stress experienced by the plant, is evident from Cu-based nanoparticles. The toxicity appears as an oxidative stress, in some cases inducing DNA damage, and a reduction in root elongation and morphological change. Oxidative stress, measured by oxidized glutathione (Dimkpa et al. 2012), has been found to be symptomatic of CuO NPs toxicity in many species (Atha et al. 2012 (ryegras and radish); Dimkpa et al. 2012 (wheat); Nair and Chung 2015a (cucumber); Kim et al. 2012 (cucumber); Nair and Chung 2015b (indian mustard)). Lee et al. (2013) found oxidative stress from Cu^0 NPs in buckwheat. Oxidatively induced DNA damage was identified in radish, perennial and annual ryegrass (Atha et al. 2012), and buckwheat (Lee et al. 2013). Strong plant growth inhibition was exhibited at 10 mg/L CuO NPs for radish and ryegrasses (Atha et al. 2012), whereas 2,000 mg/L CuO NPs over a 3 day growth period was required to affect buckwheat (Lee et al. 2013). Dimkpa et al. (2012)

observed reductions in root elongation and lateral root proliferation at 500 mg Cu/kg sand for CuO NPs.

Some uncertainty exists regarding the toxic mechanism of nanoparticles; that is, is it purely ion release from the NPs providing toxicity, or the NPs themselves? Rousk et al. (2012) maintains Cu ions released from the NPs were the source of toxicity for soil bacteria, though other studies provide evidence in plants that there is a nano-specific toxicity that cannot be mimicked by a Cu-salt (Atha et al. 2012; Shi et al. 2011; Stampoulis et al. 2009; Trujillo-Reyes et al. 2014). Shi et al. (2011) found that CuO NPs were four times more effective in reducing chlorophyll in duckweed compared to the same concentration from $CuCl_2$, implying that the phytotoxicity could not be solely explained by Cu^{2+} ions. Stampoulis et al. (2009) reported similar findings with zucchini and Cu^{o} NPs (copper metal NPs which have been shown to readily oxidize into CuO NPs), as did (Atha et al. 2012) with radish, perennial and annual ryegrass. In contrast, one mechanism discussed by Shi et al (2011) was that the increased uptake of Cu from CuO NPs was due to increased Cu^{2+} dissolved from the NPs in the acidified rhizosphere of the duckweed. This mechanism of NPs being a point source of ions close to the root surface is distinct from uptake of NPs into the plant yet could be described as a 'nano-effect' due to a differential release rate of ions; that is, a stream of ions released adjacent to the root surface. This is unique because bulk particles have not been reported to emulate this process.

Lettuce plants were hydroponically grown for 25 days and were then exposed to Cu/CuO core-shell NPs (CuO surface with a Cu center) for a further 15 days (Trujillo-Reyes et al. 2014). This treatment resulted in observations of

oxidative stress, changed uptake of other metal ions (possibly due to Cu-induced ruptured membranes), and decreased water content. It is unknown if nano-Cu caused distinct effects on the internal cells of lettuce plant from this study.

Several studies have found Cu^0 and CuO NPs internally in plants (Fig. 2-1. (C)), including wheat, maize, cucumber, radish and rice (Atha et al. 2012; Dimkpa et al. 2012; Lee et al. 2008; Peng et al. 2015; Wang et al. 2012). Wang et al. (2012) identified CuO NP, using transmission electron microscopy with energy dispersive spectroscopy (TEM-EDS), in the unexposed roots in maize grown in split-root hydroponics. CuO NPs were translocated into the plant roots, and then deposited after travelling through the xylem and down the phloem in the unexposed roots, suggesting that the CuO NPs travelled intact through the plant's vascular system. Lee et al. (2008), found that bread wheat grown in agar for 2 days took up Cu^0 NPs as identified using TEM-EDS. Kim et al. (2012) reported CuO NPs entered the root endodermis of cucumber using TEM, as did Atha et al. (2012) with radish. The interaction with bread wheat and CuO NPs has been studied in sand (Dimkpa et al. 2012, 2013). CuO (64%) and reduced Cu(I)S (36%) (Cu(I)S is known to be part of the translocation process of Cu in wheat) was found in shoot tissue after growing wheat in sand for 7 days with CuO NPs (Dimkpa et al. 2012). It was speculated that the CuO are likely nanoparticles taken up by the plant, as 64% was found in the form CuO. The authors argue that it was thermodynamically unlikely that Cu was reformed into CuO NP in the plant, implying uptake and translocation of intact CuO NPs (Dimkpa et al. 2012). Confirming findings from this previous study, Cu in the form of CuO and Cu_2-S cysteine/cysteine were found (Dimkpa et al. 2013), again

implying complete particles may have been translocated. This was the case from both nano and micro-sized CuO particles, though the smaller particle size was correlated with greater root toxicity. It was not known if NPs from the microparticle assays were taken up by the plant or if they were in the micrometer range, though in this species of wheat, 500 nm is the upper limit of transportation for particles in the xylem (Dimkpa et al. 2013). Clearly, Cu and CuO NPs at sufficient concentrations in hydroponics and sand have negative consequences in edible food growth.

Still lacking in the literature is how the exudation from wheat will impact the NPs, and if the presence of NPs will determine what exudates the wheat generates. Experiments that combine the plant exudates in a solid phase, mimicking soil, without competing influences from bacteria, seem a prudent simplification. A system that encapsulates rhizosphere chemistry from root exudates, CuO NPs and the interaction with wheat root (while removing background noise from bacterial interference and other soil complexities) should shed important light on the solution phase generated by exposing wheat to CuO NPs. The outcomes of this study, combined with other studies, provide valuable baseline data for scientist, engineers and regulators to make decisions on toxicity and therefore proper disposal and beneficial applications of CuO NPs.

REFERENCES

Ahamed, M., and Alhadlaq, H. (2014). "Synthesis, Characterization, and Antimicrobial Activity of Copper Oxide Nanoparticles." *Journal of Nanomaterials*, 10(1155), 4.

Albalasmeh, A. A., Berhe, A. A., and Ghezzehei, T. A. (2013). "A new method for rapid

determination of carbohydrate and total carbon concentrations using UV spectrophotometry." *Carbohydrate Polymers*, 97(2), 253–61.

Almaroai, Y. a., Usman, A. R. a., Ahmad, M., Kim, K.-R., Moon, D. H., Lee, S. S., and Ok, Y. S. (2012). "Effects of Synthetic Chelators and Low-Molecular-Weight Organic Acids on Chromium, Copper, and Arsenic Uptake and Translocation in Maize (*Zea mays L.*)." *Soil Science*.

Anjum, N. A., Adam, V., Kizek, R., Duarte, A. C., Pereira, E., Iqbal, M., Lukatkin, A. S., and Ahmad, I. (2015a). "Nanoscale copper in the soil–plant system – toxicity and underlying potential mechanisms." *Environmental Research*, 138(2), 306–325.

Anjum, N. A., Hasanuzzaman, M., Hossain, M. A., Thangavel, P., Roychoudhury, A., Gill, S. S., Rodrigo, M. A. M., Adam, V., Fujita, M., Kizek, R., Duarte, A. C., Pereira, E., and Ahmad, I. (2015b). "Jacks of metal/metalloid chelation trade in plants-an overview." *Frontiers in Plant Science*, 6, 192.

APHA. (2014). "APHA AWWA WEF." *Standard Methods for the Examination of Water and Wastewater*, 20.

Asli, S., and Neumann, P. M. (2009). "Colloidal suspensions of clay or titanium dioxide nanoparticles can inhibit leaf growth and transpiration via physical effects on root water transport." *Plant, Cell and Environment*, 32(5), 577–584.

Atha, D. H., Wang, H., Petersen, E. J., Cleveland, D., Holbrook, R. D., Jaruga, P., Dizdaroglu, M., Xing, B., and Nelson, B. C. (2012). "Copper oxide nanoparticle mediated DNA damage in terrestrial plant models." *Environmental science & technology*, 46(3), 1819–27.

Bais, H. P., Weir, T. L., Perry, L. G., Gilroy, S., and Vivanco, J. M. (2006). "The role of root exudates in rhizosphere interactions with plants and other organisms." *Annual Review of of Plant Biology*, Annual Reviews, 57, 233–266.

Baker, A. J. M. (1981). "Accumulators and excluders - strategies in the response of plants to heavy metals." *Journal of Plant Nutrition*, 3(1–4), 643–654.

Bechtold, T., Burtscher, E., and Turcanu, A. (2002). "Ca2+–Fe3+–D-gluconate-complexes in alkaline solution. Complex stabilities and electrochemical properties." *Journal of the Chemical Society*, (13), 2683–2688.

Blinova, I., Ivask, A., Heinlaan, M., Mortimer, M., and Kahru, A. (2010). "Ecotoxicity of nanoparticles of CuO and ZnO in natural water." *Environmental Pollution*, 158(1), 41–7.

Bondarenko, O., Ivask, A., Käkinen, A., and Kahru, A. (2012). "Sub-toxic effects of CuO nanoparticles on bacteria: kinetics, role of Cu ions and possible mechanisms of action." *Environmental Pollution*, 169, 81–9.

Braud, A., Geoffroy, V., Hoegy, F., Mislin, G. L. A., and Schalk, I. J. (2010). "Presence of the siderophores pyoverdine and pyochelin in the extracellular medium

reduces toxic metal accumulation in Pseudomonas aeruginosa and increases bacterial metal toleranceemi." *Environmental Microbiology Reports*, 2(3), 419–425.

Bravin, M. N., Garnier, C., Lenoble, V., Gérard, F., Dudal, Y., and Hinsinger, P. (2012). "Root-induced changes in pH and dissolved organic matter binding capacity affect copper dynamic speciation in the rhizosphere." *Geochimica et Cosmochimica Acta*, 84, 256–268.

Calder, A. J., Dimkpa, C. O., McLean, J. E., Britt, D. W., Johnson, W., and Anderson, A. J. (2012). "Soil components mitigate the antimicrobial effects of silver nanoparticles towards a beneficial soil bacterium, Pseudomonas chlororaphis O6." *The Science of the Total Environment*, 429, 215–22.

Callahan, D. L., Baker, A. J. M., Kolev, S. D., and Wedd, A. G. (2006). "Metal ion ligands in hyperaccumulating plants." *Journal of Biological Inorganic Chemistry*, 11(1), 2–12.

Cannan, R. K., and Kibrick, A. (1938). "Complex Formation between Carboxylic Acids and Divalent Metal Cations." *Journal of the American Chemical Society*, 60(10), 2314–2320.

Chen, H., Seiber, J., and Hotze, M. (2014). "ACS Select on Nanotechnology in Food and Agriculture: A Perspective on Implications and Applications." *Journal of Agricultural and Food Chemistry*, (62), 1209–1212.

Clemens, S. (2001). "Molecular mechanisms of plant metal tolerance and homeostasis." *Planta*, 212(4), 475–486.

Clemens, S., Palmgren, M., and Krämer, U. (2002). "A long way ahead: understanding and engineering plant metal accumulation." *Trends in Plant Science*, 1385, 309–315.

Cohen, A. C. (1959). "Simplified Estimators for the Normal Distribution When Samples Are Singly Censored or Truncated." *Technometrics*, 1(3).

Conway, J. R., Adeleye, A. S., Gardea-Torresdey, J., and Keller, A. A. (2015). "Aggregation, dissolution, and transformation of copper nanoparticles in natural waters." *Environmental Science and Technology*, 49(5), 2749–56.

Creager, M. S., Jenkins, J. E., Thagard-Yeaman, L. a., Brooks, A. E., Jones, J. a., Lewis, R. V., Holland, G. P., and Yarger, J. L. (2010). "Solid-state NMR comparison of various spiders' dragline silk fiber." *Biomacromolecules*, 11, 2039–2043.

Dakora, F., and Phillips, D. (2002). "Root exudates as mediators of mineral acquisition in low-nutrient environments." *Plant and Soil*, 35–47.

Demidchik, V. (2014). "Mechanisms and physiological roles of K+ efflux from root cells." *Journal of Plant Physiology*, 171(9), 696–707.

Deng, Z., Mortimer, G., T, S., A, M., D, M., and R., M. (2009). "Differential plasma

protein binding to metal oxide nanoparticles." *Nanotechnology*, 20(455101), 9.

Dennis, P. G., Miller, A. J., and Hirsch, P. R. (2010). "Are root exudates more important than other sources of rhizodeposits in structuring rhizosphere bacterial communities?" *FEMS Microbiology Ecology*, 72(3), 313–27.

Dimkpa, C. O. (2014). "Can nanotechnology deliver the promised benefits without negatively impacting soil microbial life?" *Journal of basic microbiology*, 54(9), 889–904.

Dimkpa, C. O., Latta, D. E., McLean, J. E., Britt, D. W., Boyanov, M. I., and Anderson, A. J. (2013). "Fate of CuO and ZnO nano- and microparticles in the plant environment." *Environmental Science and Technology*, 47(9), 4734–4742.

Dimkpa, C. O., McLean, J. E., Britt, D. W., and Anderson, A. J. (2015). "Nano-CuO and interaction with nano-ZnO or soil bacterium provide evidence for the interference of nanoparticles in metal nutrition of plants." *Ecotoxicology*, 24(1), 119–29.

Dimkpa, C. O., McLean, J. E., Latta, D. E., Manangón, E., Britt, D. W., Johnson, W. P., Boyanov, M. I., and Anderson, A. J. (2012). "CuO and ZnO nanoparticles: phytotoxicity, metal speciation, and induction of oxidative stress in sand-grown wheat." *Journal of Nanoparticle Research*, 14(9), 1125.

Djurišić, A. B., Leung, Y. H., Ng, A. M. C., Xu, X. Y., Lee, P. K. H., Degger, N., and Wu, R. S. S. (2015). "Toxicity of metal oxide nanoparticles: Mechanisms, characterization, and avoiding experimental artefacts." *Small*, 11(1), 26–44.

Dodson, J. R., Hunt, A. J., Parker, H. L., Yang, Y., and Clark, J. H. (2012). "Elemental sustainability: Towards the total recovery of scarce metals." *Chemical Engineering and Processing: Process Intensification*, 51, 69–78.

Ducic, T., and Polle, A. (2005). "Transport and detoxification of manganese and copper in plants." *Brazilian Journal of Plant Physiology*, 17(1), 103–112.

Eby, G. A. (2004). "Zinc lozenges: cold cure or candy? Solution chemistry determinations." *Bioscience reports*, 24(1), 23–39.

Feng, M.-H., Shan, X.-Q., Zhang, S.-Z., and Wen, B. (2005). "Comparison of a rhizosphere-based method with other one-step extraction methods for assessing the bioavailability of soil metals to wheat." *Chemosphere*, 59(7), 939–49.

Gajda, T., Gyurcsik, B., Jakusch, T., Burger, K., Henry, B., and Delpuech, J.-J. (1998). "Coordination chemistry of polyhydroxy acids: role of the hydroxy groups." *Inorganica Chimica Acta*, 275–276, 130–140.

Gajjar, P., Pettee, B., Britt, D. W., Huang, W., Johnson, W. P., and Anderson, A. J. (2009). "Antimicrobial activities of commercial nanoparticles against an environmental soil microbe, Pseudomonas putida KT2440." *Journal of*

Biological Engineering, 3, 9.

Gardea-Torresdey, J. L., Rico, C. M., and White, J. C. (2014). "Trophic transfer, transformation, and impact of engineered nanomaterials in terrestrial environments." *Environmental Science and Technology*, 48(5), 2526–40.

Giannousi, K., Avramidisb, I., and Dendrinou-Samara, C. (2013). "Synthesis, characterization and evaluation of copper based nanoparticles as agrochemicals against *Phytophthora infestans*." *The Royal Society of Chemistry*, (3), 21743–2175.

Grotz, N., and Guerinot, M. Lou. (2006). "Molecular aspects of Cu, Fe and Zn homeostasis in plants." *Biochimica et Biophysica Acta*, 1763(7), 595–608.

Gunawan, C., Teoh, W. Y., Marquis, C. P., and Amal, R. (2011). "Cytotoxic origin of copper(II) oxide nanoparticles: comparative studies with micron-sized particles, leachate, and metal salts." *ACS Nano*, 5(9), 7214–25.

Gustafsson, J. P. (2014). "Visual MINTEQ, A Windows version of MINTEQA2 version 4.0 MINTEQA2." <http://www2.lwr.kth.se/ English/OurSoftware/vminteq/> (Dec. 20, 2014).

Hartmann, A., Rothballer, M., and Schmid, M. (2007). "Lorenz Hiltner, a pioneer in rhizosphere microbial ecology and soil bacteriology research." *Plant and Soil*, 312(1–2), 7–14.

Haydon, M. J., and Cobbett, C. S. (2007). "Transporters of ligands for essential metal ions in plants." *The New Phytologist*, 174(3), 499–506.

Hole, D. J., Roche, D., Clawson, S. M., and S.A., Y. (2004). "Registration of 'Deloris' Wheat." *Crop Science*, 44(7498), 694–695.

Ivask, A., Juganson, K., Bondarenko, O., Mortimer, M., Aruoja, V., Kasemets, K., Blinova, I., Heinlaan, M., Slaveykova, V., and Kahru, A. (2014). "Mechanisms of toxic action of Ag, ZnO and CuO nanoparticles to selected ecotoxicological test organisms and mammalian cells in vitro: a comparative review." *Nanotoxicology*, 8 Suppl 1, 57–71.

James, D. W., and Topper, K. F. (2010). "Utah Fertilizer Guide." *AG431. Utah State University Extension, Logan*, (December).

Jones, D. L. (1998). "Organic acids in the rhizosphere – a critical review." *Plant and Soil*, 205(1), 25–44.

Jones, J., and Case, V. (1990). "Sampling, handling, and analyzing plant tissue samples." *R. L. Westerman (ed) Soil testing and plant analysis.*, American Society of Agronomy, Madison WI.

Joshi, S., Ghosh, I., Pokhrel, S., Mädler, L., and Nau, W. M. (2012). "Interactions of amino acids and polypeptides with metal oxide nanoparticles probed by fluorescent indicator adsorption and displacement." *ACS Nano*, 6(6), 5668–79.

Jośko, I., and Oleszczuk, P. (2013). "Manufactured Nanomaterials: The Connection Between Environmental Fate and Toxicity." *Critical Reviews in Environmental Science and Technology*, 43(23), 2581–2616.

Karlsson, T., Persson, P., and Skyllberg, U. (2006). "Complexation of Copper(II) in Organic Soils and in Dissolved Organic Matter – EXAFS Evidence for Chelate Ring Structures." *Environmental Science and Technology*, 40(8), 2623–2628.

Keller, A. A., Wang, H., Zhou, D., Lenihan, H. S., Cherr, G., Cardinale, B. J., Miller, R., and Ji, Z. (2010). "Stability and aggregation of metal oxide nanoparticles in natural aqueous matrices." *Environmental Science and Technology*, 44(6), 1962–7.

Kim, S., Lee, S., and Lee, I. (2012). "Alteration of Phytotoxicity and Oxidant Stress Potential by Metal Oxide Nanoparticles in *Cucumis sativus*." *Water, Air, & Soil Pollution*, 223(5), 2799–2806.

Kim, S., Lim, H., and Lee, I. (2010). "Enhanced heavy metal phytoextraction by Echinochloa crus-galli using root exudates." *Journal of Bioscience and Bioengineering*, 109(1), 47–50.

Kiser, M. A., Ladner, D. A., Hristovski, K. D., and Westerhoff, P. K. (2012). "Nanomaterial transformation and association with fresh and freeze-dried wastewater activated sludge: implications for testing protocol and environmental fate." *Environmental Science and Technology*, 46(13), 7046–53.

Kopittke, P. M., Menzies, N. W., de Jonge, M. D., McKenna, B. A., Donner, E., Webb, R. I., Paterson, D. J., Howard, D. L., Ryan, C. G., Glover, C. J., Scheckel, K. G., and Lombi, E. (2011). "In situ distribution and speciation of toxic copper, nickel, and zinc in hydrated roots of cowpea." *Plant Physiology*, 156(2), 663–73.

Kováčik, J., Klejdus, B., Hedbavny, J., Stork, F., and Grúz, J. (2012). "Modulation of copper uptake and toxicity by abiotic stresses in Matricaria chamomilla plants." *Journal of Agricultural and Food Chemistry*, 60(27), 6755–63.

Kramer, P. J., and Boyer, J. S. (1995). *Water Relations of Plants and Soils*.

Lee, J., Mahendra, S., and Alvarez, P. J. J. (2010). "Potential Environmental and Human Health Impacts of Nanomaterials Used in the Construction Industry." *ACS Nano*, 4, 3580–3590.

Lee, S., Chung, H., Kim, S., and Lee, I. (2013). "The Genotoxic Effect of ZnO and CuO Nanoparticles on Early Growth of Buckwheat, *Fagopyrum Esculentum*." *Water, Air, & Soil Pollution*, 224(9), 1668.

Lee, W.-M., An, Y.-J., Yoon, H., and Kweon, H.-S. (2008). "Toxicity and bioavailability of copper nanoparticles to the terrestrial plants mung bean (*Phaseolus radiatus*) and wheat (*Triticum aestivum*): plant agar test for water-insoluble nanoparticles." *Environmental Toxicology and Chemistry*, 27(9), 1915–1921.

Lindsay, W. L. (1979). "Chemical equilibria in soils." John Wiley and Sons Ltd.

Lynch, I., and Dawson, K. A. (2008). "Protein-nanoparticle interactions." *Nano Today*, 3(1–2), 40–47.

Ma, J. F., Kusanoa, G., Kimuraa, S., and Nomoto, K. (1993). "Specific recognition of mugineic acid-ferric complex by barley roots." *Phytochemistry*, 34(3), 599–603.

Ma, J. F., and Nomoto, K. (1993). "Inhibition of mugineic acid-ferric complex uptake in barley by copper, zinc and cobalt." *Physiologia Plantarum*, 89(2), 331–334.

Ma, J. F., and Nomoto, K. (1996). "Effective regulation of iron acquisition in graminaceous plants. The role of mugineic acids as phytosiderophores." *Physiologia Plantarum*, 97(3), 609–617.

Maksymiec, W. (1998). "Effect of copper on cellular processes in higher plants." *Photosynthetica*, 34(3), 321–342.

Manceau, A., and Matynia, A. (2010). "The nature of Cu bonding to natural organic matter." *Geochimica et Cosmochimica Acta*, 74(9), 2556–2580.

Marion, G. M., and Babcock, K. L. (1976). "Predicting Specific Conductance and Salt Concentration in Dilute Aqueous Solutions." *Soil Science*, 122(4), 181–187.

Marschner, H. (1995). *Mineral Nutrition of Higher Plants*.

Martineau, N., McLean, J. E., Dimkpa, C. O., Britt, D. W., and Anderson, A. J. (2014). "Components from wheat roots modify the bioactivity of ZnO and CuO nanoparticles in a soil bacterium." *Environmental Pollution*, 187, 65–72.

McBride, M., and MartÍnez, C. (2000). "Copper phytotoxicity in a contaminated soil: remediation tests with adsorptive materials." *Environmental Science and Technology*, (607), 4386–4391.

McLean, J. E., Pabst, M. W., Miller, C. D., Dimkpa, C. O., and Anderson, A. J. (2013). "Effect of complexing ligands on the surface adsorption, internalization, and bioresponse of copper and cadmium in a soil bacterium, *Pseudomonas putida*." *Chemosphere*, 91(3), 374–382.

Mench, M., Morel, J. L., and Guckert, A. (1987). "Metal binding properties of high molecular weight soluble exudates from maize (Zea mays L.) roots." *Biology and Fertility of Soils*, 3(3), 165–169.

Michaud, A. M., Bravin, M. N., Galleguillos, M., and Hinsinger, P. (2007). "Copper uptake and phytotoxicity as assessed in situ for durum wheat (Triticum turgidum durum L.) cultivated in Cu-contaminated, former vineyard soils." *Plant and Soil*, 298(1–2), 99–111.

Michaud, A. M., Chappellaz, C., and Hinsinger, P. (2008). "Copper phytotoxicity affects root elongation and iron nutrition in durum wheat (*Triticum turgidum durum L.*)." *Plant and Soil*, 310(1–2), 151–165.

Misra, S. K., Dybowska, A., Berhanu, D., Luoma, S. N., and Valsami-jones, E. (2012). "The complexity of nanoparticle dissolution and its importance in

nanotoxicological studies." *Science of the Total Environment*, 438, 225–232.

Mudunkotuwa, I. a., Pettibone, J. M., and Grassian, V. H. (2012). "Environmental implications of nanoparticle aging in the processing and fate of copper-based nanomaterials." *Environmental Science and Technology*, 46(13), 7001–7010.

Murakami, T., Ise, K., Hayakawa, M., Kamei, S., and Takagi, S. (1989). "Stabilities of metal complexes of mugineic acids and their specific affinities for iron(III)." *Chemistry Letters*, (12), 2137–2140.

Murphy, A., and Taiz, L. (1997). "Correlation between potassium efflux and copper sensitivity in 10 Arabidopsis ecotypes." *New Phytologist*, 136(2), 211–222.

Nair, P. M. G., and Chung, I. M. (2015a). "Biochemical, anatomical and molecular level changes in cucumber (Cucumis sativus) seedlings exposed to copper oxide nanoparticles." *Biologia*, 70(12), 1575–1585.

Nair, P. M. G., and Chung, I. M. (2015b). "Study on the correlation between copper oxide nanoparticles induced growth suppression and enhanced lignification in Indian mustard (Brassica juncea L.)." *Ecotoxicology and Environmental Safety*, 113, 302–13.

Navarro, E., Baun, A., Behra, R., Hartmann, N. B., Filser, J., Miao, A.-J., Quigg, A., Santschi, P. H., and Sigg, L. (2008). "Environmental behavior and ecotoxicity of engineered nanoparticles to algae, plants, and fungi." *Ecotoxicology*, 17(5), 372–86.

Neumann, G., and Römheld, V. (2012). *Marschner's Mineral Nutrition of Higher Plants*. *Marschner's Mineral Nutrition of Higher Plants*, Elsevier.

Nezhad, S. S., Khorasgani, M. R., Emtiazi, G., Yaghoobi, M. M., and Shakeri, S. (2014). "Isolation of copper oxide (CuO) nanoparticles resistant Pseudomonas strains from soil and investigation on possible mechanism for resistance." *World Journal of Microbiology and Biotechnology*, 30(3), 809–17.

Nian, H., Yang, Z. M., Ahn, S. J., Cheng, Z. J., and Matsumoto, H. (2002). "A comparative study on the aluminium- and copper-induced organic acid exudation from wheat roots." *Physiologia Plantarum*, 116(3), 328–335.

Oburger, E., Gruber, B., Schindlegger, Y., Schenkeveld, W. D. C., Hann, S., Kraemer, S. M., Wenzel, W. W., and Puschenreiter, M. (2014). "Root exudation of phytosiderophores from soil-grown wheat." *The New phytologist*, 203(4), 1161–74.

Odzak, N., Kistler, D., Behra, R., and Sigg, L. (2014). "Dissolution of metal and metal oxide nanoparticles in aqueous media." *Environmental Pollution*, 191, 132–8.

Odzak, N., Kistler, D., Behra, R., and Sigg, L. (2015). "Dissolution of metal and metal oxide nanoparticles under natural freshwater conditions." *Environmental Chemistry*, 12(2), 138.

Otero-González, L., Field, J. A., and Sierra-Alvarez, R. (2014). "Inhibition of anaerobic wastewater treatment after long-term exposure to low levels of CuO nanoparticles." *Water Research*, 58, 160–8.

Pallagi, A., Bajnoczi, E., Canton, S. E., Bolin, T., Peintler, G., Kutus, B., Kele, Z., Palinko, I., and Sipos, P. (2014). "Multinuclear complex formation between Ca(II) and gluconate ions in hyperalkaline solutions." *Environmental Science and Technology*, 48(12), 6604–6611.

Pallagi, A., Sebk, P., Forg, P., Jakusch, T., Palinko, I., and Sipos, P. (2010). "Multinuclear NMR and molecular modelling investigations on the structure and equilibria of complexes that form in aqueous solutions of Ca2+ and gluconate." *Carbohydrate Research*, 345(13), 1856–1864.

Paquin, P. R., Santore, R. C., Wu, K. B., Kavvadas, C. D., and Di Toro, D. M. (2000). "The biotic ligand model: a model of the acute toxicity of metals to aquatic life." *Environmental Science and Policy*, 3, 175–182.

Parker, D. R., Norvell, W. A., and Chaney, R. L. (1995). "Chemical Equilibrium and Reaction Models." *Chemical Equilibrium and Reaction Models*, SSSA Special Publication, Madison WI., 253–269.

Parker, D. R., Pedler, J. F., Ahnstrom, Z. A. S., and Resketo, M. (2001). "Reevaluating the free-ion activity model of trace metal toxicity toward higher plants: Experimental evidence with copper and zinc." *Environmental Toxicology and Chemistry*, 20(4), 899–906.

Peng, C., Zhang, H., Fang, H., Xu, C., Huang, H., Wang, Y., Sun, L., Yuan, X., Chen, Y., and Shi, J. (2015). "Natural organic matter-induced alleviation of the phytotoxicity to rice (Oryza sativa L.) caused by copper oxide nanoparticles." *Environmental Toxicology and Chemistry*, 34(9), 1996–2003.

Rachou, J., Gagnon, C., and Sauvé, S. (2007). "Use of an ion-selective electrode for free copper measurements in low salinity and low ionic strength matrices." *Environmental Chemistry*, 4, 90–97.

R Core Team. (2013). "R: A Language and Environment for Statistical Computing." R Foundation for Statistical Computing, Vienna, Austria.

Reed, S., and Martens, D. (1996). *Methods of Soil Analysis Part 3—Chemical Methods*. *Methods of Soil Analysis Part 3—Chemical Methods*, SSSA Book Series, Soil Science Society of America, American Society of Agronomy.

Reichard, P. U., Kraemer, S. M., Frazier, S. W., and Kretzschmar, R. (2005). "Goethite Dissolution in the Presence of Phytosiderophores: Rates, Mechanisms, and the Synergistic Effect of Oxalate." *Plant and Soil*, 276(1–2), 115–132.

Reichman, S. M., and Parker, D. R. (2007). "Probing the effects of light and temperature on diurnal rhythms of phytosiderophore release in wheat." *The New Phytologist*, 174(1), 101–8.

Rivera-Gil, P., Jimenez de Aberasturi, D., Wulf, V., Pelaz, B., del Pino, P., Zhao, Y., de la Fuente, J. M., Ruiz de Larramendi, I., Rojo, T., Liang, X.-J., and Parak, W. J. (2013). "The challenge to relate the physicochemical properties of colloidal nanoparticles to their cytotoxicity." *Accounts of Chemical Research*, 46(3), 743–9.

Rivera Gil, P., Oberdörster, G., Elder, A., Puntes, V., and Parak, W. J. (2010). "Correlating physico-chemical with toxicological properties of nanoparticles: the present and the future." *ACS Nano*, 4(10), 5527–31.

Roos, J. T. H., and Williams, D. R. (1977). "Formation constants for citrate-, folic acid-, gluconate- and succinate-proton, -manganese(II), and -zinc(II) systems: relevance to absorption of dietary manganese, zinc and iron." *Journal of Inorganic and Nuclear Chemistry*, 39(2), 367–369.

Rousk, J., Ackermann, K., Curling, S. F., and Jones, D. L. (2012). "Comparative toxicity of nanoparticulate CuO and ZnO to soil bacterial communities." *PloS one*, 7(3), e34197.

Rouwenhorst, R. J., Frank Jzn, J., Scheffers, W. A., and van Dijken, J. P. (1991). "Determination of protein concentration by total organic carbon analysis." *Journal of Biochemical and Biophysical Methods*, 22(2), 119–128.

Ryan, B. M., Kirby, J. K., Degryse, F., Harris, H., Mclaughlin, M. J., and Scheiderich, K. (2013). "Copper speciation and isotopic fractionation in plants: Uptake and translocation mechanisms." *New Phytologist*, 199(2), 367–378.

Sauve, S., Hendershot, W., and Allen, H. E. (2000). "Solid-Solution Partitioning of Metals in Contaminated Soils: Dependence on pH, Total Metal Burden, and Organic Matter." *Environmental Science and Technology*, 34(7).

Saxton, K. E., and Rawls, W. J. (2006). "Soil Water Characteristic Estimates by Texture and Organic Matter for Hydrologic Solutions." *Soil Science Society of America Journal*, 70(5), 1569.

Schenkeveld, W. D. C., Oburger, E., Gruber, B., Schindlegger, Y., Hann, S., Puschenreiter, M., and Kraemer, S. M. (2014). "Metal mobilization from soils by phytosiderophores - experiment and equilibrium modeling." *Plant and Soil*, 383(1–2), 59–71.

Schindlegger, Y., Oburger, E., Gruber, B., Schenkeveld, W. D. C., Kraemer, S. M., Puschenreiter, M., Koellensperger, G., and Hann, S. (2014). "Accurate LC-ESI-MS/MS quantification of 2'-deoxymugineic acid in soil and root related samples employing porous graphitic carbon as stationary phase and a $^{13}C_4$-labeled internal standard." *Electrophoresis*, 35(9), 1375–85.

Schubert, J., and Lindenbaum, A. (1952). "Stability of Alkaline Earth—Organic Acid Complexes Measured by Ion Exchange." *Journal of the American Chemical Society*, 74, 3529–3532.

Servin, A., Elmer, W., Mukherjee, A., De la Torre-Roche, R., Hamdi, H., White, J. C., Bindraban, P., and Dimkpa, C. (2015). "A review of the use of engineered nanomaterials to suppress plant disease and enhance crop yield." *Journal of Nanoparticle Research*.

Shi, J., Abid, A. D., Kennedy, I. M., Hristova, K. R., and Silk, W. K. (2011). "To duckweeds (Landoltia punctata), nanoparticulate copper oxide is more inhibitory than the soluble copper in the bulk solution." *Environmental Pollution*, 159(5), 1277–82.

Sinhal, V. K., Srivastava, A., and Singh, V. P. (2010). "EDTA and citric acid mediated phytoextraction of Zn, Cu, Pb and Cd through marigold (Tagetes erecta)." *Journal of Environmental Biology*, 31(3), 255–9.

Sousa, V. S., and Teixeira, M. R. (2013). "Aggregation kinetics and surface charge of CuO nanoparticles: the influence of pH, ionic strength and humic acids." *Environmental Chemistry*, 10(4), 313.

Stampoulis, D., Sinha, S. K., and White, J. C. (2009). "Assay-dependent phytotoxicity of nanoparticles to plants." *Environmental Science and Technology*, 43(24), 9473–9.

Studer, A. M., Limbach, L. K., Van Duc, L., Krumeich, F., Athanassiou, E. K., Gerber, L. C., Moch, H., and Stark, W. J. (2010). "Nanoparticle cytotoxicity depends on intracellular solubility: comparison of stabilized copper metal and degradable copper oxide nanoparticles." *Toxicology Letters*, 197(3), 169–74.

Terzano, R., Cesco, S., and Mimmo, T. (2015). "Dynamics, thermodynamics and kinetics of exudates: crucial issues in understanding rhizosphere processes." *Plant and Soil*, 386(1–2), 399–406.

Thakali, S., Allen, H. E., Di Toro, D. M., Ponizovsky, A. A., Rooney, C. P., Zhao, F.-J., and McGrath, S. P. (2006). "A Terrestrial Biotic Ligand Model. 1. Development and Application to Cu and Ni Toxicities to Barley Root Elongation in Soils." *Environmental Science and Technology*, 40(22), 7085–7093.

Thakkar, K. N., Mhatre, S. S., and Parikh, R. Y. (2010). "Biological synthesis of metallic nanoparticles." *Nanomedicine : Nanotechnology, Biology, and Medicine*, 6(2), 257–62.

Treeby, M., Marschner, H., and Römheld, V. (1989). "Mobilization of iron and other micronutrient cations from a calcareous soil by plant-borne, microbial, and synthetic metal chelators." *Plant and Soil*, 114(2), 217–226.

Trujillo-Reyes, J., Majumdar, S., Botez, C. E., Peralta-Videa, J. R., and Gardea-Torresdey, J. L. (2014). "Exposure studies of core-shell Fe/Fe(3)O(4) and Cu/CuO NPs to lettuce (Lactuca sativa) plants: Are they a potential physiological and nutritional hazard?" *Journal of Hazardous Materials*, 267, 255–63.

Tsednee, M., Mak, Y.-W., Chen, Y.-R., and Yeh, K.-C. (2012). "A sensitive LC-ESI-Q-TOF-MS method reveals novel phytosiderophores and phytosiderophore-iron complexes in barley." *The New Phytologist*, 195(4), 951–61.

USEPA. (1979). "'Methods for Chemical Analysis of Water and Wastes.'" *EPA 600 Series*, Washington, D.C., D.C., EPA 600 Se(USEPA-600), 4-79–20.

USEPA. (1996). *Test Methods for Evaluating Solid Waste. Method 3050B-1. Acid Digestion of Sediments, Sludges, and Soils. Revision 2. EPA/SW-846.*, National Technical Information Service, Springfield, Va.

Wang, L.-F., Habibul, N., He, D.-Q., Li, W.-W., Zhang, X., Jiang, H., and Yu, H.-Q. (2015). "Copper release from copper nanoparticles in the presence of natural organic matter." *Water Research*, 68, 12–23.

Wang, S., Nan, Z., Liu, X., Li, Y., Qin, S., and Ding, H. (2009). "Accumulation and bioavailability of copper and nickel in wheat plants grown in contaminated soils from the oasis, northwest China." *Geoderma*, 152(3–4), 290–295.

Wang, Z., Von Dem Bussche, A., Kabadi, P. K., Kane, A. B., and Hurt, R. H. (2013). "Biological and environmental transformations of copper-based nanomaterials." *ACS Nano*, 7(10), 8715–8727.

Wang, Z., Xie, X., Zhao, J., Liu, X., Feng, W., White, J. C., and Xing, B. (2012). "Xylem- and phloem-based transport of CuO nanoparticles in maize (Zea mays L.)." *Environmental Science and Technology*, 46(8), 4434–41.

Watson, J.-L., Fang, T., Dimkpa, C. O., Britt, D. W., McLean, J. E., Jacobson, A., and Anderson, A. J. (2014). "The phytotoxicity of ZnO nanoparticles on wheat varies with soil properties." *Biometals*, 28(1), 101–112.

White, P. J., and Broadley, M. R. (2009). "Biofortification of crops with seven mineral elements often lacking in human diets--iron, zinc, copper, calcium, magnesium, selenium and iodine." *The New Phytologist*, 182(1), 49–84.

von Wiren, N. (2000). "Hydroxylated Phytosiderophore Species Possess an Enhanced Chelate Stability and Affinity for Iron(III)." *Plant Physiology*, 124(3), 1149–1158.

Von Wiren, N., Romheld, V., Morel, J., Guckert, A., and Marchner, H. (1993). "Influence of microorganisms on iron acquisition in maize." *Soil Biology and Biochemistry*, 25(3), 371–376.

Wu, S. G., Kong, I.-C., Tang, Y. J., Huang, L., J, H., DR, C., and IC, K. (2012). "Phytotoxicity of Metal Oxide Nanoparticles is Related to Both Dissolved Metals Ions and Adsorption of Particles on Seed Surfaces." *Journal of Petroleum and Environmental Biotechnology*, 3(126).

Xu, M., Li, J., Iwai, H., Mei, Q., Fujita, D., Su, H., Chen, H., and Hanagata, N. (2012). "Formation of nano-bio-complex as nanomaterials dispersed in a biological solution for understanding nanobiological interactions." *Nature*, 2, 406.

Xuan, Y., Scheuermann, E. B., Meda, A. R., Hayen, H., von Wirén, N., and Weber, G. (2006). "Separation and identification of phytosiderophores and their metal complexes in plants by zwitterionic hydrophilic interaction liquid chromatography coupled to electrospray ionization mass spectrometry." *Journal of Chromatography A*, 1136(1), 73–81.

Zuverza-Mena, N., Medina-Velo, I. A., Barrios, A. C., Tan, W., Peralta-Videa, J. R., and Gardea-Torresdey, J. L. (2015). "Copper nanoparticles/compounds impact agronomic and physiological parameters in cilantro (Coriandrum sativum)." *Environmental Science*, 17(10), 1783–93.

CHAPTER 3

RHIZOSPHERE INTERACTIONS BETWEEN COPPER OXIDE NANOPARTICLES AND WHEAT ROOT EXUDATES IN A SAND MATRIX; INFLUENCES ON BIOAVAILABILITY AND UPTAKE

Abstract

Copper oxide nanoparticles (CuO NPs) are used in an expanding range of industries including a potential for agricultural application as a fertilizer or as a fungicide. Accidental spills or misapplication of CuO NPs may lead to soil contamination. This work was directed towards understanding which exudates from wheat roots force increased solubility of CuO NPs, and to determine whether this solubility is related to increased plant uptake. Additionally, we determined if the level of NPs in the growth matrix has a feedback regarding composition and quantity of exudates.

Bread wheat (*Triticum aestivum* cv Deloris) was grown for 10 days in sand with the addition of 0 to 300 mg Cu/kg sand as CuO NPs. The plants responded to increased nanoparticle doses via a dose-dependent increase in root exudation, and a corresponding increased dissolution of Cu from the NPs at higher NP doses, despite recurrence of higher pH.

Toxicity to the wheat plant resulting in reduced root elongation was likely due to a combination of CuO NPs, and dissolved Cu complexes, since Cu^{2+} measured by an ion selective electrode was < 5 μg/L, and not clearly related to CuO NP dose.

The majority of Cu was by a wheat phytosiderophore deoxymugineic acid (DMA) and citrate, with DMA dominant at higher CuO NP doses, predicted by M'INTEQ.

Increased uptake of Cu as well as reduced levels of Ca, Mg, Mn, K and Fe in shoots was found at CuO NP levels of 100 mg Cu/kg sand and above, and correlated with geochemical modeling predictions of increased CuDMA formation. The increased presence of CuO NPs interfered with Fe nutrition particularly due to increased formation of CuDMA over FeDMA.

Keywords
Copper oxide nanoparticles, copper toxicity, root exudates, wheat, complexation, deoxymugineic acid

1. Introduction

Copper oxide nanoparticles (CuO NPs) are a potential environmental contaminant. CuO NPs have industrial applications in sensors, catalysts, solar energy conversion, electronic printing, surfactants and antimicrobials (Ahamed and Alhadlaq 2014; Bondarenko et al. 2012; Wang et al. 2013). However, CuO NPs are infrequently studied in an environmental context (Gardea-Torresdey et al. 2014), such as impacts of CuO NPs on soil biota. CuO NPs are bacteriostatic to soil microbes (Gajjar et al. 2009) and phytotoxic in hydroponics (Trujillo-Reyes et al. 2014; Wang et al. 2012) and in a sand matrix (Dimkpa et al. 2012, 2013, 2015). CuO NPs may be intentionally applied as fertilizers or fungicides, or incidentally contaminate soils via waste streams and biosolids application (Lee et al. 2010; Rivera Gil et al. 2010). This

necessitates an increased understanding of their mechanisms of toxicity in an agricultural context.

Copper ions have significance as an essential micronutrient for plant growth, but at elevated levels Cu becomes toxic (Marschner 1995; Michaud et al. 2007, 2008). Plants have developed various mechanisms for maintaining homeostasis of Cu by regulating Cu uptake, including production of root exudates to increase or decrease bioavailability of Cu. Specific metallochaperones move Cu internally, with sequestration as a non-harmful form. Specific efflux pumps remove Cu from the cells (Clemens et al. 2002). Toxicity occurs when these systems are overwhelmed. Uncertainty remains regarding whether CuO NPs inflict toxicity directly, or whether the toxicity is due to Cu released from the CuO NPs (Anjum et al. 2015 a; Atha et al. 2012; Shi et al. 2011; Stampoulis et al. 2009; Trujillo-Reyes et al. 2014).

The bioavailability of Cu is controlled by solution phase chemistry, particularly in the soil closest to the roots, the rhizosphere. pH and dissolved organic carbon (DOC) are most influential on Cu mobility and bioavailability (Michaud et al. 2007; Sauve et al. 2000). Cu can exist in solution as a free ion (Cu^{2+}) or complexed with inorganic or organic ligands. The presence of ligands, including plant and bacterial exudates, changes Cu mineral dissolution, desorption and bioavailability.

Specifically, wheat plants grown under Fe-deficient conditions up regulate production of the phytosiderophores deoxymugineic acid (DMA) that form strong Cu-complexes (Ma and Nomoto 1993, 1996; Xuan et al. 2006). Fe nutrition is affected in shoots of wheat grown in Cu contaminated soils (Michaud et al. 2008),

which we speculate may be due to phytosiderophore-Cu complexation limiting Fe uptake. Additionally, low molecular weight organic acids (LMWOAs) such as citrate and malate, can solubilize metals that are otherwise not bioavailable (Anjum et al. 2015 b; Dakora and Phillips 2002). Increased solubility through complexation can drive uptake into the plant or bacteria. For example, citrate, a bacterial and root exudate, complexes Cu and enhances uptake by a soil bacterium, *Pseudomonas putida* (McLean et al. 2013). Indeed, the root exudates, oxalate and citrate from *Belamcanda chinensis,* when applied to soil, increased Cu uptake in the grass, *Echinochloa crus-galli* (Kim et al. 2010). Amino acids leach high levels of Cu from CuO NPs, causing toxicity to the bacteria *E. coli* in culture solutions (Gunawan et al. 2011). Amino acids and polypeptides can sorb to CuO NPs with different affinities (Joshi et al. 2012). Competing stabilities between complexes make this system non-trivial (Callahan et al. 2006). Thus organic ligands play a crucial role in defining the rhizosphere and controlling Cu uptake, and the concentrations of these exudates may be driven by increased amounts of Cu (Nian et al. 2002). Of pertinence to a plant-NP system is the solution phase biogeochemistry, particularly the interplay between the NP dose and the exudation of organic carbon by the roots of wheat plant. Since such organic carbon will affect CuO NP aggregation-dissolution, the uptake of metal into the plant is influenced. Exudation of different ligands, which may vary with CuO NP dose, may have implications for metal uptake and homeostasis in the plant (Clemens 2001).

Solution properties will affect NP solubility, through chelation, and ligands can increase bioavailable Cu to plants as seen in hydroponic studies (Michaud et al.

2008; Parker et al. 2001; Ryan et al. 2013). However, hydroponic systems imply several shortcomings from a morphologic and geochemical perspective. Jones (1998) highlights that roots grown hydroponically are morphologically and physiologically different from those grown in solid systems, including the lack of root hairs, mechanical impedance and water stress. Conversely, wheat grown in a solid matrix allows CuO NPs to interact more realistically with quantities of ligands produced in rhizosphere processes (e.g., phytosiderophores are produced up to 10x higher in hydroponics compared to soil systems (Oburger et al. 2014)) and, thus, the NPs surface properties, rates of aggregation and dissolution to be investigated more realistically.

This study evaluates the interactions between root exudates of bread wheat (*Triticum aestivum*) and CuO NPs at sub-lethal levels in a sand matrix, along with a control without NPs. This interaction will model rhizosphere processes, and isolate plant-NP interactions (in the absence of microbes) to assess how plant exudates may defend against toxicity, or drive dissolution of the NP into Cu^{2+} ions and complexes, and affect Cu uptake by the wheat plant. The solution phase of this system was analyzed to better understand the CuO NP-wheat root exudate interplay. From this, the mechanisms of CuO NP toxicity were inferred, and the plant response and ability to manage metal homeostasis investigated at the end of the growth period.

2. Materials and methods

2.1 Characterization of NPs

CuO NPs obtained from Sigma-Aldrich (MO, USA) were characterized in deionized water and in sand for aggregation, shape evolution, dissolution, and surface charge (Dimkpa et al. 2012, 2013, 2015). In water the CuO NPs aggregated to an average diameter of 318 nm, while in planted sand the NPs had an average diameter of 317 nm. The CuO NPs contained Al (216 μg/g), Fe (814 μg/g), Mn (130 μg/g) and Zn (153 μg/g). In sand, the zeta potential of particles in suspension was reduced from -27 mV to -18 mV when plants were present.

2.2 Plant growth conditions

White silica sand (UNIMIN Corp., ID, US) was washed by deionized water (DI) three times, and heated overnight in a 550° muffle furnace to remove organic matter. After washing in DI again, sand was oven dried at 150°. Some soluble organic matter remained despite the muffle furnace treatment (1.5 mg/L each of formate, acetate and gluconate reducing background DOC to < 5mg/L in a 2:1 water:sand extraction with 10 g sand).

Nitric acid digestion of the sand showed small amounts of Al, Fe and very little Cu, though much of this was not water-soluble (Table 3-1.) Diethylene triamine pentaacetic acid (DTPA)-ammonium bicarbonate extraction (ABC) (Reed and Martens 1996) was performed to assess plant available metals in the sand. DTPA-ABC is a standard test to define nutrient requirements for various crops,

including wheat. The sand is deficient in Fe, Zn, Mn and Cu for plant growth (Table 3-1.

Table 3-1. DTPA and nitric acid digestion of muffle furnace treated sand (mg metal/kg dry sand). Water-soluble metals were obtained by shaking 20 g dry sand in 40 mL deionized water for 24 hours.

mg metal /kg dry sand	Al	Fe	Zn	Mn	Cu
Water-soluble (2:1 DI:sand)	5.4	1.4	0.01	0.08	0.01
Nitric acid digestion (EPA Method 3050)	746	347	2.2	3.6	0.4
DTPA-ABC extraction	2.6	2.8	0.1	0.03	0.3
Nutrient requirement considered low for generalized fertility (DTPA extractable) (James and Topper 2010)	NA	<3	<1	<1	<0.2

The experiment was a randomized block design with studies being blocked on time, due to limitations on handling the number of pots at harvesting and analytical support. Each study was repeated three times, with triplicate replications within each study time. The studies were replicated completely, as opposed to one CuO NP dose each time, to avoid biological and procedural bias. The first two experimental replicate sets were identical in design and analysis. The third experimental replicate included two additional doses of CuO NPs (10 and 200 mg/kg) and additional NP separation methods.

Within each study, CuO NPs were added to the sand at doses of 0, 30, 100, 300 mg Cu/kg and shaken for 30 minutes in acid-washed 1,000 ml Nalgene bottles to homogenize the samples. The sand/NP samples were then autoclaved, and distributed into the Magenta boxes (21 x 7 x 7 cm, Sigma Aldrich MO USA) used for

planting. A $Ca(NO_3)_2$ filter sterilized solution (0.7mM) was amended to the sand in the Magenta boxes for background ionic strength and Ca for seed germination and root growth. The higher NP doses are sub-lethal (Dimkpa et al. 2012), but cause a significant decrease in root length (Dimkpa et al. 2012) and oxidative stress (Dimkpa et al. 2012).

Initially 300 g of sand was used for plant growth at all concentrations of CuO NPs. With the lower doses, the roots extended throughout the boxes, but at the higher dosing, the roots penetrated only the top 2 cm of the sand. To ensure the roots were fully distributed throughout the sand for all treatments (all the sand and CuP NPs are rhizosphere influenced), the mass of sand was reduced proportionally (Table 3-2.). The 0.7 mM $Ca(NO_3)_2$ solution was added to the sand at 1.5 times field capacity. Field capacity of the sand was determined by allowing the saturated sand to freely drain overnight and the results were as reported by Saxton and Rawls (2006) for sand. Experimental set-up is summarized in Table 3-2. Additional CuO NP doses at 10 and 200 (in triplicate) were added to the final study to assess Cu solubility at 6 levels for correlations and plant response purposes.

Seeds were surface sterilized with 3% NaOCl (Clorox, CA, USA) and pre-germinated on Luria Bertani (LB) media plates for 4 days, to assess microbial sterility. 25 seedlings (on plates free from microbial growth) per Magenta box were then transferred to the treated sand. Plants were grown for 10 days under fluorescent lights (28 °C, 16 hours light, 8 hours dark, generating a photosynthetic photon flux density of 144 pmol m^{-2} s^{-1} at the box surface) in conditions previously described (Dimkpa et al. 2012, 2013). All boxes were placed under the light so that

the level of the sand was the same for all treatments and rotated daily, minimizing photo effects on the shoots. Equivalent treatments without plants were included as controls.

Table 3-2. Experimental conditions – within each experiment treatments were replicated 3 times (9 Magenta boxes per treatment). Unplanted treatments were prepared to control for dissolution of CuO NPs in the calcium nitrate solution. Treatments with * were only evaluated in experiment 3.

CuO NPs (mg Cu/ kg dry sand)	Sand (g)	0.7 mM $Ca(NO_3)_2$ solution (mL) Initial	0.7 mM $Ca(NO_3)_2$ solution (mL) Flush	Replication (Magenta boxes)
0	300	45	45	9
10	220	33	33	3*
30	160	24	24	9
100	110	16.5	16.5	9
200	90	13.5	13.5	3*
300	70	10.5	15.5	9

2.3 Analysis of plant tissues and sand after harvesting

After growth, 0.7 mM $Ca(NO_3)_2$ solution was added to flush exudates from roots. This process was started 3 h after the start of the photoperiod for maximum phytosiderophore exudation (Oburger et al. 2014). The volume used for each treatment was equivalent to the volume added before plant growth, apart from the 300 mg Cu/kg dose (Table 3-2). Addition of this solution was necessary to provide adequate volume for analyses. The solution was equilibrated with the sand in the presence of the plants for 15 minutes. Plants were then removed from the sand, measured for longest root and shoot, and roots washed thoroughly with deionized water. Shoots were cut above the coleoptile, since our observations indicate that

CuO NPs are bound to this tissue, distorting uptake results. Tissue was dried overnight at 60 °C, digested using nitric acid (Jones and Case 1990) and analyzed for Cu, Fe, Mn, Ca, Mg and K by inductively coupled plasma mass spectroscopy (ICPMS) (Agilent 7700x) (EPA method 6030). The sand was digested using nitric acid and hydrogen peroxide (USEPA 1996 method 3050) with analyses for trace elements and major cations by ICPMS.

2.4 Analysis of water extraction

Solution was removed from sand by pouring the contents of the boxes into autoclaved 100 mm diameter long stem glass funnels stopped with glass wool place onto vacuum flasks. Extraction of the liquid from the sand was aided with application of a vacuum. The collected solution was then filtered through a 0.2-µm nylon filter (Environmental Express Charleston SC) for sterility.

Metals were determined in the filtered solution by ICPMS after centrifugation to remove nanoparticles greater than 10 nm by (Eppendorf centrifuge 8504, Eppendorf rotor F45-30-11). Samples were centrifuged at 14,000 x *g* for 14 minutes (Dimkpa et al. 2012, 2013). Based on Stokes Einstein equation, this procedure will remove CuO particles greater than 10 nm ($Cu_{<10}$), as confirmed by dynamic light scattering (DLS, DynaPro NanoStar, Wyatt Technology Corporation, Santa Barbara, CA) to remove all (Cu and otherwise) particles above the 10 nm (personal communication with Josh Hortin 2016). In water quality analysis dissolved has been traditional defined by filtration with 0.45 µm or more recently 0.2 µm. These

filtration methods however are not adequate with NPs, since the filters will not remove nano-sized material that would be inappropriate defined as dissolved.

pH (Accumet Excel XL25, Fisher Scientific) was determined on the 0.2 µm filtered solution by standard methods (Method 4500, APHA 2014). Dissolved organic carbon (DOC) was determined in this filtered solution by combustion with IR detection TOC analyzer (Apollo 9000, Teledyne Tekmar, Method 5310 B (APHA 2014)). Amino acids were also determined from the 0.2 µm filtered solution by HPLC (Aquity, MA, USA) (Creager et al. 2010). Ion chromatography using a Dionex ICS-3000 equipped with a Dionex IonPac AS11-HC analytical column and guard column and a Dionex ASRS-ULTRA Anion Self-Regenerating Suppressor (Dionex Corp., Sunnyvale, CA) determined low molecular weight organic acids and nitrate. For total sugars, a sulfuric acid method with a glucose standard was used, with quantification using a Genesys 6 UV-Visible Spectrophotometer (Thermo Scientific, Madison WI) at 315 nm as per Albalasmeh et al. (2013). Protein concentration was resolved via BCA Protein Assay kit (Thermo scientific, Rockford, IL) under the 5 - 250 µg/mL method, measured by the UV Vis spectrometer at 576 nm. Acetone precipitation was used to minimize interferences.

The phytosiderophore, 2' deoxymugeinic acid (DMA), was determined after the 3 kDa microcentrifuged filtrate (discussed further in section 2.5) (Millipore, MA, USA) (2700 x *g* for 30 min). DMA was quantified against a certified standard (Toronto Research Chemical, Toronto, Canada) by liquid chromatography triple quadrupole MS (LC-QqQ-MS) (Agilent 1290 ultra HPLC 6490) with zwitterionic column (150 mm x 1.0 mm I.D.) and guard column (14 mm x 1.0 mm I.D.) from

SeQuant (Umea, Sweden)). The LC-QqQ-MS was operated using multiple reaction monitoring and the mobile phase was 0.1% formic acid, similar to the method described by Schindlegger et al. (2014). The 3 kDa microcentrifuged filtrate was analyzed since the <10 nm fraction led to carry over of Cu during analysis. The samples were acidified to replace Cu or Fe from the molecule for analysis of total DMA.

2.5 Metal uptake into the wheat plant, against metal and DOC size distribution

To evaluate metal speciation in more detail, metals (M) were size differentiated by two methods, microcentrifugation and 3kDA ultra filtration in Experiment 3. The microcentrifugation, described above, removed particles greater than 10 nm ($M_{<10}$). This supernatant includes nanoparticles <10 nm, complexed metals and free metal ions. The 3-kDa ultrafiltration removed all particles above 1 nm ($M_{<1}$). This filtrate includes metal complexes less than 3 kDa, and free metals (Table **3**-**3**.). Specifically, the 0.2 µm filtered solution was also centrifuged using a 3 kDa spin filters (Millipore, MA, USA) (2700 x *g* for 30 min) calculated to remove CuO NPs above 1 nm ($Cu_{<1}$). Size partitioning was confirmed by DLS to remove all particles > 1 nm. All of the above particles would normally be classified as "dissolved" (being less than 0.45-µm in environmental science) but in the context of nano toxicology, further distinctions are important, since the size of particle has implications for bioavailability and toxicity (Mudunkotuwa et al. 2012).

Free Cu^{2+} activity was measured using a Cu ion selective electrode (Orion 96-29 ionplus) following the procedures described by Rachou et al. (2007) for solutions

with low ionic strength and DOC. DOC was also determined on the microcentrifuged sample defining < 10 nm fraction ($DOC_{<10}$), and in the filtrate of the 3-kDa spin filter ($DOC_{<1}$).

Using $M_{<1}$ and ligand concentrations from Experiment 3 (Table 3-5), MINTEQ (Gustafsson 2014) geochemical modeling was employed to assess Cu-speciation in more detail, as well as CuO dissolution into the solution.

Electrical conductivity (EC) (Accumet model 30 conductivity meter) was determined on the solution after 0.2 µm nylon filter (Environmental Express Charleston SC) and analyzed by standard methods (Method 2510 APHA 2014).

Table 3-3. Nomenclature relating Cu and other metals (M) and DOC size fractions, analytical techniques and symbols.

Symbol	**Technique**	**Size fractions**	**Includes**
Cu_{aq}	0.2 µm filter	Removes > 0.2 µm particles	M-complexes, free ions, small sized precipitates/nano aggregates and colloids
$Cu_{<10}$, $M_{<10}$, $DOC_{<10}$	Microcentrifuge	Removes particles > 10 nm	M-complexes, free ions, small nano particles
$Cu_{<1}$, $M_{<1}$, $DOC_{<1}$	3 kDa spin filter, centrifugation	Removes particles > 1 nm	Complexes, free ions
Cu^{2+}	Cu ion selective electrode		Free Cu^{2+} ions only (no complexes)

3. Data analysis and statistics

In order to have the rooting system distributed throughout the sand for each dosing of NPs, the volume of sand used, 0.7 mM $Ca(NO_3)_2$ solution applied and the

0.7 mM $Ca(NO_3)_2$ solution used for extraction was varied for each treatment (Table 3-2.). Water loss during growth was assessed in a separate experiment, with identical conditions as above. After 10 days of growth plants were removed carefully, the remaining sand was mixed thoroughly then triplicate samples from each magenta box were taken and dried (60°C). The percentage moisture ((wet – dry)/dry) was used to assess how much water remained in the sand. The same was done for unplanted replicates. Since each treatment used a different volume of $Ca(NO_3)_2$ for planting and extraction and the treatment affected water loss, volumes were normalized to the volume of water in the sand after harvesting. This factor was applied to all concentrations (metals and ligands) to account for dilution by extraction volume.

3.1 Statistical Analysis

JMP 8 (SAS Institute, Inc. 5.01) was used for one-way Analysis of Variance (ANOVA) blocked on three experiments repeated over time and Tukey's Honestly Significant Difference (HSD) to compare significant responses from different nanoparticle doses. Transformations (log) were performed to satisfy constant variance and normality when required. Power of the test was also calculated at >75% power with n=9. Data below method detection limit (<MDL) were determined by a log-normal distribution of above MDL data, and assigned a value randomly based on an extrapolation of that log-normal distribution (Cohen 1959). Pearson's correlation coefficients (R) were also generated to assess relationships between variables.

Geochemical modeling

Cu complexes were modeled using MINTEQ (Gustafsson 2014) in the rhizosphere using data from Experiment 3 (n=3). Model inputs included ligands determined from chromatography, soluble metals ICPMS from spin filters ($M_{<1}$) (Table 3-8) and pH. Stability constants for DMA (Murakami et al. 1989), gluconate (Bechtold et al. 2002; Gajda et al. 1998) and amino acids from GEOCHEM (Parker et al. 1995) were added to the model's database (Supporting information Table 3-7). The model was run with precipitation allowed (indicating equilibrium). CuO NPs were modeled with a finite solid phase of crystalline tenorite, calculated as total mass of CuO NPs added initially to the Magenta boxes per volume of solution at the end of the growth period (Supporting information Table 3-8). From X-ray diffraction analysis, CuO NP were best described as crystalline (personal communication with Josh Horton.)

3.2 Quality Control

Solution and one root from each box were plated on LB media to assess microbial contamination after the growth period. Overall 75% of plant roots and solution plated onto LB showed no culturable bacterial or fungal infection after 5 days of plating. After 10 days presumed dormant bacterial endophytes were evident in some root samples.

All treatments were replicated in triplicate within each experimental set-up. For NP dosing at 0, 30, 100, and 300 mg Cu/kg the experimental set-up was

repeated three times over a three-month period to account for biological variability (triplicate within experiment x three experimental set-ups, n = 3 x 3 = 9). For NP 10 and 200 mg Cu/kg the experimental set-up was performed once with each treatment in triplicate in Experiment 3 (n=3). This was done for both planted and unplanted Magenta boxes. Plants without NP addition were a control on plant concentration of Cu due to distribution from the seed. Unplanted controls were used to show CuO dissolution in 0.7 mM $Ca(NO_3)_2$ matrix, and to ensure DOC was derived from biological exudates.

EPA QC protocols for ensuring accuracy and precision were followed for all analyses, including the use of blanks, calibration check samples, replicate analyses and matrix spike samples. Mass balance on Cu was performed on Cu distributed in solution, sand, and plant tissue. Mass recovery for Cu was between 40 - 60%, with 10% being lost to process of application, and some to 0.2-µm filtration**.** The process of CuO NP application was confirmed successful by dry application and 100% recovery of Cu into sand. The process of recovery from wet sand was investigated step by step, and was not found to be problematic in terms of Cu recovery. Its possible losses of Cu occurred sporadically throughout the process culminating in larger losses.

4. Results and discussion

4.1 Rhizosphere solution characterization and geochemical modeling

Size differentiation of Cu particles was evident at all NP doses (Fig. 3-1) in the rhizosphere solution, with only 57% Cu being truly dissolved, passing through the 3 kDa (1 nm) filter, the remaining Cu associated with colloidal material or NPs with sizes between 1 and 10 nm. Over 60% of the Fe and Al were associated with the larger size fraction (Fig. 3-1) (Full data set SI Fig. 3-7). $Fe_{<1}$ in solution was unaffected by CuO NP dose (average 324 ± standard deviation 187 µg/L) whereas for $Al_{<1}$, CuO NP doses 100 - 300 mg Cu/kg sand were not significantly different (2770 ± 876 µg/L), but distinct to CuO NP doses 0 to 100 mg Cu/kg sand (1080 ± 607 µg/L) (Tukey's HSD $\alpha = 0.05$) (SI Table 3-8).

Ca, Mg, K and Na (SI Table 3-10) showed no significant difference between microcentrifuged ($M_{<10}$) samples and respective 3-kDa-filtered sample ($M_{<1}$), implying these metals did not precipitate, nor sorb to sand or CuO particles.

In the dissolved organic carbon fractions, DOC_{aq} (0.2 µm) and $DOC_{<10}$ (below 10 nm) were not statistically different from $DOC_{<1}$ (below 1 nm fraction) (ANOVA, α=0.05); all DOC was below 1nm, or 3 kDa (Fig. 3-7). That is, > 3kDa DOC such as proteins, border cells and large polysaccharides such as polygalacturonic acid contributed negligibly to carbon exudation (Dakora and Phillips 2002; Mench et al. 1987; Neumann and Römheld 2012). This shows that the difference between $Cu_{<1}$ and $Cu_{<10}$ were not associations with organic colloids, and therefore must be fine sand grains, NPs, or inorganic colloids containing Al and Fe.

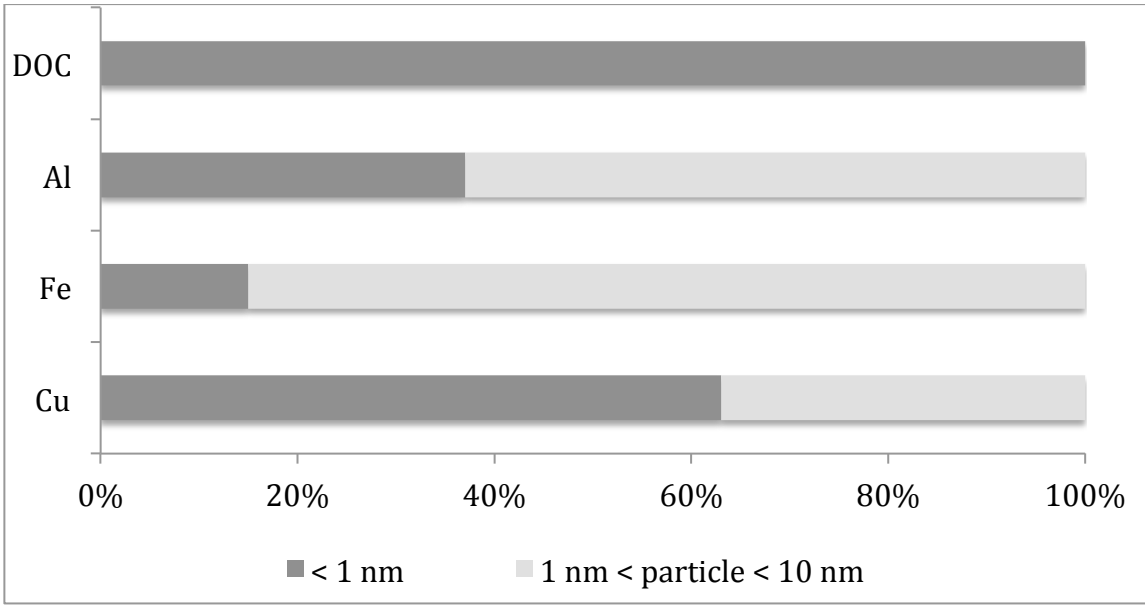

Fig. 3-1. Size distribution of particles below 10 nm of planted samples for DOC (mg/L) and Al, Fe, and Cu (µg/L). Particles between 1 and 10 nm were calculated as difference in concentration between $M_{<10}$ and $M_{<1}$.

In planted samples, DOC and soluble Cu ($Cu_{<10}$, $Cu_{<1}$) were correlated (**Fig. 3-2**), suggesting that biological exudates drove NP dissolution. It's possible that exposure of the CuO NPs to the wheat exudates dissolves Cu from the NPs, thus subjecting the plants to Cu toxicity, driving the wheat plant to release more exudates (whether by root damage or metabolic response), in a feed forward mechanism specific to nanoparticle exposure. The presence of increased root hairs in higher CuO NP doses, and their reduced root length shows that roots are morphologically different which may indicate a distinct pattern of exudate release. More dynamic studies, such as sacrificing Magenta boxes through time, may shed light on this.

Size differentiation of Cu is shown across CuO NP doses (**Fig. 3-2** a). Both Cu fractions increased with dose until stabilizing by 200 mg Cu/kg dry sand as CuO NPs. DOC increased across CuO NP doses above 100 mg Cu/kg (**Fig. 3-2** b). Clearly,

both Cu size fractions and DOC were substantially higher in planted compared to unplanted systems (**Fig. 3-2** a and b respectively), suggesting a biological driver of Cu solubility, likely related to biological exudates.

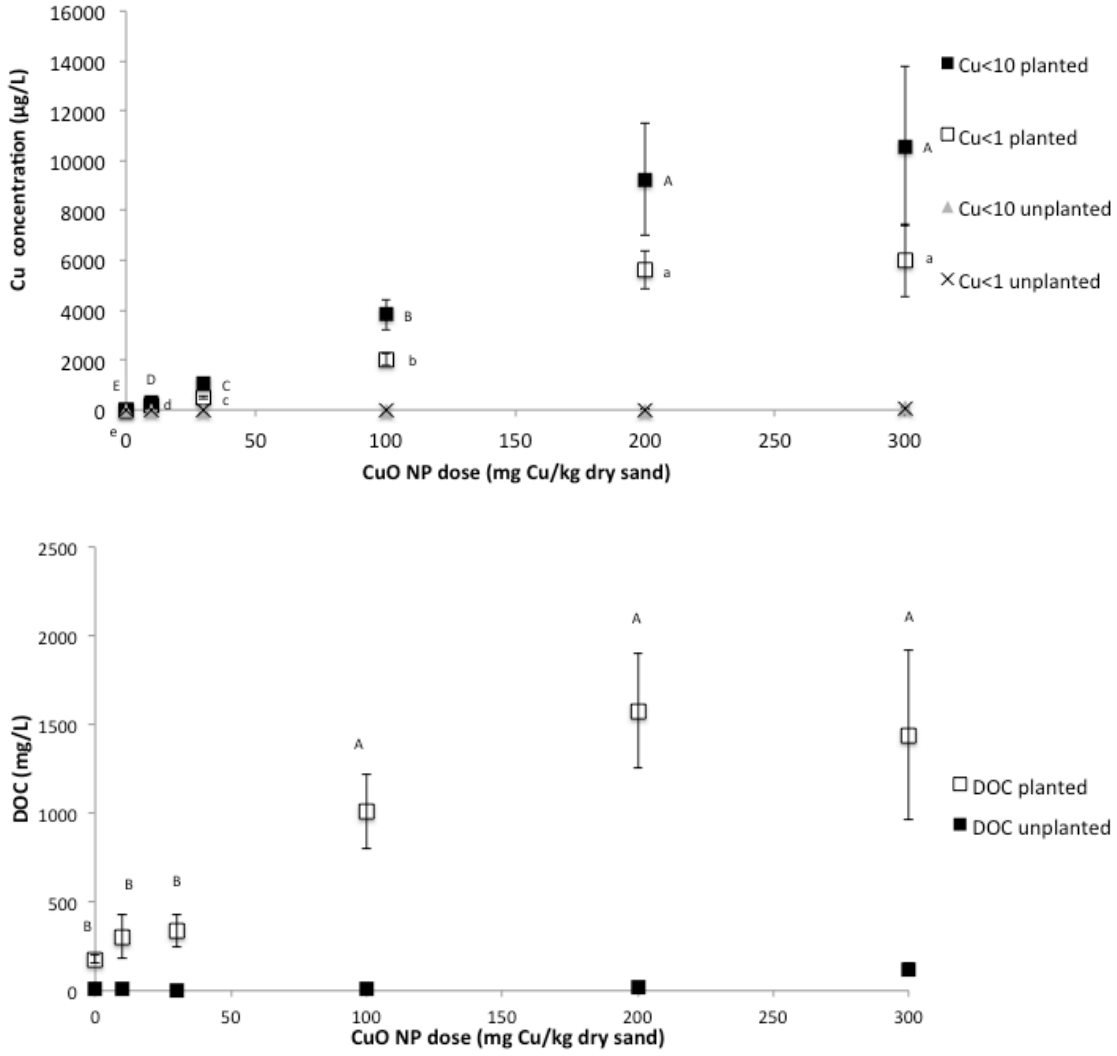

Fig. 3-2. Experiment 3: Planted and unplanted Cu and DOC, as $Cu_{<10}$ and $Cu_{<1}$, (mg Cu/L) (a), and DOC (mg C/L) (no difference between $DOC_{<1}$ and $DOC_{<10}$) (b) across doses of CuO NP (mg Cu/kg dry sand). Planted treatments with the same letters are not significantly different (α=0.05) by Tukey's HSD (run across CuO NP doses) after log transformation. Error bars indicate standard deviation (n=3).

There was a solution pH-CuO NP dose dependency at the end of the growth period; the pH of CuO NP 300 and 200 was significantly higher (ANOVA α=0.05) (7.5 ± 0.3) from CuO NP doses 0, 10 and 30 (6.7 ± 0.14) (SI **Table 3-9**), perhaps driven by Cu dissolution (CuO dissolution produces two hydroxide ions, increasing the pH), or proton sorption onto CuO NPs from water ionization. The solubility of tenorite increases an order of magnitude with every 0.5 pH unit decrease (Lindsay 1979), so dissolution observed here not simply a pH effect since the opposite is observed. The solubility of CuO NPs with pH changes has not been conclusively studied in comparison with bulk CuO (tenorite), though kinetics of CuO NP dissolution are likely faster than bulk counter parts (Misra et al. 2012). pH also has implications on aggregation of the NPs depending on the point of zero charge (PZC) which has not been defined here, and can vary significantly depending on crystalline structure and surface area (Conway et al. 2015; Sousa and Teixeira 2013). Despite pH driving Cu dissolution at lower pH, data from our growth systems showed higher dissolution at higher pH, showing other factors at play.

Geochemical modeling by MINTEQ, using the <1 nm solution data supported the observation of Cu and Al being associated with colloids. In the controls 99.99% of Al was predicted to precipitate as diaspore (Al_2O_3), while all Fe remained in solution, complexed with Ca-gluconate. Only a small percentage of CuO dissolved, proportionally less at higher CuO NP doses, and almost no aluminum was predicted in solution at any NP dose (Table 3-4). A small amount of Ca(oxalate) was predicted at CuO NP dose of 200 mg Cu/kg (Table 3-4).

Table 3-4. MINTEQ predictions for precipitation of metals at equilibrium (% of metal as precipitate).

% of metal as precip / NP dose	Al as diaspore (Al_2O_3)	Cu as tenorite (CuO)	Ca as Ca-oxalate
0	99.99	0.00	0.00
10	99.99	97.00	0.00
30	99.99	98.23	0.00
100	99.99	99.89	0.00
200	99.99	99.99	0.13
300	99.99	99.98	0.00

Taking geochemical data and measured DOC data together, Fe in colloids between 1 and 10 nm exists as Fe ions sorbed to Al_2O_3 sand particles or CuO NPs. Addition of $Fe_{<10}$ (approximately 5 – 10 times higher concentration than $Fe_{<1}$) into the MINTEQ model did not result in any Fe precipitates, giving further credence to this.

To understand the driver of Cu dissolution from CuO NPs, DOC was further investigated, and analyzed for proteins, sugars, LMWOAs, amino acids and the wheat phytosiderophore DMA. Solubilization of Cu has been correlated with increasing DOC in soil (McBride and Martinez 2000), and in particular with CuO NPs with certain DOC ligands (Conway et al. 2015; Wang et al. 2015, 2013), though the propensity of species of DOC to chelate or complex Cu varies with Cu-ligand stability.

Sugars and carbohydrates (assumed as glucose 40% C) contributed 89 ± 22% of DOC, proteins (assumed 53% C (Rouwenhorst et al. 1991)) was 28 ± 13%. LMWOAs, AAs and DMA combined contributed 15 ± 5%. Sugars are expected to play a minor role in dissolution of Cu from the CuO NPs, since they lack carboxylic, S or N based functional groups involved in Cu complexation, and were shown not to drive dissolution of CuO NPs in supporting information by Wang et al. (2013). It's possible that certain large carbohydrates may bind and cap the CuO NPs, though no literature was found at this stage to qualify this. Proteins however, can act as surface "coronas" on NPs (Lynch and Dawson 2008; Xu et al. 2012) impacting the bioavailability and bio-reactivity of the NPs. Peptides have been shown to adsorb to CuO NPs (Joshi et al. 2012), potentially altering the CuO NP bio-reactivity. Proteins and peptides also act as chelators for Cu ions, driving dissolution of the CuO NPs.

The stability of complexes is highly specific to DOC components. Of particular interest are AAs, DMA and LMWOAs as their affinity to Cu is high. Amino acids were highly variable in concentration in the rhizosphere sand solution, and all were less than 3 mg/L (Table 3-8). The UV detector HPLC method for amino acids detection has been reported to be subject to significant variability (up to 35% variation in standards), and levels in the treatments were near the detection limit of the method used (personal communication with Dr. Justin Jones, USU Innovation Laboratory).

In Fig. 3-3. (a – d respectively), DMA and the LMWOAs gluconate, citrate, and malate increased with CuO NP dose before stabilizing at CuO NP dose 100 mg Cu/kg dry sand and above. The plants responded to elevated concentrations of NPs and soluble Cu, with increased production of root exudates. Nian et al. (2002) also

observed enhanced root exudates (malate and citrate) in wheat exposed to 40 µM (2540 µg/L) Cu ions, as $CuCl_2$. Whether the increase production of the root exudates was a direct metabolic response of the plant to increase dosing of the NPs or the response was due to leaking of DOC due to root wall damage was not the focus of this study, though thin, brittle roots with necrotic lesions were reported in similar studies (Dimkpa et al. 2012). Unplanted treatments had no citrate, malate or DMA, and gluconate was more than 70% lower in unplanted samples compared to the respective planted CuO NP dose, showing that LMOWAs and DMA were plant associated.

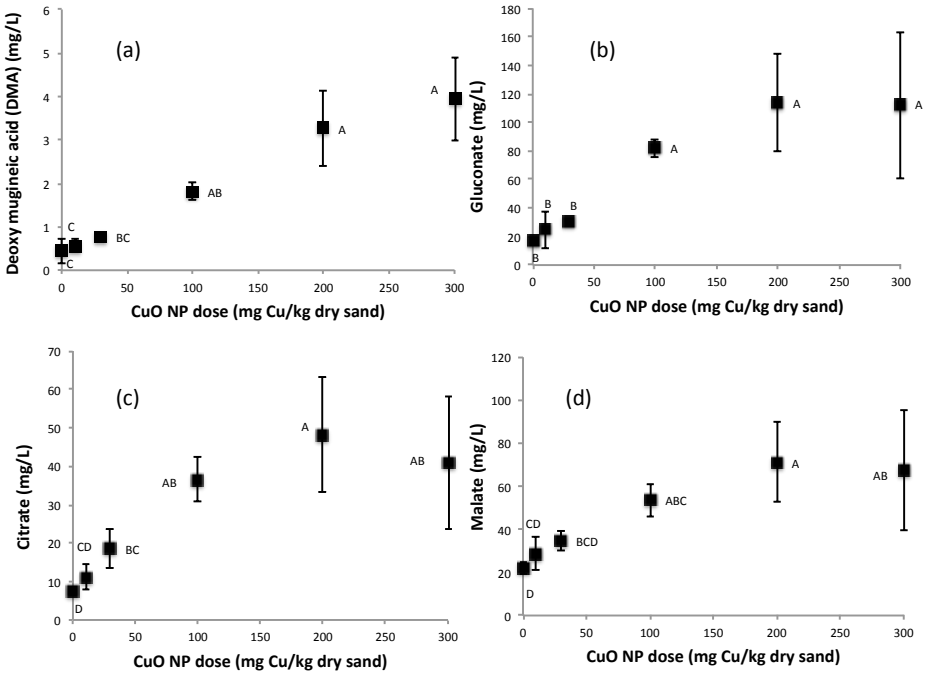

Fig. 3-3. DMA (a) LMWOAs gluconate (b), citrate (c), and malate (d) concentrations from Experiment 3 across CuO NP doses (n=3) (mg/L). Treatments with the same letters are not significantly different (α=0.05) by Tukey's HSD after log transformation. Error bars indicate standard deviation (n=3).

MINTEQ geochemical modeling was analyzed to understand equilibrium solution conditions. In terms of complexation, Cu citrate was predicted to be the dominant form of Cu in solution at CuO NP doses of 100 mg Cu /kg or less (Fig. 3-4). Citrate is likely to play a role in Cu solubilization from the CuO NPs; one study showed citrate interacting CuO NPs dissolved up to 10x more Cu irrespective of pH (Mudunkotuwa et al. 2012). Cu-malate was also predicted in significant amounts, particularly at CuO NP doses of 10 and 30 mg Cu/kg sand. At Cu at 300 and 200 mg Cu/kg sand, DMA played a central role in complexing Cu from the CuO NPs, along with citrate (Fig. 3-4).

No particular amino acid was involved in the majority of Cu complexation at any CuO NP dose, though cumulatively amino acids complexed up to 30 % of Cu at NP dose 300 mg Cu/kg sand, while only contributing 10% at the lowest NP dose. At higher doses, glycine and arginine were highest contributors to complexation, while at lower doses valine and arginine played a role (Fig. 3-4).

A sensitivity analysis showed that dissolution of CuO in MINTEQ was governed by pH, particularly below pH 7, and decreasing pH and increasing citrate or DMA concentration solubilized significantly more Cu (Supporting Information Fig. 3-12.). Indeed, using the full triplicate measurements as inputs to the MINTEQ model show that there variation on Cu solubility is about 25% of the mean dissolution, though the major ligands driving Cu complexation were not changed (Supporting Information **Table 3-13**).

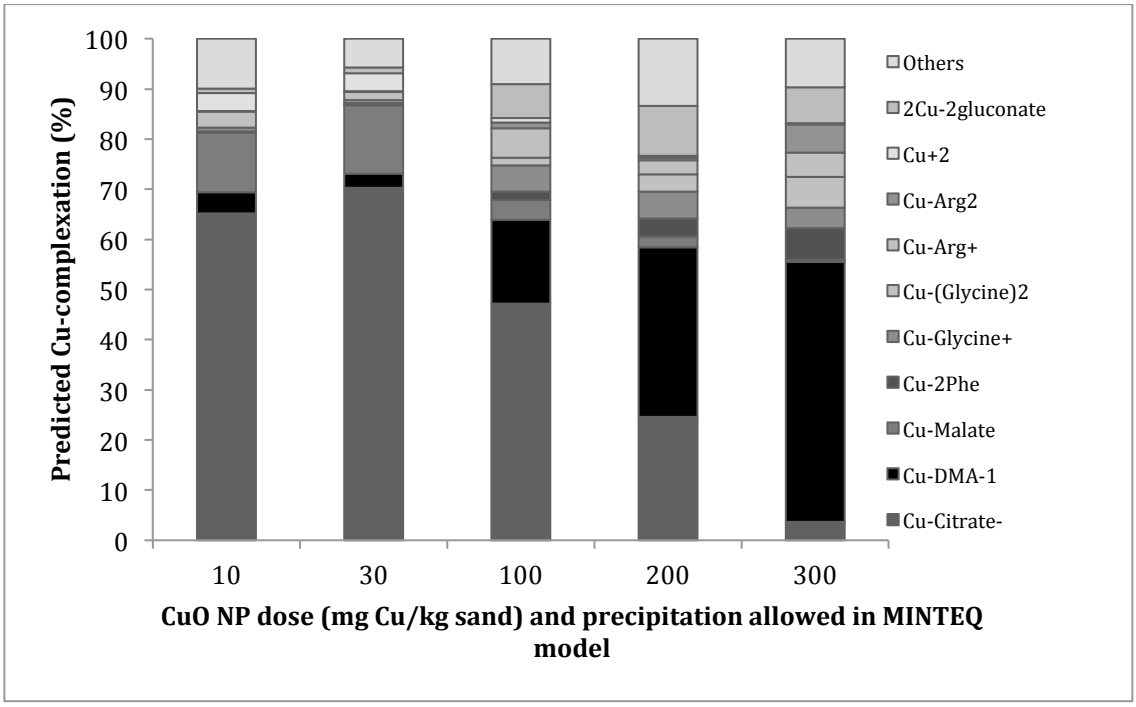

Fig. 3-4. Cu Complexes (%) predicted by MINTEQ at different NP doses (n=3). MINTEQ model will precipitate any species above saturation. Legend is shown in order of data on bar graphs.

Cu dissolution was compared between that predicted by the model and experimental data (Table 3-5.). Only a small fraction of the CuO NPs was dissolved according to the model with 2.98% at CuO NP 10, but only 0.02% at the highest CuO NP dose of 300 mg Cu/kg sand. The low proportion of soluble Cu was supported by empirical data (Table 3-5.). The empirical data showed 0.2% of CuO NPs dissolved at 10 mg Cu/kg, while 0.06% dissolved at 300 mg Cu/kg as CuO NP. A slight change in % dissolved resulted in a much larger dissolution concentration, showing how little Cu dissolved from the CuO NPs. Removing the solid phase CuO from MINTEQ was also investigated, and found that at low pH restricting a solid phase drove the model to agree with empirical values, whereas at higher CuO NP doses, the lack of

dissolution predicted by the model made the solid phase inconsequential **Table 3-12**).

Table 3-5. Comparison of $Cu_{<1}$ and Cu^{2+} from experimental data (n=3 average) and MINTEQ model. Solid phase of tenorite (CuO) crystalline was imposed to model CuO NPs. NA = not applicable.

CuO NP dose (mg Cu/kg sand)	0	10	30	100	200	300
pH	6.69	6.78	6.63	7.17	7.36	7.67
% sol Cu/total CuO solid (MINTEQ)	NA	2.98 %	1.77 %	0.11 %	0.04 %	0.02 %
% sol Cu/total CuO solid (measured)	NA	0.20 %	0.16 %	0.10 %	0.12 %	0.06 %
Soluble Cu µg/L (MINTEQ)	10	2839	5629	2242	2012	1589
$Cu_{<1}$ µg/L (measured)	10	189	495	2037	5610	5998
Cu^{2+} µg/L (MINTEQ)	0.00	13	203	18	8.0	2.16
Cu^{2+} µg/L (measured)	0.40	0.31	1.15	0.90	1.88	3.59

The model underestimated soluble Cu concentration at CuO NP 200 and 300 mg Cu/kg sand, but overestimated at CuO NP 10 and 30 mg Cu/kg sand. It is possible that some components in the DOC which were not captured in the model solubilized Cu, or that $Cu_{<1}$ measured may have included some small precipitates. At pH 7.55, the model results would match that of observed dissolved Cu (495 µg/L) for dosing at 30 mg Cu/kg sand. At CuO NP dose 100 mg Cu/kg sand (pH 7.17), the model predicted $Cu_{<1}$ most accurately of the NP doses (SI Fig. 3-11.) As discussed, below pH 7, dissolved Cu is particularly sensitive to slight (0.1) pH changes (SI Fig. 3-12.), in addition to pH measurements being inherently difficult to take around

neutral pH. It's also possible that at low CuO NP doses, the surface chemistry of the NPs was affected by exudates that stabilized and resulted in lower dissolution than predicted, and that these exudates (for example peptides and proteins have a surface affinity to CuO NPs that is quite specific (Joshi et al. 2012; Lynch and Dawson 2008) - not examined in detail here) were not produced by the wheat plant when stressed by high CuO NP doses. The charge balance in MINTEQ was less than 15% (low on anions) (SI Table 3-11) across all CuO NP doses.

The underlying assumptions of geochemical modeling include equilibrium, both between the solid and solution phases, and within the solution phase. In a rhizosphere context, this may not be appropriate, since this interaction is dynamic and the plant may respond (Schenkeveld et al. 2014; Terzano et al. 2015). There may be spatial considerations: phytosiderophores are thought to be released only from the root apex to avoid consumption by microorganisms (Von Wiren et al. 1993), concentrating DMA at the root tip. Additionally, the roots may release compounds that are synergistic; oxalate and DMA were found to release more Fe compared to DMA alone in goethite (FeO(OH)) (Reichard et al. 2005). Kinetics may play a part in this release, but are little studied (Schenkeveld et al. 2014; Terzano et al. 2015), especially in the context of nanoparticles in the rhizosphere. Further, the model only considers solution phase complexation competition. Schenkeveld et al (2012) however demonstrated replacement of Fe in a FeEDDHA complex sorbed to the surface of goethite by Cu; a surface reaction not considered in geochemical modeling. The high surface area of CuO NP may enhance sorption of metal complexes.

Though released by wheat to acquire Fe particularly in alkaline soils, DMA is also a strong Cu chelator (Murakami et al. 1989). In the presence of CuO NPs, this may have implications for dissolution; the excess DMA may dissolve Cu from NPs and have potential implications for Cu and Fe uptake into shoots (Ma et al. 1993; Ma and Nomoto 1993). To the author's knowledge, this is the first study to analyze release of phytosiderophores in the context of CuO NPs. DMA concentrations were higher than those reported by Oburger et al. (2014) in alkaline soils by a factor of 2 - 3. Differences in DMA production may be due to the lower available Fe levels in the sand (Table 3-1.) compared to soils, microbial consumption of DMA in the soils, differences in methods and timing for collecting or because of large amounts of CuO NPs and Cu around roots binding DMA. Formation of CuDMA complex would likely drive the wheat plant to release more DMA, as phytosiderophore production is driven in part by Fe limitations in the plant (Oburger et al. 2014).

Planted systems showed a lower ratio of $Cu^{2+}/Cu_{<1}$ compared to unplanted treatments; in unplanted systems, up to 88% of the $Cu_{<1}$ was as the free ion Cu^{2+} whereas Cu^{2+} represented far less than 1% of $Cu_{<1}$ in planted samples, indicating again that complexation was a major driver in dissolution of CuO NPs in planted systems (SI Fig. 3-8), Cu2+ did not contribution to toxicity (Table 3-5.).

Cu^{2+} measured in the rhizosphere solution was most accurately predicted in CuO NP 100 and 300 mg Cu/kg sand in MINTEQ (Table 3-5.) CuO NP 30 mg Cu/kg sand had large differences in Cu^{2+} predictions, the model overestimating compared to measurements taken by the Cu^{2+} ion selective electrode. This was driven in part

by high soluble Cu predictions by MINTEQ, caused by low pH compared to CuO NP 100 and 300 mg Cu/kg sand.

4.2 Plant morphology and metal homeostasis

Based on the solution chemistry outlined above, the wheat roots were subjected to a range of compounds, including increased amounts of metal-organic complexes, and several morphologic and metal uptake responses were significant. A randomized blocked design, repeated 3 times across several months, involving three different experiments at 0, 30, 100 and 300 mg Cu/kg dry sand as CuO NPs provided an indication of biological reproducibility, with the solution chemistry following the same trends outlined in section 4.2 (Fully replicated data set: Appendix E).

Dose dependent reduction in root elongation was observed, as reported previously (Dimkpa et al. 2012, 2013). Roots showed a dose dependent decrease in both mass and length. Root dry mass decreased by 50% for the dose of 300 mg Cu/kg sand compared to the control (SI Fig. 3-9.)

Minimal chlorosis (1-2 leaves per box and only slight yellowing) was found at the end of the 10-day growth period, even in the control with no NPs, and thus occurred without Cu exposure, suggesting CuO NP exposure did not drive chlorosis in the growth period.

To determine whether CuO NPs affected plant water management, wet shoots directly out of Magenta boxes were weighed, then oven dried at 60° overnight and reweighed. Control shoots had significantly less water loss compared

to plants subjected to CuO NP doses of 200 and 300 mg Cu/kg: there was 12 % lower mass of water in shoots dosed with 300 mg/kg sand CuO NP compared with control shoots (SI **Fig. 3-10.**). CuO NPs also adversely impacted the moisture content of roots and shoots in maize (Wang et al. 2012) and lettuce plants (Trujillo-Reyes et al. 2014). Another study suggested hydraulic conductance was decreased following exposure of TiO_2 NP to maize plants, not due to toxic effects, but inhibition of apoplastic flow by clogging of nano- sized root cell wall pores (Asli and Neumann 2009).

Marschner (1995) suggests an upper threshold of 20 – 30 mg Cu/kg dry shoot mass for wheat, to provide this essential nutrient without toxicity, with deficiency suggested below 1 - 5 mg Cu/kg dry shoot. This Cu homeostasis (Clemens 2001) in shoots was not maintained at NP dose of 300 mg Cu/kg sand (Fig. 3-5. a), and even at 100 mg Cu/kg sand, Cu in shoots was at the upper limit.

Root associated Cu increased dose dependently (Fig. 3-5. e). Root associated Cu was not differentiated between Cu inside tissue versus Cu associated with the root surface. Roots were simply rinsed with deionized water to avoid tissue damage and leakage that occurs with more rigorous cleaning methods. The determination of solution chemistry of 60% Cu complexes ($Cu_{<1}$) and 40% Cu associated with 1 to 10 nm particles (Fig. 3-1 and Fig. 3-4), suggests that complexes and Cu containing nanoparticles surrounded the root surface.

The concentration of Cu associated with the roots was orders of magnitude higher than in the shoots, implying additionally that translocation of Cu was controlled within the plant, seen also with rice (Peng et al. 2015). In soil grown

wheat, the shoot to root ratio of Cu when wheat was exposed to high levels of Cu (around 150 mg Cu/kg soil) never exceeded 0.2 (Michaud et al. 2007; Wang et al. 2009).

Transport of Cu^{2+} within a normally functioning plant is tightly controlled by ligand exchange reactions, and excess Cu is secured in vacuoles within the roots (Clemens et al. 2002), an exclusion strategy (Baker 1981). The translocation and subsequent dissolution of CuO NPs *in planta* however is a potential mechanism for increased uptake into the shoot (Wang et al. 2012), in this study 100 mg Cu/kg sand and above had increased Cu uptake compared to control plants. The composition of this Cu was not determined from this study, however this could be assisted by CuO NP damage to the root plasmalemma (Lee et al. 2008) allowing ingress of NPs along with Cu^{2+} or Cu complexes. Together, a wheat plant exposed to high concentrations of CuO NPs may suffer Cu toxicity and root damage due to high dissolved Cu. The root damage may accentuate the problem of CuO NP ingress, driving *in planta* uptake of CuO NPs and dissolution once into the shoots. This is likely a mechanism that the wheat plant's defenses are inadequate to defend against, since Cu ions and complexes are more common in soil systems. Taken together, these potential mechanisms makes CuO NP toxicity a specific problem, due to CuO NPs faster dissolution rates, and ability to enter the plant's root pores due to their small size, a "Trojan horse" type mechanism (Studer et al. 2010; Wang et al. 2013).

Fe in shoots significantly decreased at CuO NP doses of 100 and 300 mg Cu/kg sand compared to control plants (Fig. 3-5. c), coinciding with the highest DMA exudation (Fig. 3-3 a). As discussed previously, higher Cu in the rhizosphere

(particularly CuO NPs which have a large surface area) has been linked with decreased Fe uptake, probably due to the formation of CuDMA complexes (Fig. 3-4), which interrupt the Fe uptake mechanism of Strategy II (those that produce phytosiderophores) monocots such as wheat (Michaud et al. 2007; Oburger et al. 2014; Ryan et al. 2013). Fe in roots could not be accurately ascertained due to sand contributing Fe to the digestion.

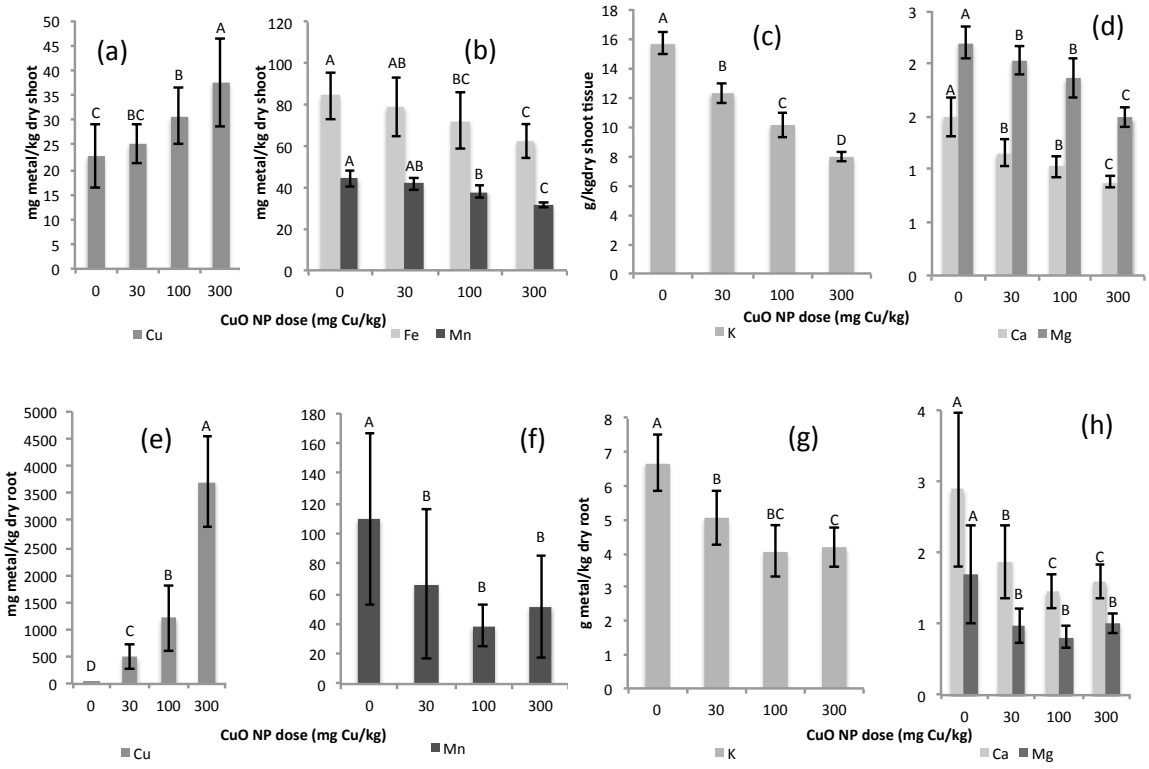

Fig. 3-5. Metal uptake into wheat plant: Cu (a) Fe and Mn (b) and K (c), Ca and Mg (d) and in shoot tissue over 10 days in sand with 0, 30, 100, or 300 mg Cu/kg sand as CuO NPs (n = 9). Cu (e), Mn (f), and K (g), Ca and Mg (h) in root tissue (n = 9). Fe in roots not shown as it was impacted by sand attached to roots resulting in unrealistically high Fe results. Columns with the same letters are not significantly different (α=0.05) by Tukey's HSD. Error bars represent standard deviation.

A significant reduction in K in shoots and roots was found (Fig. 3-5. c and g respectively), being more severe at higher NP dose, consistent with Dimkpa et al. (2012) studying wheat subjected to CuO NP, Wang et al. (2012) with maize and CuO NP, and Kováčik et al. (2012) using chamomilla plants subjected to Cu salts. This was also supported by higher K^+ in solution at higher NP doses (SI Table 3-8). K^+ efflux is linked to oxidative stress (Murphy and Taiz 1997), a symptom of the wheat root exposed to Cu^{2+} and a resultant increase in unquenched reactive oxygen species (ROS) (Dimkpa et al. 2012).

Ca and Mg were dose dependently lower in the shoot and root tissue (Fig. 3-5. d and h respectively). Given Mg and Ca are both competing cations with a +2 charge, it is possible that Cu in solution from the CuO NPs outcompeted Ca and Mg onto the root surface, preventing uptake. Ca and Mg are up taken via non selective pores that may be blocked in the presence of excess Cu. CuO NPs at 20 and 80 mg Cu/kg soil depressed Ca and Mg in shoots of cilantro in potting mix soil (Zuverza-Mena et al. 2015). Mn decreased significantly in shoot tissue only at CuO NP doses at 100 mg Cu/kg sand or above compared with the control (Fig. 3-5. b), whereas root Mn decreased significantly at all CuO NP doses relative to the control (Fig. 3-5. f), also seen in cilantro shoots subjected to CuO NPs in potting soil (Zuverza-Mena et al. 2015).

4.3 Cu toxicity: traditional models and specific CuO NP toxicity

There are several models that describe Cu toxicity to plants. These include the free ion activity model (FIAM), where toxicity is driven from the activity of the free Cu ion, here measured by ISE as Cu^{2+}. Root related Cu is correlated to Cu^{2+}, (

Fig. 3-6.), but so is complexed Cu. Differentiating toxicity due to CuO NPs versus ions or Cu-organic matter complexes is a point of difficulty in defining nano-toxicity, but one that requires resolution (Ivask et al. 2014). In this section, we relate detail on mechanisms of CuO NP toxicity and relate the mechanisms to species of Cu (small CuO NPs, Cu ions or Cu complexes), and how this may influence bioavailability.

This study did not control the aqueous concentration of Cu or the concentration of exudates, meaning observations may have fed back on each other, in terms of exudation and then Cu dissolution, leading to some autocorrelation. However, shoot Cu concentrations were most correlated with $Cu_{<10}$, ($R = 0.84$) (

Fig. 3-6. a). In terms of complexes predicted by MINTEQ, only CuDMA was correlated with uptake and translocation of Cu into the plant shoots (**Fig. 3-6.** b).

In an experiment with Cu toxicity on wheat, Parker et al. (2001) showed that complexation in hydroponics by malonate or malate decreased toxicity of Cu, but Cu-citrate did not decrease toxicity. The group suggested that transport of Cu-citrate into the wheat plant contributes to the toxicity and potentially to Cu uptake, thus showing that contribution of Cu-complexes to toxicity and uptake may be ligand specific. 10 - 13% Cu malate was predicted by MINTEQ at CuO NP 10 and 30 mg Cu/kg sand, potentially alleviating some toxic effects, though 65 - 70% of the Cu was

present as Cu-citrate (Fig. 3-4) which may have contributed to Cu uptake and reduced root length, consistent with Parker et al. (2001). A non-significant correlation between Cu citrate and Cu in the shoots (

Fig. 3-6. b) may indicate Cu citrate is toxic to roots, but this complex is not translocated, such as being sequestered into root cell vacuoles.

Citrate has been used in phytoremediation studies to improve metals uptake (Almaroai et al. 2012; Sinhal et al. 2010) and to assess bioavailability and uptake in wheat in contaminated soils (Feng et al. 2005), showing that Cu complexes such as Cu-citrate can drive both solubility and uptake of metals into plants. Cu in solution complexed with DMA and citrate primarily at the highest CuO NP doses (Fig. 3-4), corresponding with reduced root length and Cu toxicity.

The terrestrial biotic ligand model (TBLM) describes the competitive effect cations such as Ca, Mg and especially protons have on reducing Cu toxicity on a biotic ligand such a plant root (Thakali et al. 2006). Cations sorption creates a bridge between negatively charges CuO NPs (flocculation) and increasing ionic strength tends to drive CuO NP aggregation (Conway et al. 2015), suggesting that NP dissolution is negatively correlated with the presence of major cations. However, sorption of CuO NP to the root and localized Cu release (Shi et al. 2011) is not accounted for in TBLM or FIAM.

The addition of CuO NPs adds particles with significantly higher surface area to volume ratio compared with the sand, implying thermodynamic as well as spatial likelihood of Cu complex formation. For example, 300 mg Cu/kg sand as CuO NP would increase available surface area by a factor of 20, compared to the same mass of sand without NPs (CuO NP surface area from (Mudunkotuwa et al. 2012), sand

assumed surface area of 0.00038 m^2/g). A DMA ion diffusing from the root surface would therefore have greater likelihood of chelating Cu from a CuO NP than Fe from a sand or soil particle, increasing the likelihood of a Cu-DMA complex formation over Fe-DMA.

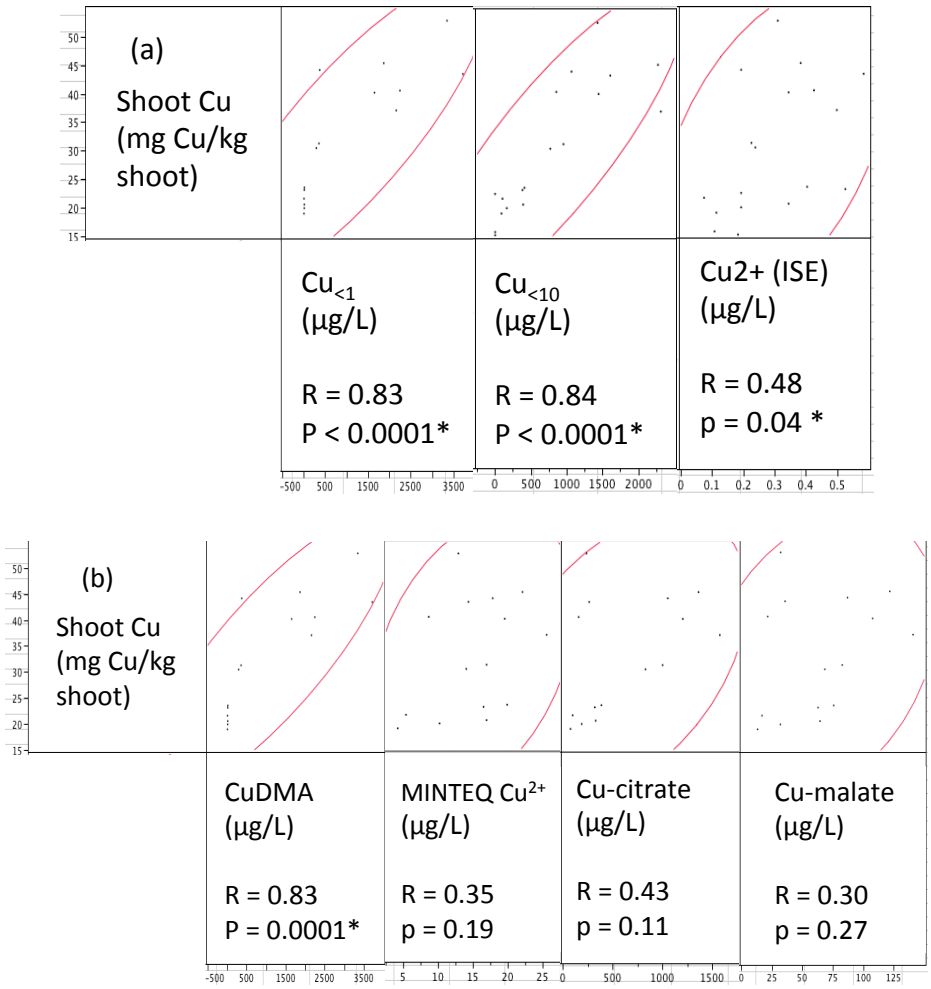

Fig. 3-6. (a) $Cu_{<1}$, $Cu_{<10}$ and Cu^{2+} measured by Cu^{2+} ion selective electrode (ISE) (ug/L) and **(b)** complexes CuDMA, Cu2+, Cu citrate and Cu malate as predicted by the MINTEQ model correlated with Cu uptake in shoot Cu (mg Cu/kg tissue). Red ellipses represent 95% confidences intervals around the correlation (n=18). All significant at $\alpha = 0.05$, apart from MINTEQ prediction of Cu^{2+}, Cu malate and Cu citrate.

This is empirically supported by lower Fe uptake in shoots in higher NP doses, and increased Cu uptake (Fig. 3-5. a and b), as well as Fe being predominately in small nano particulate form, probably associated with small Al_2O_3 particles from the sand (Fig. 3-7 b.) MINTEQ predicted no FeDMA complex formation in this system, with all soluble Fe as various Fe-Ca-gluconate complexes.

An increase in CuDMA formation in CuO NP 100 mg Cu/kg sand (Fig. 3-5. a) was associated with a threshold break (30 mg Cu/kg shoot (Neumann and Römheld 2012)) in Cu uptake (Fig. 3-5. a and **Fig. 3-6.** b). CuDMA formation is therefore correlated with increased Cu uptake, in addition to a decrease in Fe in shoots. As discussed, FeDMA was not predicted to form at any CuO NP dose, including the control, but as CuO NP dose increased, so does release of DMA, and therefore formation of CuDMA. CuDMA is likely taken up in oats (Ryan et al. 2013), though CuDMA uptake is subject to some uncertainty in barley (Ma et al. 1993; Ma and Nomoto 1993), and has not been studied in wheat. Oats and barley are both strategy II monocots, using phytosiderophores (similar to DMA) to chelate and uptake Fe. An antagonism between high Cu and low Fe in shoots was also demonstrated in hydroponics with durum wheat (Michaud et al. 2008). At low levels, CuO NPs had little impact on Fe homeostasis (Fig. 3-5. b) meaning a dose under 30 mg Cu/kg sand as CuO NP did not adversely affect plant growth, at least over this growth period.

A bacterium originating from soil, *Pseudomonas aeruginosa* PAOI, was found to release its siderophore pyoverdine (PVD) in response to high Cu levels, as a defensive mechanism (Braud et al. 2010). Since CuPVD is uptaken more slowly than FePVD, complexing Cu with PVD is a response of the microbe to limit to Cu toxicity.

Given CuDMA is reportedly taken up more slowly than FeDMA in barley (Ma and Nomoto 1993), in spite, or perhaps because of FeDMA having a specific uptake mechanism (Ma et al. 1993), the same strategy may be taking place.

Modeling CuO NP toxicity is still in its infancy; no model of NP uptake or direct toxicity yet exists, despite several studies showing uptake of CuO NP is possible in hydroponics (e.g. Peng et al. 2015 (rice); Wang et al. 2012 (maize)). Taken together, this may mean that Cu toxicity from CuO NPs is derived from all forms; including small NPs (Mudunkotuwa et al. 2012), in addition to certain bioavailable complexes and to a lesser extent free Cu^{2+} ions.

Clearly, the specific exposure media is highly influential in terms of CuO NPs and their biogeochemistry (Wang et al. 2013) and toxic mechanisms of CuO NPs remain inconclusive (Djurišić et al. 2015). For example, low pH systems may drive toxicity purely from ion release from the CuO NPs (Misra et al. 2012; Shi et al. 2011), whereas higher pH systems such as calcareous soils (pH > 8) CuO NP toxicity could be driven by CuO NP uptake, dissolution by complexation, and *in planta* dissolution. From our studies, at higher pH, complexation becomes a more dominant form of dissolution and potential toxicity (such as Cu-DMA or Cu-citrate), implying a greater understanding of the components of DOC is crucial in making a deterministic toxicity model to describe how CuO NPs may be transformed in agricultural settings.

5. Conclusion

Effects of CuO NP on wheat growth and uptake of Cu and other micronutrients involve complex processes occurring in the rhizosphere. Challenges to wheat roots with high concentration (>100 mg Cu/kg sand) of CuO NPs result in greater root exudation enhancing Cu solubility, Cu uptake and plant toxicity response (observed as decreased root length and biomass production). Small (<10 nm) Cu containing particles, in addition to bioavailable Cu complexes, were correlated with this plant response.

Root exudation may serve as a defense mechanism against metal toxicity, but at higher dosing may involve increased plant uptake, overwhelming defense strategies of the plant. The presence of CuO NPs, favorable to quick dissolution kinetics, near wheat roots may make these dissolution processes particularly toxic. The interplay between higher concentrations of NPs and DOC, in particular DMA and citrate, was found to drive dissolution. This interplay may have aided the solubilization of small CuO NPs and Cu complexes onto the root surface, damaging the plant and exacerbating this dissolution process in a feed forward mechanism. The increased uptake of Cu into shoots and adhering to roots coincided with lower levels of Ca, Mg, Mn, K and Fe in the wheat shoots compared to controls. Fe uptake in particular in this system may be at a competitive disadvantage resultant from conditions favorable to CuDMA over FeDMA complexation.

This work has implications in agricultural contexts for CuO NPs since understanding the biogeochemistry of CuO NPs in the rhizosphere of wheat is

essential for a complete picture of CuO NP toxicity. Applications include beneficially using NPs as more efficient fertilizers (Anjum et al. 2015 a; Dimkpa et al. 2015; Servin et al. 2015), and more efficient phytoremediation. Greater investigation of these processes in soil and over longer time frames would be a prudent extension to this work.

REFERENCES

Ahamed, M., and Alhadlaq, H. (2014). "Synthesis, Characterization, and Antimicrobial Activity of Copper Oxide Nanoparticles." *Journal of Nanomaterials*, 10(1155), 4.

Albalasmeh, A. A., Berhe, A. A., and Ghezzehei, T. A. (2013). "A new method for rapid determination of carbohydrate and total carbon concentrations using UV spectrophotometry." *Carbohydrate Polymers*, 97(2), 253–61.

Almaroai, Y. a., Usman, A. R. a., Ahmad, M., Kim, K.-R., Moon, D. H., Lee, S. S., and Ok, Y. S. (2012). "Effects of Synthetic Chelators and Low-Molecular-Weight Organic Acids on Chromium, Copper, and Arsenic Uptake and Translocation in Maize (*Zea mays L.*)." *Soil Science*.

Anjum, N. A., Adam, V., Kizek, R., Duarte, A. C., Pereira, E., Iqbal, M., Lukatkin, A. S., and Ahmad, I. (2015a). "Nanoscale copper in the soil–plant system – toxicity and underlying potential mechanisms." *Environmental Research*, 138(2), 306–325.

Anjum, N. A., Hasanuzzaman, M., Hossain, M. A., Thangavel, P., Roychoudhury, A., Gill, S. S., Rodrigo, M. A. M., Adam, V., Fujita, M., Kizek, R., Duarte, A. C., Pereira, E., and Ahmad, I. (2015b). "Jacks of metal/metalloid chelation trade in plants-an overview." *Frontiers in Plant Science*, 6, 192.

APHA. (2014). "APHA AWWA WEF." *Standard Methods for the Examination of Water and Wastewater*, 20.

Asli, S., and Neumann, P. M. (2009). "Colloidal suspensions of clay or titanium dioxide nanoparticles can inhibit leaf growth and transpiration via physical effects on root water transport." *Plant, Cell and Environment*, 32(5), 577–584.

Atha, D. H., Wang, H., Petersen, E. J., Cleveland, D., Holbrook, R. D., Jaruga, P., Dizdaroglu, M., Xing, B., and Nelson, B. C. (2012). "Copper oxide nanoparticle mediated DNA damage in terrestrial plant models." *Environmental science & technology*, 46(3), 1819–27.

Bais, H. P., Weir, T. L., Perry, L. G., Gilroy, S., and Vivanco, J. M. (2006). "The role of root exudates in rhizosphere interactions with plants and other organisms."

Annual Review of of Plant Biology, Annual Reviews, 57, 233–266.
Baker, A. J. M. (1981). "Accumulators and excluders - strategies in the response of plants to heavy metals." *Journal of Plant Nutrition*, 3(1–4), 643–654.
Bechtold, T., Burtscher, E., and Turcanu, A. (2002). "Ca2+–Fe3+–D-gluconate-complexes in alkaline solution. Complex stabilities and electrochemical properties." *Journal of the Chemical Society*, (13), 2683–2688.
Blinova, I., Ivask, A., Heinlaan, M., Mortimer, M., and Kahru, A. (2010). "Ecotoxicity of nanoparticles of CuO and ZnO in natural water." *Environmental Pollution*, 158(1), 41–7.
Bondarenko, O., Ivask, A., Käkinen, A., and Kahru, A. (2012). "Sub-toxic effects of CuO nanoparticles on bacteria: kinetics, role of Cu ions and possible mechanisms of action." *Environmental Pollution*, 169, 81–9.
Braud, A., Geoffroy, V., Hoegy, F., Mislin, G. L. A., and Schalk, I. J. (2010). "Presence of the siderophores pyoverdine and pyochelin in the extracellular medium reduces toxic metal accumulation in Pseudomonas aeruginosa and increases bacterial metal toleranceemi." *Environmental Microbiology Reports*, 2(3), 419–425.
Bravin, M. N., Garnier, C., Lenoble, V., Gérard, F., Dudal, Y., and Hinsinger, P. (2012). "Root-induced changes in pH and dissolved organic matter binding capacity affect copper dynamic speciation in the rhizosphere." *Geochimica et Cosmochimica Acta*, 84, 256–268.
Calder, A. J., Dimkpa, C. O., McLean, J. E., Britt, D. W., Johnson, W., and Anderson, A. J. (2012). "Soil components mitigate the antimicrobial effects of silver nanoparticles towards a beneficial soil bacterium, Pseudomonas chlororaphis O6." *The Science of the Total Environment*, 429, 215–22.
Callahan, D. L., Baker, A. J. M., Kolev, S. D., and Wedd, A. G. (2006). "Metal ion ligands in hyperaccumulating plants." *Journal of Biological Inorganic Chemistry*, 11(1), 2–12.
Cannan, R. K., and Kibrick, A. (1938). "Complex Formation between Carboxylic Acids and Divalent Metal Cations." *Journal of the American Chemical Society*, 60(10), 2314–2320.
Chen, H., Seiber, J., and Hotze, M. (2014). "ACS Select on Nanotechnology in Food and Agriculture: A Perspective on Implications and Applications." *Journal of Agricultural and Food Chemistry*, (62), 1209–1212.
Clemens, S. (2001). "Molecular mechanisms of plant metal tolerance and homeostasis." *Planta*, 212(4), 475–486.
Clemens, S., Palmgren, M., and Krämer, U. (2002). "A long way ahead: understanding and engineering plant metal accumulation." *Trends in Plant Science*, 1385, 309–315.
Cohen, A. C. (1959). "Simplified Estimators for the Normal Distribution When Samples Are Singly Censored or Truncated." *Technometrics*, 1(3).
Conway, J. R., Adeleye, A. S., Gardea-Torresdey, J., and Keller, A. A. (2015). "Aggregation, dissolution, and transformation of copper nanoparticles in natural waters." *Environmental Science and Technology*, 49(5), 2749–56.
Creager, M. S., Jenkins, J. E., Thagard-Yeaman, L. a., Brooks, A. E., Jones, J. a., Lewis, R.

V., Holland, G. P., and Yarger, J. L. (2010). "Solid-state NMR comparison of various spiders' dragline silk fiber." *Biomacromolecules*, 11, 2039–2043.
Dakora, F., and Phillips, D. (2002). "Root exudates as mediators of mineral acquisition in low-nutrient environments." *Plant and Soil*, 35–47.
Demidchik, V. (2014). "Mechanisms and physiological roles of K+ efflux from root cells." *Journal of Plant Physiology*, 171(9), 696–707.
Deng, Z., Mortimer, G., T, S., A, M., D, M., and R., M. (2009). "Differential plasma protein binding to metal oxide nanoparticles." *Nanotechnology*, 20(455101), 9.
Dennis, P. G., Miller, A. J., and Hirsch, P. R. (2010). "Are root exudates more important than other sources of rhizodeposits in structuring rhizosphere bacterial communities?" *FEMS Microbiology Ecology*, 72(3), 313–27.
Dimkpa, C. O. (2014). "Can nanotechnology deliver the promised benefits without negatively impacting soil microbial life?" *Journal of basic microbiology*, 54(9), 889–904.
Dimkpa, C. O., Latta, D. E., McLean, J. E., Britt, D. W., Boyanov, M. I., and Anderson, A. J. (2013). "Fate of CuO and ZnO nano- and microparticles in the plant environment." *Environmental Science and Technology*, 47(9), 4734–4742.
Dimkpa, C. O., McLean, J. E., Britt, D. W., and Anderson, A. J. (2015). "Nano-CuO and interaction with nano-ZnO or soil bacterium provide evidence for the interference of nanoparticles in metal nutrition of plants." *Ecotoxicology*, 24(1), 119–29.
Dimkpa, C. O., McLean, J. E., Latta, D. E., Manangón, E., Britt, D. W., Johnson, W. P., Boyanov, M. I., and Anderson, A. J. (2012). "CuO and ZnO nanoparticles: phytotoxicity, metal speciation, and induction of oxidative stress in sand-grown wheat." *Journal of Nanoparticle Research*, 14(9), 1125.
Djurišić, A. B., Leung, Y. H., Ng, A. M. C., Xu, X. Y., Lee, P. K. H., Degger, N., and Wu, R. S. S. (2015). "Toxicity of metal oxide nanoparticles: Mechanisms, characterization, and avoiding experimental artefacts." *Small*, 11(1), 26–44.
Dodson, J. R., Hunt, A. J., Parker, H. L., Yang, Y., and Clark, J. H. (2012). "Elemental sustainability: Towards the total recovery of scarce metals." *Chemical Engineering and Processing: Process Intensification*, 51, 69–78.
Ducic, T., and Polle, A. (2005). "Transport and detoxification of manganese and copper in plants." *Brazilian Journal of Plant Physiology*, 17(1), 103–112.
Eby, G. A. (2004). "Zinc lozenges: cold cure or candy? Solution chemistry determinations." *Bioscience reports*, 24(1), 23–39.
Feng, M.-H., Shan, X.-Q., Zhang, S.-Z., and Wen, B. (2005). "Comparison of a rhizosphere-based method with other one-step extraction methods for assessing the bioavailability of soil metals to wheat." *Chemosphere*, 59(7), 939–49.
Gajda, T., Gyurcsik, B., Jakusch, T., Burger, K., Henry, B., and Delpuech, J.-J. (1998). "Coordination chemistry of polyhydroxy acids: role of the hydroxy groups." *Inorganica Chimica Acta*, 275–276, 130–140.
Gajjar, P., Pettee, B., Britt, D. W., Huang, W., Johnson, W. P., and Anderson, A. J. (2009). "Antimicrobial activities of commercial nanoparticles against an environmental soil microbe, Pseudomonas putida KT2440." *Journal of*

Biological Engineering, 3, 9.
Gardea-Torresdey, J. L., Rico, C. M., and White, J. C. (2014). "Trophic transfer, transformation, and impact of engineered nanomaterials in terrestrial environments." *Environmental Science and Technology*, 48(5), 2526–40.
Giannousi, K., Avramidisb, I., and Dendrinou-Samara, C. (2013). "Synthesis, characterization and evaluation of copper based nanoparticles as agrochemicals against *Phytophthora infestans*." *The Royal Society of Chemistry*, (3), 21743–2175.
Grotz, N., and Guerinot, M. Lou. (2006). "Molecular aspects of Cu, Fe and Zn homeostasis in plants." *Biochimica et Biophysica Acta*, 1763(7), 595–608.
Gunawan, C., Teoh, W. Y., Marquis, C. P., and Amal, R. (2011). "Cytotoxic origin of copper(II) oxide nanoparticles: comparative studies with micron-sized particles, leachate, and metal salts." *ACS Nano*, 5(9), 7214–25.
Gustafsson, J. P. (2014). "Visual MINTEQ, A Windows version of MINTEQA2 version 4.0 MINTEQA2." <http://www2.lwr.kth.se/ English/OurSoftware/vminteq/> (Dec. 20, 2014).
Hartmann, A., Rothballer, M., and Schmid, M. (2007). "Lorenz Hiltner, a pioneer in rhizosphere microbial ecology and soil bacteriology research." *Plant and Soil*, 312(1–2), 7–14.
Haydon, M. J., and Cobbett, C. S. (2007). "Transporters of ligands for essential metal ions in plants." *The New Phytologist*, 174(3), 499–506.
Hole, D. J., Roche, D., Clawson, S. M., and S.A., Y. (2004). "Registration of 'Deloris' Wheat." *Crop Science*, 44(7498), 694–695.
Ivask, A., Juganson, K., Bondarenko, O., Mortimer, M., Aruoja, V., Kasemets, K., Blinova, I., Heinlaan, M., Slaveykova, V., and Kahru, A. (2014). "Mechanisms of toxic action of Ag, ZnO and CuO nanoparticles to selected ecotoxicological test organisms and mammalian cells in vitro: a comparative review." *Nanotoxicology*, 8 Suppl 1, 57–71.
James, D. W., and Topper, K. F. (2010). "Utah Fertilizer Guide." *AG431. Utah State University Extension, Logan*, (December).
Jones, D. L. (1998). "Organic acids in the rhizosphere – a critical review." *Plant and Soil*, 205(1), 25–44.
Jones, J., and Case, V. (1990). "Sampling, handling, and analyzing plant tissue samples." *R. L. Westerman (ed) Soil testing and plant analysis.*, American Society of Agronomy, Madison WI.
Joshi, S., Ghosh, I., Pokhrel, S., Mädler, L., and Nau, W. M. (2012). "Interactions of amino acids and polypeptides with metal oxide nanoparticles probed by fluorescent indicator adsorption and displacement." *ACS Nano*, 6(6), 5668–79.
Jośko, I., and Oleszczuk, P. (2013). "Manufactured Nanomaterials: The Connection Between Environmental Fate and Toxicity." *Critical Reviews in Environmental Science and Technology*, 43(23), 2581–2616.
Karlsson, T., Persson, P., and Skyllberg, U. (2006). "Complexation of Copper(II) in Organic Soils and in Dissolved Organic Matter − EXAFS Evidence for Chelate Ring Structures." *Environmental Science and Technology*, 40(8), 2623–2628.
Keller, A. A., Wang, H., Zhou, D., Lenihan, H. S., Cherr, G., Cardinale, B. J., Miller, R., and

Ji, Z. (2010). "Stability and aggregation of metal oxide nanoparticles in natural aqueous matrices." *Environmental Science and Technology*, 44(6), 1962–7.

Kim, S., Lee, S., and Lee, I. (2012). "Alteration of Phytotoxicity and Oxidant Stress Potential by Metal Oxide Nanoparticles in *Cucumis sativus*." *Water, Air, & Soil Pollution*, 223(5), 2799–2806.

Kim, S., Lim, H., and Lee, I. (2010). "Enhanced heavy metal phytoextraction by Echinochloa crus-galli using root exudates." *Journal of Bioscience and Bioengineering*, 109(1), 47–50.

Kiser, M. A., Ladner, D. A., Hristovski, K. D., and Westerhoff, P. K. (2012). "Nanomaterial transformation and association with fresh and freeze-dried wastewater activated sludge: implications for testing protocol and environmental fate." *Environmental Science and Technology*, 46(13), 7046–53.

Kopittke, P. M., Menzies, N. W., de Jonge, M. D., McKenna, B. A., Donner, E., Webb, R. I., Paterson, D. J., Howard, D. L., Ryan, C. G., Glover, C. J., Scheckel, K. G., and Lombi, E. (2011). "In situ distribution and speciation of toxic copper, nickel, and zinc in hydrated roots of cowpea." *Plant Physiology*, 156(2), 663–73.

Kováčik, J., Klejdus, B., Hedbavny, J., Stork, F., and Grúz, J. (2012). "Modulation of copper uptake and toxicity by abiotic stresses in Matricaria chamomilla plants." *Journal of Agricultural and Food Chemistry*, 60(27), 6755–63.

Kramer, P. J., and Boyer, J. S. (1995). *Water Relations of Plants and Soils*.

Lee, J., Mahendra, S., and Alvarez, P. J. J. (2010). "Potential Environmental and Human Health Impacts of Nanomaterials Used in the Construction Industry." *ACS Nano*, 4, 3580–3590.

Lee, S., Chung, H., Kim, S., and Lee, I. (2013). "The Genotoxic Effect of ZnO and CuO Nanoparticles on Early Growth of Buckwheat, *Fagopyrum Esculentum*." *Water, Air, & Soil Pollution*, 224(9), 1668.

Lee, W.-M., An, Y.-J., Yoon, H., and Kweon, H.-S. (2008). "Toxicity and bioavailability of copper nanoparticles to the terrestrial plants mung bean (*Phaseolus radiatus*) and wheat (*Triticum aestivum*): plant agar test for water-insoluble nanoparticles." *Environmental Toxicology and Chemistry*, 27(9), 1915–1921.

Lindsay, W. L. (1979). "Chemical equilibria in soils." John Wiley and Sons Ltd.

Lynch, I., and Dawson, K. A. (2008). "Protein-nanoparticle interactions." *Nano Today*, 3(1–2), 40–47.

Ma, J. F., Kusanoa, G., Kimuraa, S., and Nomoto, K. (1993). "Specific recognition of mugineic acid-ferric complex by barley roots." *Phytochemistry*, 34(3), 599–603.

Ma, J. F., and Nomoto, K. (1993). "Inhibition of mugineic acid-ferric complex uptake in barley by copper, zinc and cobalt." *Physiologia Plantarum*, 89(2), 331–334.

Ma, J. F., and Nomoto, K. (1996). "Effective regulation of iron acquisition in graminaceous plants. The role of mugineic acids as phytosiderophores." *Physiologia Plantarum*, 97(3), 609–617.

Maksymiec, W. (1998). "Effect of copper on cellular processes in higher plants." *Photosynthetica*, 34(3), 321–342.

Manceau, A., and Matynia, A. (2010). "The nature of Cu bonding to natural organic matter." *Geochimica et Cosmochimica Acta*, 74(9), 2556–2580.

Marion, G. M., and Babcock, K. L. (1976). "Predicting Specific Conductance and Salt Concentration in Dilute Aqueous Solutions." *Soil Science*, 122(4), 181–187.
Marschner, H. (1995). *Mineral Nutrition of Higher Plants*.
Martineau, N., McLean, J. E., Dimkpa, C. O., Britt, D. W., and Anderson, A. J. (2014). "Components from wheat roots modify the bioactivity of ZnO and CuO nanoparticles in a soil bacterium." *Environmental Pollution*, 187, 65–72.
McBride, M., and MartÍnez, C. (2000). "Copper phytotoxicity in a contaminated soil: remediation tests with adsorptive materials." *Environmental Science and Technology*, (607), 4386–4391.
McLean, J. E., Pabst, M. W., Miller, C. D., Dimkpa, C. O., and Anderson, A. J. (2013). "Effect of complexing ligands on the surface adsorption, internalization, and bioresponse of copper and cadmium in a soil bacterium, *Pseudomonas putida*." *Chemosphere*, 91(3), 374–382.
Mench, M., Morel, J. L., and Guckert, A. (1987). "Metal binding properties of high molecular weight soluble exudates from maize (Zea mays L.) roots." *Biology and Fertility of Soils*, 3(3), 165–169.
Michaud, A. M., Bravin, M. N., Galleguillos, M., and Hinsinger, P. (2007). "Copper uptake and phytotoxicity as assessed in situ for durum wheat (Triticum turgidum durum L.) cultivated in Cu-contaminated, former vineyard soils." *Plant and Soil*, 298(1–2), 99–111.
Michaud, A. M., Chappellaz, C., and Hinsinger, P. (2008). "Copper phytotoxicity affects root elongation and iron nutrition in durum wheat (*Triticum turgidum durum L.*)." *Plant and Soil*, 310(1–2), 151–165.
Misra, S. K., Dybowska, A., Berhanu, D., Luoma, S. N., and Valsami-jones, E. (2012). "The complexity of nanoparticle dissolution and its importance in nanotoxicological studies." *Science of the Total Environment*, 438, 225–232.
Mudunkotuwa, I. a., Pettibone, J. M., and Grassian, V. H. (2012). "Environmental implications of nanoparticle aging in the processing and fate of copper-based nanomaterials." *Environmental Science and Technology*, 46(13), 7001–7010.
Murakami, T., Ise, K., Hayakawa, M., Kamei, S., and Takagi, S. (1989). "Stabilities of metal complexes of mugineic acids and their specific affinities for iron(III)." *Chemistry Letters*, (12), 2137–2140.
Murphy, A., and Taiz, L. (1997). "Correlation between potassium efflux and copper sensitivity in 10 Arabidopsis ecotypes." *New Phytologist*, 136(2), 211–222.
Nair, P. M. G., and Chung, I. M. (2015a). "Biochemical, anatomical and molecular level changes in cucumber (Cucumis sativus) seedlings exposed to copper oxide nanoparticles." *Biologia*, 70(12), 1575–1585.
Nair, P. M. G., and Chung, I. M. (2015b). "Study on the correlation between copper oxide nanoparticles induced growth suppression and enhanced lignification in Indian mustard (Brassica juncea L.)." *Ecotoxicology and Environmental Safety*, 113, 302–13.
Navarro, E., Baun, A., Behra, R., Hartmann, N. B., Filser, J., Miao, A.-J., Quigg, A., Santschi, P. H., and Sigg, L. (2008). "Environmental behavior and ecotoxicity of engineered nanoparticles to algae, plants, and fungi." *Ecotoxicology*, 17(5), 372–86.

Neumann, G., and Römheld, V. (2012). *Marschner's Mineral Nutrition of Higher Plants*. *Marschner's Mineral Nutrition of Higher Plants*, Elsevier.
Nezhad, S. S., Khorasgani, M. R., Emtiazi, G., Yaghoobi, M. M., and Shakeri, S. (2014). "Isolation of copper oxide (CuO) nanoparticles resistant Pseudomonas strains from soil and investigation on possible mechanism for resistance." *World Journal of Microbiology and Biotechnology*, 30(3), 809–17.
Nian, H., Yang, Z. M., Ahn, S. J., Cheng, Z. J., and Matsumoto, H. (2002). "A comparative study on the aluminium- and copper-induced organic acid exudation from wheat roots." *Physiologia Plantarum*, 116(3), 328–335.
Oburger, E., Gruber, B., Schindlegger, Y., Schenkeveld, W. D. C., Hann, S., Kraemer, S. M., Wenzel, W. W., and Puschenreiter, M. (2014). "Root exudation of phytosiderophores from soil-grown wheat." *The New phytologist*, 203(4), 1161–74.
Odzak, N., Kistler, D., Behra, R., and Sigg, L. (2014). "Dissolution of metal and metal oxide nanoparticles in aqueous media." *Environmental Pollution*, 191, 132–8.
Odzak, N., Kistler, D., Behra, R., and Sigg, L. (2015). "Dissolution of metal and metal oxide nanoparticles under natural freshwater conditions." *Environmental Chemistry*, 12(2), 138.
Otero-González, L., Field, J. A., and Sierra-Alvarez, R. (2014). "Inhibition of anaerobic wastewater treatment after long-term exposure to low levels of CuO nanoparticles." *Water Research*, 58, 160–8.
Pallagi, A., Bajnoczi, E., Canton, S. E., Bolin, T., Peintler, G., Kutus, B., Kele, Z., Palinko, I., and Sipos, P. (2014). "Multinuclear complex formation between Ca(II) and gluconate ions in hyperalkaline solutions." *Environmental Science and Technology*, 48(12), 6604–6611.
Pallagi, A., Sebk, P., Forg, P., Jakusch, T., Palinko, I., and Sipos, P. (2010). "Multinuclear NMR and molecular modelling investigations on the structure and equilibria of complexes that form in aqueous solutions of Ca2+ and gluconate." *Carbohydrate Research*, 345(13), 1856–1864.
Paquin, P. R., Santore, R. C., Wu, K. B., Kavvadas, C. D., and Di Toro, D. M. (2000). "The biotic ligand model: a model of the acute toxicity of metals to aquatic life." *Environmental Science and Policy*, 3, 175–182.
Parker, D. R., Norvell, W. A., and Chaney, R. L. (1995). "Chemical Equilibrium and Reaction Models." *Chemical Equilibrium and Reaction Models*, SSSA Special Publication, Madison WI., 253–269.
Parker, D. R., Pedler, J. F., Ahnstrom, Z. A. S., and Resketo, M. (2001). "Reevaluating the free-ion activity model of trace metal toxicity toward higher plants: Experimental evidence with copper and zinc." *Environmental Toxicology and Chemistry*, 20(4), 899–906.
Peng, C., Zhang, H., Fang, H., Xu, C., Huang, H., Wang, Y., Sun, L., Yuan, X., Chen, Y., and Shi, J. (2015). "Natural organic matter-induced alleviation of the phytotoxicity to rice (Oryza sativa L.) caused by copper oxide nanoparticles." *Environmental Toxicology and Chemistry*, 34(9), 1996–2003.
Rachou, J., Gagnon, C., and Sauvé, S. (2007). "Use of an ion-selective electrode for free copper measurements in low salinity and low ionic strength matrices."

Environmental Chemistry, 4, 90–97.
R Core Team. (2013). "R: A Language and Environment for Statistical Computing." R Foundation for Statistical Computing, Vienna, Austria.
Reed, S., and Martens, D. (1996). *Methods of Soil Analysis Part 3—Chemical Methods*. *Methods of Soil Analysis Part 3—Chemical Methods*, SSSA Book Series, Soil Science Society of America, American Society of Agronomy.
Reichard, P. U., Kraemer, S. M., Frazier, S. W., and Kretzschmar, R. (2005). "Goethite Dissolution in the Presence of Phytosiderophores: Rates, Mechanisms, and the Synergistic Effect of Oxalate." *Plant and Soil*, 276(1–2), 115–132.
Reichman, S. M., and Parker, D. R. (2007). "Probing the effects of light and temperature on diurnal rhythms of phytosiderophore release in wheat." *The New Phytologist*, 174(1), 101–8.
Rivera-Gil, P., Jimenez de Aberasturi, D., Wulf, V., Pelaz, B., del Pino, P., Zhao, Y., de la Fuente, J. M., Ruiz de Larramendi, I., Rojo, T., Liang, X.-J., and Parak, W. J. (2013). "The challenge to relate the physicochemical properties of colloidal nanoparticles to their cytotoxicity." *Accounts of Chemical Research*, 46(3), 743–9.
Rivera Gil, P., Oberdörster, G., Elder, A., Puntes, V., and Parak, W. J. (2010). "Correlating physico-chemical with toxicological properties of nanoparticles: the present and the future." *ACS Nano*, 4(10), 5527–31.
Roos, J. T. H., and Williams, D. R. (1977). "Formation constants for citrate-, folic acid-, gluconate- and succinate-proton, -manganese(II), and -zinc(II) systems: relevance to absorption of dietary manganese, zinc and iron." *Journal of Inorganic and Nuclear Chemistry*, 39(2), 367–369.
Rousk, J., Ackermann, K., Curling, S. F., and Jones, D. L. (2012). "Comparative toxicity of nanoparticulate CuO and ZnO to soil bacterial communities." *PloS one*, 7(3), e34197.
Rouwenhorst, R. J., Frank Jzn, J., Scheffers, W. A., and van Dijken, J. P. (1991). "Determination of protein concentration by total organic carbon analysis." *Journal of Biochemical and Biophysical Methods*, 22(2), 119–128.
Ryan, B. M., Kirby, J. K., Degryse, F., Harris, H., Mclaughlin, M. J., and Scheiderich, K. (2013). "Copper speciation and isotopic fractionation in plants: Uptake and translocation mechanisms." *New Phytologist*, 199(2), 367–378.
Sauve, S., Hendershot, W., and Allen, H. E. (2000). "Solid-Solution Partitioning of Metals in Contaminated Soils: Dependence on pH, Total Metal Burden, and Organic Matter." *Environmental Science and Technology*, 34(7).
Saxton, K. E., and Rawls, W. J. (2006). "Soil Water Characteristic Estimates by Texture and Organic Matter for Hydrologic Solutions." *Soil Science Society of America Journal*, 70(5), 1569.
Schenkeveld, W. D. C., Oburger, E., Gruber, B., Schindlegger, Y., Hann, S., Puschenreiter, M., and Kraemer, S. M. (2014). "Metal mobilization from soils by phytosiderophores - experiment and equilibrium modeling." *Plant and Soil*, 383(1–2), 59–71.
Schindlegger, Y., Oburger, E., Gruber, B., Schenkeveld, W. D. C., Kraemer, S. M., Puschenreiter, M., Koellensperger, G., and Hann, S. (2014). "Accurate LC-ESI-

MS/MS quantification of 2'-deoxymugineic acid in soil and root related samples employing porous graphitic carbon as stationary phase and a $^{13}C_4$-labeled internal standard." *Electrophoresis*, 35(9), 1375–85.

Schubert, J., and Lindenbaum, A. (1952). "Stability of Alkaline Earth—Organic Acid Complexes Measured by Ion Exchange." *Journal of the American Chemical Society*, 74, 3529–3532.

Servin, A., Elmer, W., Mukherjee, A., De la Torre-Roche, R., Hamdi, H., White, J. C., Bindraban, P., and Dimkpa, C. (2015). "A review of the use of engineered nanomaterials to suppress plant disease and enhance crop yield." *Journal of Nanoparticle Research*.

Shi, J., Abid, A. D., Kennedy, I. M., Hristova, K. R., and Silk, W. K. (2011). "To duckweeds (Landoltia punctata), nanoparticulate copper oxide is more inhibitory than the soluble copper in the bulk solution." *Environmental Pollution*, 159(5), 1277–82.

Sinhal, V. K., Srivastava, A., and Singh, V. P. (2010). "EDTA and citric acid mediated phytoextraction of Zn, Cu, Pb and Cd through marigold (Tagetes erecta)." *Journal of Environmental Biology*, 31(3), 255–9.

Sousa, V. S., and Teixeira, M. R. (2013). "Aggregation kinetics and surface charge of CuO nanoparticles: the influence of pH, ionic strength and humic acids." *Environmental Chemistry*, 10(4), 313.

Stampoulis, D., Sinha, S. K., and White, J. C. (2009). "Assay-dependent phytotoxicity of nanoparticles to plants." *Environmental Science and Technology*, 43(24), 9473–9.

Studer, A. M., Limbach, L. K., Van Duc, L., Krumeich, F., Athanassiou, E. K., Gerber, L. C., Moch, H., and Stark, W. J. (2010). "Nanoparticle cytotoxicity depends on intracellular solubility: comparison of stabilized copper metal and degradable copper oxide nanoparticles." *Toxicology Letters*, 197(3), 169–74.

Terzano, R., Cesco, S., and Mimmo, T. (2015). "Dynamics, thermodynamics and kinetics of exudates: crucial issues in understanding rhizosphere processes." *Plant and Soil*, 386(1–2), 399–406.

Thakali, S., Allen, H. E., Di Toro, D. M., Ponizovsky, A. A., Rooney, C. P., Zhao, F.-J., and McGrath, S. P. (2006). "A Terrestrial Biotic Ligand Model. 1. Development and Application to Cu and Ni Toxicities to Barley Root Elongation in Soils." *Environmental Science and Technology*, 40(22), 7085–7093.

Thakkar, K. N., Mhatre, S. S., and Parikh, R. Y. (2010). "Biological synthesis of metallic nanoparticles." *Nanomedicine : Nanotechnology, Biology, and Medicine*, 6(2), 257–62.

Treeby, M., Marschner, H., and Römheld, V. (1989). "Mobilization of iron and other micronutrient cations from a calcareous soil by plant-borne, microbial, and synthetic metal chelators." *Plant and Soil*, 114(2), 217–226.

Trujillo-Reyes, J., Majumdar, S., Botez, C. E., Peralta-Videa, J. R., and Gardea-Torresdey, J. L. (2014). "Exposure studies of core-shell Fe/Fe(3)O(4) and Cu/CuO NPs to lettuce (Lactuca sativa) plants: Are they a potential physiological and nutritional hazard?" *Journal of Hazardous Materials*, 267, 255–63.

Tsednee, M., Mak, Y.-W., Chen, Y.-R., and Yeh, K.-C. (2012). "A sensitive LC-ESI-Q-TOF-MS method reveals novel phytosiderophores and phytosiderophore-iron complexes in barley." *The New Phytologist*, 195(4), 951–61.

USEPA. (1979). "'Methods for Chemical Analysis of Water and Wastes.'" *EPA 600 Series*, Washington, D.C., D.C., EPA 600 Se(USEPA-600), 4-79–20.

USEPA. (1996). *Test Methods for Evaluating Solid Waste. Method 3050B-1. Acid Digestion of Sediments, Sludges, and Soils. Revision 2. EPA/SW-846.*, National Technical Information Service, Springfield, Va.

Wang, L.-F., Habibul, N., He, D.-Q., Li, W.-W., Zhang, X., Jiang, H., and Yu, H.-Q. (2015). "Copper release from copper nanoparticles in the presence of natural organic matter." *Water Research*, 68, 12–23.

Wang, S., Nan, Z., Liu, X., Li, Y., Qin, S., and Ding, H. (2009). "Accumulation and bioavailability of copper and nickel in wheat plants grown in contaminated soils from the oasis, northwest China." *Geoderma*, 152(3–4), 290–295.

Wang, Z., Von Dem Bussche, A., Kabadi, P. K., Kane, A. B., and Hurt, R. H. (2013). "Biological and environmental transformations of copper-based nanomaterials." *ACS Nano*, 7(10), 8715–8727.

Wang, Z., Xie, X., Zhao, J., Liu, X., Feng, W., White, J. C., and Xing, B. (2012). "Xylem- and phloem-based transport of CuO nanoparticles in maize (Zea mays L.)." *Environmental Science and Technology*, 46(8), 4434–41.

Watson, J.-L., Fang, T., Dimkpa, C. O., Britt, D. W., McLean, J. E., Jacobson, A., and Anderson, A. J. (2014). "The phytotoxicity of ZnO nanoparticles on wheat varies with soil properties." *Biometals*, 28(1), 101–112.

White, P. J., and Broadley, M. R. (2009). "Biofortification of crops with seven mineral elements often lacking in human diets--iron, zinc, copper, calcium, magnesium, selenium and iodine." *The New Phytologist*, 182(1), 49–84.

von Wiren, N. (2000). "Hydroxylated Phytosiderophore Species Possess an Enhanced Chelate Stability and Affinity for Iron(III)." *Plant Physiology*, 124(3), 1149–1158.

Von Wiren, N., Romheld, V., Morel, J., Guckert, A., and Marchner, H. (1993). "Influence of microorganisms on iron acquisition in maize." *Soil Biology and Biochemistry*, 25(3), 371–376.

Wu, S. G., Kong, I.-C., Tang, Y. J., Huang, L., J, H., DR, C., and IC, K. (2012). "Phytotoxicity of Metal Oxide Nanoparticles is Related to Both Dissolved Metals Ions and Adsorption of Particles on Seed Surfaces." *Journal of Petroleum and Environmental Biotechnology*, 3(126).

Xu, M., Li, J., Iwai, H., Mei, Q., Fujita, D., Su, H., Chen, H., and Hanagata, N. (2012). "Formation of nano-bio-complex as nanomaterials dispersed in a biological solution for understanding nanobiological interactions." *Nature*, 2, 406.

Xuan, Y., Scheuermann, E. B., Meda, A. R., Hayen, H., von Wirén, N., and Weber, G. (2006). "Separation and identification of phytosiderophores and their metal complexes in plants by zwitterionic hydrophilic interaction liquid chromatography coupled to electrospray ionization mass spectrometry." *Journal of Chromatography A*, 1136(1), 73–81.

Zuverza-Mena, N., Medina-Velo, I. A., Barrios, A. C., Tan, W., Peralta-Videa, J. R., and

Gardea-Torresdey, J. L. (2015). “Copper nanoparticles/compounds impact agronomic and physiological parameters in cilantro (Coriandrum sativum).” *Environmental Science*, 17(10), 1783–93.

Supporting information

Material and Methods – Supporting Information

Table 3-6. Correction Factors to account for water losses and dilutions in exudate extraction.

	CuO NP Dose	Initial Solution Added (mL)	Solution Loss (mL)	Solution Left in sand (mL)	Flush water added (mL)	Total water (mL)	Correction factor (Compare between planted treatments)	Correction factor (Compare to unplanted treatments)
Planted	0	45	14.4	30.6	45	75.6	2.5	1.7
	30	24	9.9	14.1	24	38.1	2.7	1.6
	10	16.5	11.2	5.3	16.5	21.8	4.1	1.3
	30	10.5	8.3	2.2	15.5	17.7	8.1	1.7
Unplanted	0	45	16.5	28.5	45	73.5	NA	1.63
	30	24	4.3	19.7	24	43.7	NA	1.82
	10	16.5	5.3	11.2	16.5	27.7	NA	1.68
	30	10.5	7.6	2.9	15.5	18.4	NA	1.75

Table 3-7. Thermodynamic database inputs for DMA and gluconate.

p = metal (cation), q =ligand (as anion), r = proton (H).

Complex	notation (pqr)	log K	Source
HGluconate	011	3.66	(Bechtold et al. 2002)
CuGluconate	110	2.51	(Gajda et al. 1998)
$CuGluconate(OH)_3$	11-3	-20.96	(Gajda et al. 1998)
$CuGluconate_2$	120	4.59	(Gajda et al. 1998)
$CuGluconate_2(OH)$	12-1	-0.6	(Gajda et al. 1998)
$CuGluconate_2(OH)_2$	12-2	-8.28	(Gajda et al. 1998)
$Cu_2Gluconate_2(OH)_3$	22-3	-7.25	(Gajda et al. 1998)
$Cu_2Gluconate_2(OH)_4$	22-4	-15.46	(Gajda et al. 1998)
FeGluconate	110	10.51	(Bechtold et al. 2002)
FeGluconate(OH)	11-1	9.03	(Bechtold et al. 2002)

Complex	notation (pqr)	log K	Source
$FeGluconate(OH)_2$	11-2	6.35	(Bechtold et al. 2002)
$FeGluconate(OH)_3$	11-3	1.78	(Bechtold et al. 2002)
$FeGluconate(OH)_4$	11-4	-8.4	(Bechtold et al. 2002)
$FeGluconate_2$	120	22.23	(Bechtold et al. 2002)
$FeGluconate_2(OH)$	12-1	18.22	(Bechtold et al. 2002)
$FeGluconate_2(OH)_2$	12-2	15.3	(Bechtold et al. 2002)
$FeGluconate_2(OH)_3$	12-3	9.84	(Bechtold et al. 2002)
$FeGluconate_2(OH)_4$	12-4	-1.15	(Bechtold et al. 2002)
$FeGluconate_2(OH)_5$	12-5	-20	(Bechtold et al. 2002)
$Fe_2Gluconate_2(OH)_7$	22-7	-1.42	(Bechtold et al. 2002)
$CaFeGluconate_2$		20.96	(Bechtold et al. 2002)
$CaFeGluconate_2(OH)$		22.47	(Bechtold et al. 2002)
$CaFeGluconate_2(OH)_2$		19.06	(Bechtold et al. 2002)
$CaFeGluconate_2(OH)_3$		14.82	(Bechtold et al. 2002)
$CaFeGluconate_2(OH)_4$		6.65	(Bechtold et al. 2002)
$CaFeGluconate_2(OH)_5$		-2.63	(Bechtold et al. 2002)
CaFeGluconate		16.26	(Bechtold et al. 2002)
CaFeGluconate(OH)		13.89	(Bechtold et al. 2002)
$CaFeGluconate(OH)_2$		11.21	(Bechtold et al. 2002)
$CaFeGluconate(OH)_3$		7.13	(Bechtold et al. 2002)
$CaFeGluconate(OH)_4$		-1	(Bechtold et al. 2002)
$CaFeGluconate(OH)_5$		-11.01	(Bechtold et al. 2002)
ZnGluconate	110	1.7	(Cannan and Kibrick 1938)
ZnGluconate	11-1?	1.49	(Roos and Williams 1977)
ZnGluconate(OH)	11-1	9.76	(Eby 2004)
CaGluconate	110	1.21	(Cannan and Kibrick 1938)
CaGluconate	110	1.22	(Schubert and Lindenbaum 1952)
CaGluconate estimate as IS->0	110	1.8	(Pallagi et al. 2010)
CaGluconate pH 6	110	0.99	(Pallagi et al. 2010)
CaGluconate pH 8	110	1.05	(Pallagi et al. 2010)
CaGluconate	110	0.37	(Pallagi et al. 2014)
CaGluonate(OH)	11-1	2.82	(Pallagi et al. 2014)
$Ca_2Gluconate(OH)_3$	21-3	8.04	(Pallagi et al. 2014)
$Ca_3Gluconate_2(OH)_4$	32-4	12.44	(Pallagi et al. 2014)
Cu-DMA	110	18.7	(Murakami et al. 1989)
Fe-DMA	110	18.38	(Murakami et al. 1989)
Fe-DMA-OH	11-1	16.25	(Murakami et al. 1989)

Table 3-8. Inputs used in MINTEQ (units as indicated).

MINTEQ DATA INPUTS EXPT 3 ONLY

mg/L	0	10	30	100	200	300
Cu2+ ISE ug/L	0.40	0.31	1.15	0.90	1.88	3.59
mg/L						
<1 nm Na	28	35	35	88	122	181
<1 nm Mg	4	5	6	12	17	25
<1 nm Ca	21	25	28	51	66	130
<1 nm K	8	5	6	12	13	24
<1 nm Al	0.59	0.86	0.89	1.99	3.18	3.14
<1 nm Mn	0.03	0.03	0.05	0.01	0.05	0.03
<1 nm Fe	0.20	0.32	0.28	0.37	0.51	0.26
<1 nm Cu	0.01	0.19	0.49	2.04	5.61	6.00
<1 nm Zn	0.05	0.02	0.03	0.05	0.07	0.04
<1 nm Ni	0.02	0.02	0.04	0.03	0.05	0.09
mg/L						
Gluconate	16.7	24.6	30.7	81.9	114.1	111.9
Oac (acetate)	0.5	0.5	0.9	2.8	3.0	5.9
Formate	2.4	0.9	2.9	4.0	4.9	5.4
Chloride	2.1	2.8	3.1	6.0	9.1	12.9
Nitrate	119	124	164	278	336	665
Malate	22.1	28.7	34.8	53.6	71.1	67.7
Oxalate	0.2	0.2	0.3	0.5	1.0	0.6
Citrate	7.3	11.2	18.5	36.6	48.1	40.8
DMA	0.44	0.57	0.77	1.80	3.26	3.94
Ala	0.20	0.06	0.04	0.14	0.15	0.31
Arg	0.59	0.40	0.38	0.95	0.50	1.56
Asp	0.28	0.12	0.27	0.41	0.88	2.19
Glu	0.22	0.13	0.09	0.12	0.20	0.38
Gly	0.18	0.07	0.25	0.92	1.29	1.50
Ile	0.12	0.44	0.29	0.71	1.06	1.11
Leu	0.13	0.53	0.32	0.87	1.27	1.48
Lys	0.12	0.08	0.05	0.06	0.06	0.11
Met		0.05	0.07	0.13	0.16	0.21
Phe	0.15	0.40	0.23	0.79	1.14	1.36
Pro	0.23	0.91	0.38	1.23	2.19	0.83
Ser	0.15	0.41	0.13	0.52		
Thr	0.18	0.10	0.10	0.10	0.14	0.18
Tyr	0.10	0.11	0.07	0.18	0.18	0.17
Val	0.41	0.70	0.24	0.59	1.42	1.60
pH	6.69	6.78	6.63	7.17	7.36	7.67
EC uS/cm	117	139	153	190	222	225
Solid CuO mM	0	2	5	32	76	150

Supporting Information: Results and discussion

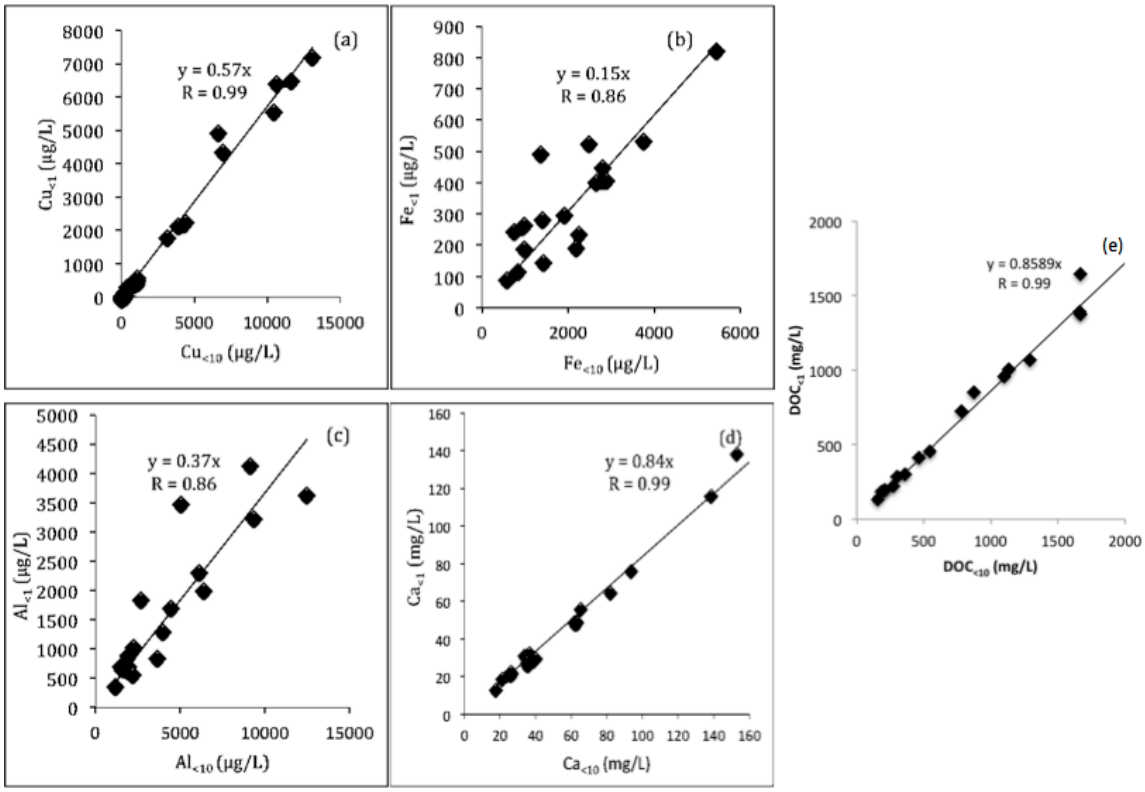

Fig. 3-7. Correlation between planted samples $M_{<1}$ and $M_{<10}$ of Cu (a), Fe (b), Al (c), and Ca (d) (µg/L) and $DOC_{<1}$ and $DOC_{<10}$ (mg/L) from final experiment (n=18) at different CuO NP doses. Pearson's correlations coefficients are shown (R). Unplanted Fe and Al (not shown) were below detection limit.

Table 3-9. pH of sand extract solution over the 3 separate studies.

	Study 1		Study 2		Study 3	
CuO NP dose	Planted	Unplanted	Planted	Unplanted	Planted	Unplanted
0	6.28	6.18	6.29	6.69	6.78	6.39
0	6.40	6.11	7.50	7.38	6.57	8.33
0	6.32	6.13	6.40	6.64	6.73	7.65
10	NA	NA	NA	NA	6.79	6.94
10	NA	NA	NA	NA	6.94	6.92
10	NA	NA	NA	NA	6.61	7.13
30	6.27	6.32	6.79	8.06	6.52	6.93
30	6.36	6.11	6.84	7.35	6.78	7.96
30	6.21	6.28	7.31	8.40	6.59	8.40
100	5.88	6.46	6.52	7.32	7.19	7.99
100	5.83	6.37	9.06	6.76	7.09	7.64
100	6.24	6.37	6.71	6.67	7.23	NA
200	NA	NA	NA	NA	7.14	8.51
200	NA	NA	NA	NA	7.32	7.61
200	NA	NA	NA	NA	7.63	6.63
300	5.75	6.37	6.61	7.42	7.41	6.51
300	6.2	6.3	6.72	6.61	7.67	6.73
300	6.03	6.34	6.67	6.85	7.94	6.68

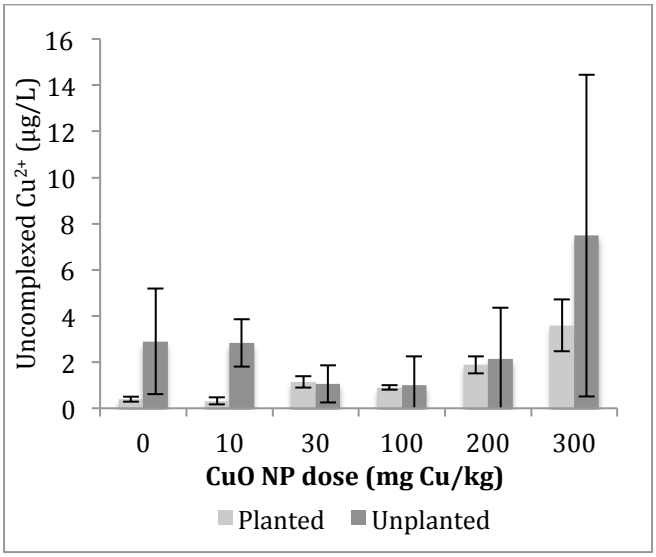

Fig. 3-8. Cu^{2+} measured from a Cu^{2+} ion selective electrode in planted and unplanted samples (n=3). Error bars indicate standard deviation.

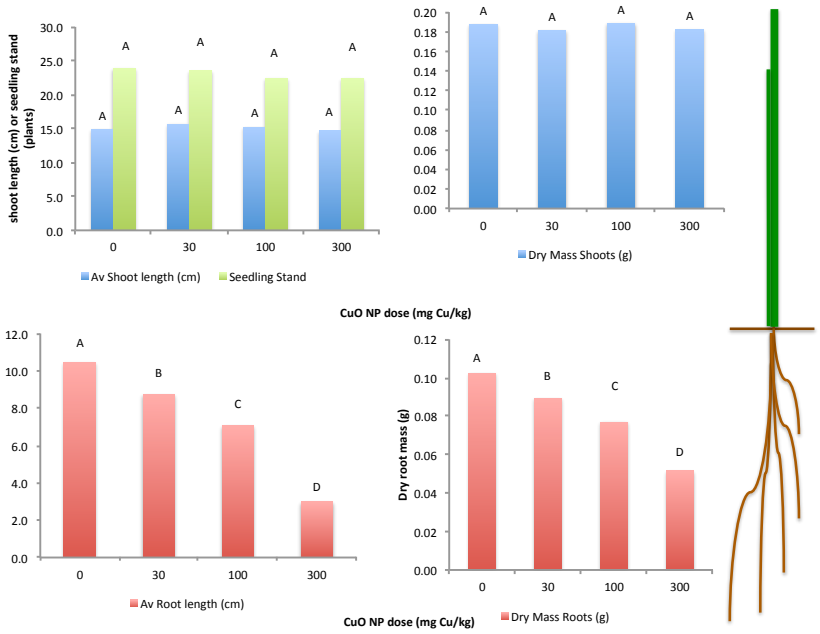

Fig. 3-9. Plant morphology in response to CuO NP dose (n = 9, apart from CuO NP 10, 200 n=3). Columns with the same letters are not significantly different (α=0.05) by Tukey's HSD.

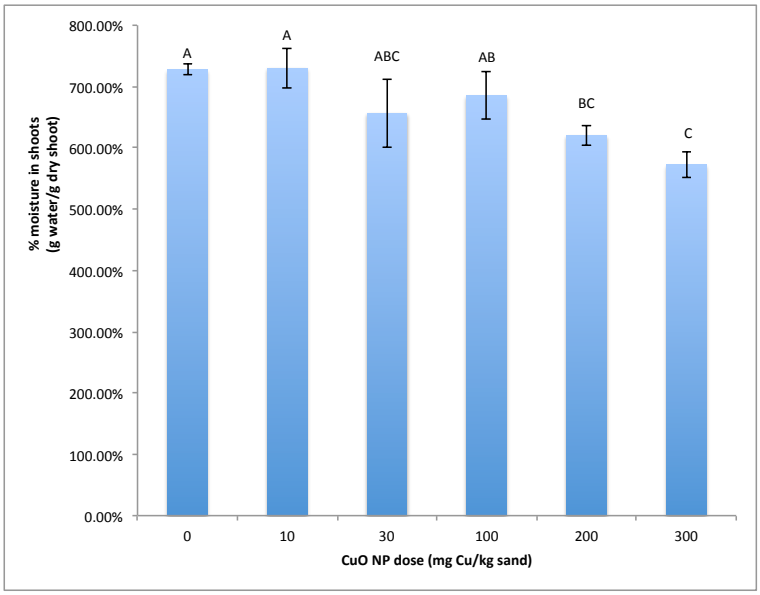

Fig. 3-10. Water content (g water/g dry shoot) across CuO NP doses (n=3). Columns with the same letters are not significantly different (α=0.05) by Tukey's HSD. Error bars represent standard deviation.

Table 3-10. Comparison of average $M_{<10}$ and $M_{<1}$ show the majority of Al and Fe particles are in the 1 – 10 nm range (n=3) across NP doses (mg Cu/kg dry sand).

ug/L	**0**	**30**	**100**	**300**
$Al_{<10}$	1423	3282	5649	5604
$Al_{<1}$	587	893	1990	3135
$Fe_{<10}$	770	2032	2482	1954
$Fe_{<1}$	197	284	367	265
mg/L	**0**	**30**	**100**	**300**
$Ca_{<10}$	24	37	63	152
$Ca_{<1}$	21	27	51	130
$Mg_{<10}$	4	7	14	29
$Mg_{<1}$	4	5	12	25
$K_{<10}$	9	7	14	27
$K_{<1}$	7	6	12	24
$Na_{<10}$	32	44	99	201
$Na_{<1}$	28	35	88	181

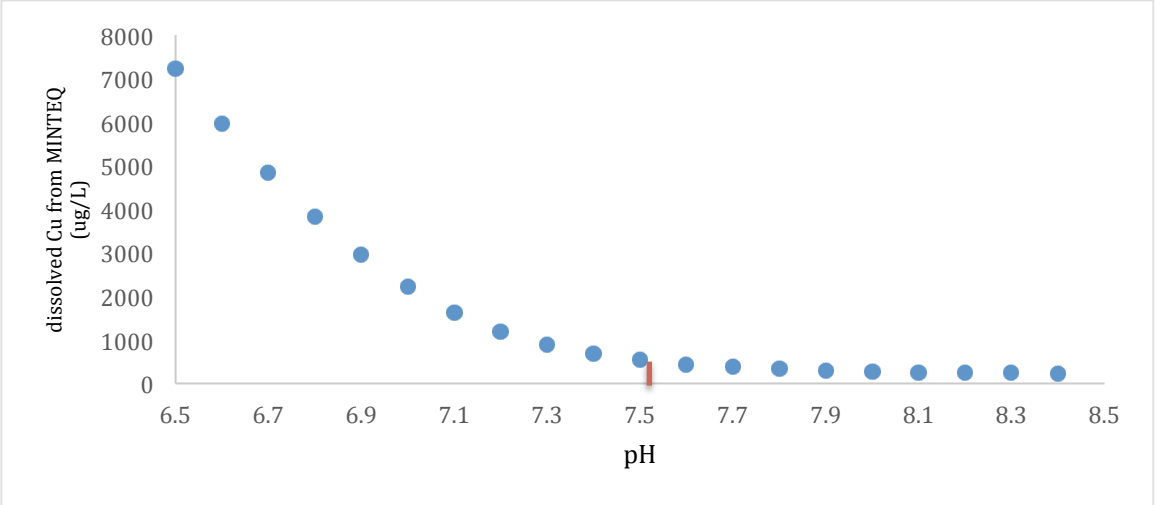

Fig. 3-11. CuO NP dose of 30 mg/kg: sensitivity to pH changes. Red mark indicates where model agrees with observed results (pH 7.55).

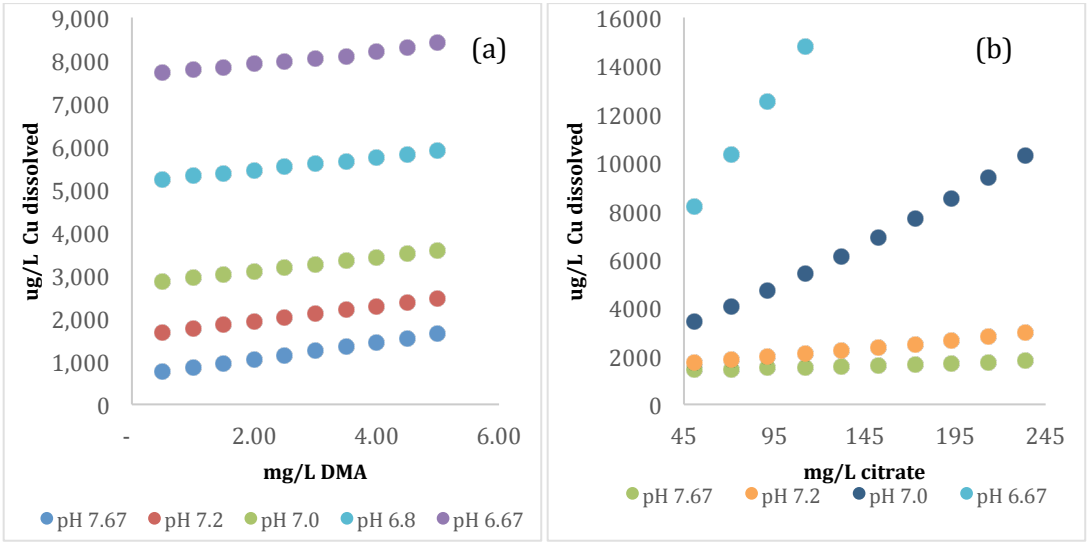

Fig. 3-12. Using 300 mg Cu/k as CuO NP sensitivity to DMA (a) and citrate (b) concentration is shown at pH range from 6.67 to 7.67, from MINTEQ geochemical model.

Table 3-11. Ionic strength comparisons in planted samples from experiment 3 from MINTEQ model and measured data (converted from EC as per (Marion and Babcock 1976)).

CuO NP dose	Charge Balance (% diff)	I (mM) (MINTEQ)	I (mM) (Measured)
0	7% low anions	3.3	4.7
10	11% low anions	3.8	5.5
30	5% low anions	4.4	6.7
100	12% low anions	8.3	12.5
200	15% low anions	10.6	16.5
300	14% low anions	18.2	29.6

Table 3-12. Comparison between dissolved Cu with a solid and no solid phase added to MINTEQ. The MINTEQ model was run with and without a solid CuO (crystalline) phase. The results are below (Table 0-5 and Fig. 0-2). At the lower NP

doses, the model fit better to measured data without the solid phase, while at the higher CuO NP doses, it was irrelevant due to high precipitation.

	Dissolved Cu (ug/L)		
CuO NP dose (mg Cu/kg)	No solid phase	Added CuO solid	pH
0	10	10	6.69
10	189	2,839	6.78
30	490	5,629	6.63
100	2,039	2,242	7.17
200	2,012	2,012	7.36
300	1,589	1,589	7.67

Table 3-13. Sensitivity of MINTEQ models to triplicate measurements of rhizosphere solution characteristics at CuO NP doses 30 and 100 mg Cu/kg dry sand. The mean of all inputs was used as the basis of that CuO NP dose over the triplicates measured. To assess the sensitivity of the model to individual inputs, especially pH, DMA and citrate concentrations, all the inputs were used to understand how they would impact the level of Cu dissolved in the MINTEQ model. A summary at CuO NP doses 30 and 100 mg Cu/kg dry sand are shown, along with probable drivers of the differences in Cu solubility.

CuO NP 30 mg Cu/kg sand

pH	dis Cu ug/L	Citrate (mg/L)	Probable driver?
6.52	5403	13.2	
6.78	4113	18.8	higher pH, higher citrate
6.59	7117	23.5	higher citrate, low pH

mean	5545
stdev	1507

5629	Using mean values (Table 3-5)

CuO NP
100 mg
Cu/kg
sand

pH	dis Cu ug/L	Citrate (mg/L)	Probable driver?
7.19	2734	43.2	
7.09	2445	33.8	lower citrate
7.23	1607	32.8	lower citrate, higher pH

mean	2262
stdev	585

2242	Using mean values (Table 3-5)

CHAPTER 4

ENGINEERING SIGNIFICANCE

Increased use of CuO NPs in agriculture and industry leads to increased likelihood of contamination in soil and water systems. It is crucial to understand under which agriculturally relevant scenarios (that is soils and soil processes) these nanoparticles present the greatest toxicity, and how the performance of wheat, a commercially significant crop, may be impacted. Rhizosphere processes are increasingly being recognized for their importance in consideration of pollutant, in addition to being the gateway of nutrient uptake into plants.

Conversely, as copper supplies across the world become more scarce (Dodson et al. 2012), CuO NPs may present opportunities for a more efficient delivery method in Cu deficient environments, or as fungicide and therefore the dynamics of plant-soil-NP interaction are especially important to investigate. With an increasing global population, land use will be an issue of critical importance to generate sufficient food supplies. Remediation of marginal lands is one way to increase land use, of which phytoremediation is an application. A better understanding of rhizosphere processes may uncover opportunities to make this process more effective.

Additionally, inefficient application of fertilizer has negative ramifications for water quality. NPs show a strong potential in effective delivery of nutrients, in

particular when designed to respond to plant exudates signaling a deficiency – analogously to how nanomedicines can be targeted in cancer applications. Capping a nanoparticle in a corona that responds specifically to a plant exudate, and releases a nutrient "on demand," may be a way to circumvent over application of fertilizers. For example, in calcareous soils, high pH drives low Fe and other micronutrient bioavailability. Chemical complexation is the mechanism that winter wheat employs to obtain Fe, releasing DMA and complexing Fe from solid phase, enabling plant uptake. Our work here provides some new additions to a rapidly expanding field of nano-agricultural applications.

Further Work

Extrapolating the findings of this simplified system into an agricultural context requires many modifications. Particularly, LMWOAs, AA and DMA (Von Wiren et al. 1993) are highly consumable by bacteria which are numerous in a soil system. Distance from the wheat root in general means lower LMWOAs and DMA (Von Wiren et al. 1993). This may reduce the concentration and thus their role in CuO NP dissolution, providing plant defense. Alternatively, bacteria and fungi produce siderophores that can chelate Cu and increase CuO NP solubility. Additionally, as outlined in Appendix B, soil systems have DOC that is multifaceted and highly complex. Components such as fulvic and humic acid (Watson et al. 2014) may reduce or increase solubility of Cu from the CuO NPs. Furthermore, soil may provide sorption sites, or provide inorganic anions (PO_4^{3-} and CO_3^{2-} for example) to

form Cu precipitates or cap the CuO NPs in coronas, impacting the forms of Cu available to the wheat plant. More investigation is required to completely understand the implications of increased CuO NP presence in soil.

APPENDICES

Appendix A: Soil components and copper availability

Understanding the factors in soil that mitigate or enhance the impact of CuO NPs and released Cu ions on the wheat plant is necessary to appreciate the transport of NPs, as well as the factors impacting Cu ions released from the CuO NPs.

pH

Lower pH will decrease available sorption sites in the soil, promoting soluble Cu, with higher pH increasing both soil sorption sites on soil organic matter and clays (Suave 1997, 2000) as well as precipitating Cu from solution. Thus, dissolution of CuO NPs is increased under acidic pH. The caveat is complex formation between Cu and dissolved organic matter from the soil, and bacterial and root exudates. Complexation is enhanced with increasing pH, as ligands are deprotonated.

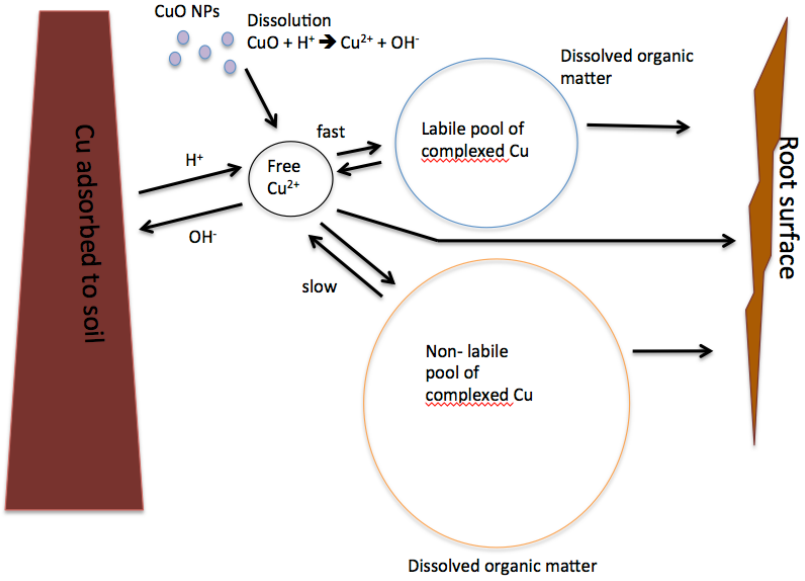

Fig. 0-1. Relationship between soil solid and solution phase, and impact on bioavailable Cu (modified from (McBride and MartÍnez 2000)).

Organic matter

Organic matter (decaying plant or animal matter) in soils may be dissolved or be in solid phase, called soil organic matter (SOM). SOM increases the cation exchange capacity (CEC) of the soil; in other words, the soil's ability to sorb Cu out of solution (Kramer and Boyer 1995).

DOC is contained in the solution phase of soils in varying quantities originating from different sources including organic matter breakdown and bacterial and root exudates. As suggested by Michaud et al. (2008), the DOC in soil has a large influence on the proportion of Cu remaining in solution, especially with increasing pH. For example, Blinova et al. (2010) analyzed several water types alongside CuO NPs to determine toxicity on bacteria and found that the proportion of DOC was highly significant in lowering the bioavailability of Cu in solution, the main driver of bacterial toxicity in this case; although the bioavailability was also impacted by ligand speciation. As indicated in Fig 6, DOC can bond with Cu in labile (easily exchangeable ligands) and non-labile pools, and provide a large buffer of Cu ions, even at high pH. The DOC species attached to Cu will affect bioavailability.

Soil solid phase

Sorption sites for Cu on soil minerals and SOM control how much of the Cu will be available in solution, providing a Cu buffer to the soil solution. The solid phase Cu supplies the labile, non-labile and free pools of soluble Cu (Fig. 0-1). Depending on the pH, soil type, and surface charge on the soil particle, the sorption capacity of soils for Cu vary greatly. In general, higher proportions of clay and SOM will increase a soil's cation exchange capacity CEC (Kramer and Boyer 1995).

Ionic strength

Increasing ionic strength, specifically polyvalent cations, decreases solution activity of other free ions, changing the behavior of that species in solution, and changing solubility of solid phase constituents. In the presence of other polyvalent cations Cu has less potential to sorb to a biological site of significance (fish gills, or plant roots for example.). The Biotic Ligand Model (BLM) considers competition between Cu and hardness cations (Ca and Mg) for bacterial or root sorption sites in aquatic systems (Paquin et al. 2000).

Soil bacteria

Rhizosphere bacteria represent the plant's "second genome" due to a strong symbiosis, providing defense against toxins at the root apices especially (Dennis et al. 2010). If bacteria in the rhizosphere are directly altered as a result of interaction with CuO NPs, the plant may be more susceptible to damage. For example, *Pseudomonas putida KT2440* was effected distinctly by CuO NPs as opposed to bulk CuO, suggesting aggregation of NPs may reduce their toxicity to soil microbes and hence soil health (Gajjar et al. 2009). NP behavior has been demonstrably different than 'bulk' CuO; both bioavailable Cu (complexed or free Cu^{2+}) and CuO NPs directly affected *Pseudamonas flourescens* bacteria (Kakinen et al 2011). It is therefore important to consider the impact of CuO NPs on soil bacterial communities in soil, and the potential for resulting symbiotic loss to the wheat plant in soils. Exudates from the root are key metabolites for microbial production of ethylene, a plant

signal controlling development, and the rate of exudation is increased in the presence of microbes (Dakora and Phillips 2002).

Appendix B: Preliminary experiments

A preliminary experiment comprising 2 treatments (with and without Fe solution) was performed to elucidate the concentration and type of root exudates in this sand-wheat system. Pre-germinated shoots over 3 days were placed on LB medium as a way to reduced shoot-media contamination, as well as being able to ensure wheat plants are grown in aseptic conditions. Treatments were grown over 14 days in sand, with 5 mM $CaCl_3$, 0.8 mM BO_3 and 50 µM $FeCl_3$ for all +Fe treatments.

For metal-organic complexes, I have begun testing for EDTA-Cu as an infusion (direct infusion bypassing the column) in an EIS-TOF as the first step for this process with assistance from the UWRL chromatography technician. EDTA-Cu has been detected at 1 mM Cu and 1.5 mM EDTA using formic acid mobile phase suggested by Tsednee et al. (2012). Cu-fumarate was not detected as a complex, only a fumarate ion, likely due to lower stability constant compared to EDTA at low pH ~3 under the same conditions. This will be followed by analyzing exudates from the preliminary study with pre-germinated wheat grown for 13 days in sand with +/- Fe.

A second preliminary study with control ±Fe and 300 mg/kg CuO NPs ±Fe was also performed (2.5 mM $CaCl_3$ was used to lower Cl levels for the IC, all other solutions were as above). Root exudates were analyzed using techniques above, and DOC as shown (**Table 0-1.**) (Background DOC at 10 mg/L from unplanted systems in sand was observed in Control +Fe replicate 5.) A particularly high value in –Fe CuO NP dose of 74 mg/L increased the standard deviation of this treatment. There was a

trend for higher DOC in NP treatments. Initial tests suggest background DOC will likely be lowered to < 5 mg/L by muffle furnace treated sand (550 °C) and using a Buchner funnel without GF/B, which is hoped will reduce standard deviation between treatments.

Table 0-1. DOC results from sand grown 17 day old wheat with/without Fe (50uM) solution and CuO NPs (N=5, apart from +Fe Control where N=4)

mg/L DOC ± Std Dev	+Fe	-Fe
Control	8±5	18±9
300 mg/kg CuO NP	19±4	41±19

LMWOA variability was high, and in many cases levels were low (<0.5 mg/L). Options to alleviate this issue include planting more plants per Magenta box (10 suggested as opposed to 5 per box here) or using a longer loop for the IC (increasing sensitivity).

Table 0-2. LMWOA resulting from sand grown 17 day old wheat with/without Fe solution and CuO NPs (N=5, apart from +Fe Control where N=4). All others <0.5 mg/L.

mg/L Butyrate ± Std Dev	+Fe	-Fe
Control	0.40±0.42	0±0
300 mg/kg CuO NP	3.33±0.64	0±0
mg/L Acetate ± Std Dev	+Fe	-Fe
Control	2.76±3.83	1.87±1.31
300 mg/kg CuO NP	0.74±0.40	1.97±0.71

Appendix C: Procedural development TOF and QqQ

- Challenges:
  - Difficulty with metal contamination
  - Fe/Cu from samples makes CCV recovery poor
  - DMA level at 0.2 μM, close to limit of detection (LOD)
- Initial drive to use Time Of Flight Mass spec to assess all Cu compounds
  - Concentration of individual complexes low, making detection difficult
- Used Ion Chromatography to TOF link to verify VFAs
  - DMA didn't elute off IC column
  - Confirmation of VFAs was possible – ammonia injection greatly aided sensitivity
- Tried QqQ MS
  - Initially infusion (no column) – MRM method 10^3 lower LOD
  - Zwitterionic column exceeded pressure threshold (broken column)
  - Chromatography poor and replication difficult to obtain
  - New zwitterionic column purchased
  - Direct to source syringe injection attempted
    - Lowest metal contamination so far
    - Suspect high Cu in solution (ions/complexes/NPs) that diverges from Xuan et al 2006 that method was modeled off
    - Sample clean up with ultra filtration/3 kDa spin filters next
  - Used MRM to detect DMA down to 0.1 uM levels

Appendix D: Detailed materials and methods

Experimental design

A randomized factorial design with CuO NPs at four concentrations (including 0) was used in this study. To have enough plant tissue for analysis 25 plants were grown per Magenta growth box (Sigma Aldrich, St Louis, MO, USA), with 9 replicated boxes for each treatment. Dry-weight root mass with 25 plants (1 Magenta box) for the most toxic dose CuO NPs (300 mg Cu/kg) yielded 0.05 g of tissue (determined from previous experiments), sufficient enough to determine uptake of metals into roots per kg of dry plant mass accurately. Plants grown without NPs served as the control. A Cu ion control, using Cu chloride salt, was not used. Ion controls have been used to compare ion versus NP effects, but the dissolution rate of CuO NPs is difficult to emulate (Dimkpa et al. 2012) , and may be highly dependent on proximity of the NP to the root surface (Shi et al. 2011).

Each Magenta box was treated as an independent microcosm. Shoot tissue, root tissue and sand solution were linked for statistical comparisons **Fig. 0-2.**

Material and methods

Sources of NPs and sand

The CuO NPs were obtained from Sigma-Aldrich Chemical Company (St Louis, MO), have been previously characterized by our group. The CuO NPs were characterized using the methods used by this research group to characterize other NPs (Table 0-3.). The sand used as a growth matrix (muffle oven heated to 550 °C to

remove background DOC, rinsed thoroughly with de-ionized water 5 times, then oven dried overnight) was white silica sand, purchased from UNIMIN Corp., ID, US.

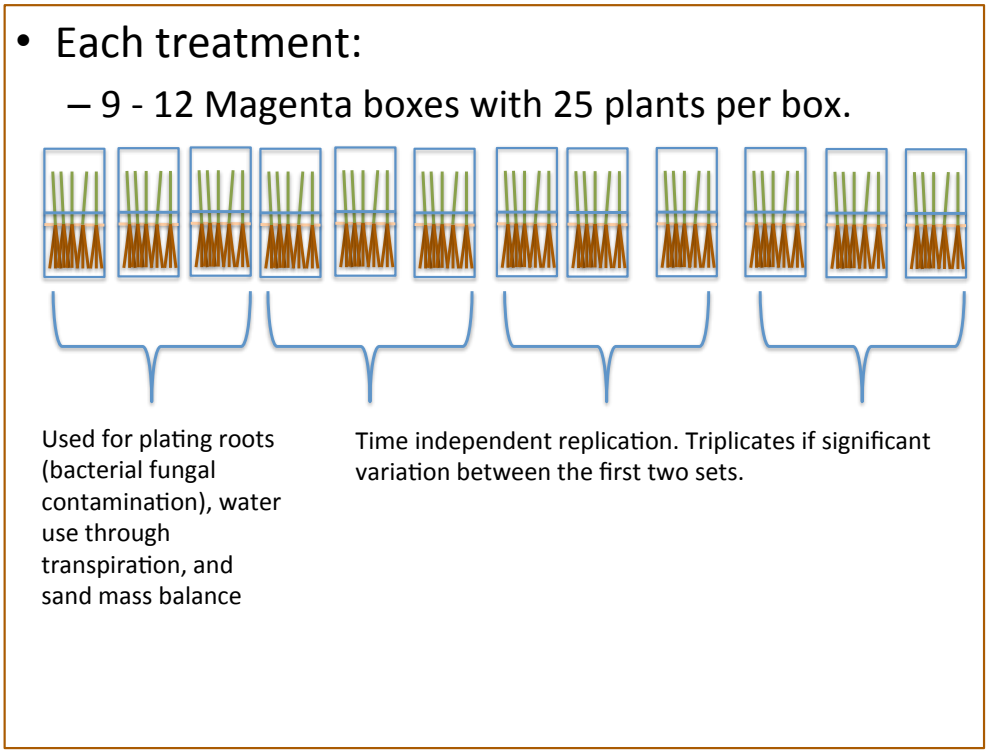

Fig. 0-2. Each treatment comprised of 12 Magenta boxes; 3 used for water transpiration measurements and plant roots plated to test for bacterial contamination, the remaining 9 were run through the process in Fig. 6.

The wheat seeds (*Triticum aestivum* cv Deloris) were obtained from Green Mountain LLC (Mountain green UT). This is an organic hard red winter wheat developed by Dr David Hole (Utah State University).

Table 0-3. Characterization of CuO NPs

Measure	Method	Result	Reference
Size distribution (nm)	DynaPro NanoStar Dynamic Light Scattering	Sigma Aldrich, dry particles < 50 nm	(Dimkpa et al. 2012)

	(Wyatt Technology Corporation, Santa Barbara, CA)	In H_2O 318 nm (mean), some particles < 100 nm In sand matrix, larger aggregates formed	
Elemental composition (μg/g) (mean)	Nitric Acid Digestion (Method 3050 USEPA 1996), followed by ICP-MS (Agilent 7700x ICP-MS)	69.4% Cu Fe 814 μg/g Si 500 μg/g Al 216 μg/g	(Dimkpa et al. 2012)
Zeta-potential (mV)	Zeta Meter Inc., VA, USA	-27.0 (pH 7.2) (in sand without plants)	(Dimkpa et al. 2013)

Plant growth conditions

The commercial NPs were added to sand as combined 6 boxes of sand, then split into Magenta growth boxes (21 cm x 7 cm x 7 cm, Sigma-Aldrich Chemical Company, St Louis, MO), at doses and mass of sand described in Table 5. To ensure homogeneous distribution of the NPs, the contents will be shaken in acid washed 1 L Nalgene bottles. The sand will be moistened with 45 mL/300 g sand, as shown in Table 5 of an 0.7 mM $Ca(NO_3)2$ aqueous solution. The addition of Ca is necessary for seed germination and the Ca salt will provide a low and consistent background ionic strength solution. This ratio of sand and solution represents 1.5 times field capacity (m/m) (Saxton and Rawls 2006). The sand-water mixture was aerated by mixing.

All solutions, sand and Magenta boxes were autoclaved to minimize microbial contamination.

The wheat seeds were surface sterilized by submerging the seeds in 3% Bleach (Chlorox) in DI water for 10 minutes, before being thoroughly washed with sterile DI water 5 times. To pre-germinate seedlings, seeds were germinated for 4 days on LB nutrient agar plates. Twenty five seedlings were added to each Magenta box (selected based on absence of microbial growth from the agar plates), planted to ensure the sand/NP mix does not touch the shoots, and the boxes placed under lights (fluorescent growth lights at 28 °C, 16 hours light, 8 hours dark, generating a photosynthetic photon flux density of 144 pmol m^{-2} s^{-1} at the box surface, at 28 °C, with no additional watering (Dimkpa et al. 2013)) for an additional 10 days of growth. This light level is acknowledged as low; full sunlight PPFD can reach 2000 pmol m^{-2} s^{-1}. Boxes will be rotated every 24 hours to ensure even distribution of light.

Controls (wheat grown as above without NPs) were used to assess standard level of exudation, metal uptake into shoots and morphological features. Unplanted treatments with the same sand and solution as described above, were prepared as further controls, to compare to the effect of CuO NP dissolution from plant based exudate complexation. Based on previous results (Dimkpa et al. 2012), the doses proposed (Table **0**-**4**.) are sub-lethal, causing morphological and biochemical changes to the plant, but not death. The growth period was chosen since 10 days has been sufficient time for plants to begin producing phytosiderophores (PSs) as they become reliant on external sources of the micronutrient Fe (Oburger et al. 2014;

Reichman and Parker 2007). Plants release PSs especially in Fe deficient conditions (Michaud et al. 2007). Plants will not produce PSs if there is sufficient Fe present in the growth matrix. 10 days of growth was chosen to avoid complexation competition from other nutrient additions (e.g. FeEDTA, PO_4^{3-}), since seeds have nutrition for the plants for 9 days.

Table 0-4. Experimental conditions – all treatments will be replicated 2 - 3 times per treatment over time (6 - 9 Magenta boxes). Planted and unplanted treatments as below will be prepared to control for dissolution of CuO NPs in the calcium nitrate solution.

	CuO NPs (mg Cu/ kg dry sand)	**Sand (g)**	**0.7 mM $Ca(NO_3)_2$ solution (mL) Initial**	**0.7mM $Ca(NO_3)_2$ solution (mL) Flush**
Control	0	300	45	45
Low CuO NP	30	160	24	24
Mid CuO NP	100	110	16.5	16.5
High CuO NP	300	70	10.5	15.5

To ensure photo effects are minimized, the height of the sand was equalized by propping up the Magenta boxes with cardboard or styrofoam plates (Fig. 0-3.). Evident also, is lack of chlorosis, implying that nutrient deficiency was not a major factor on the plants' physiological status.

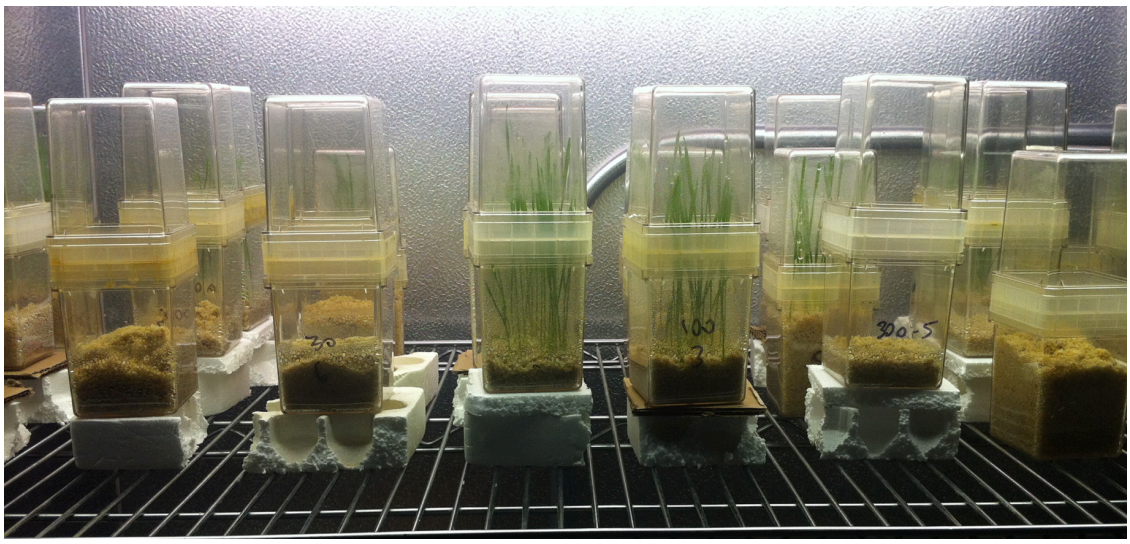

Fig. 0-3. To avoid light gradients, Magenta boxes were compensated for less sand by being propped up underneath.

Methods

An overview of the process is presented in **Fig. 0-3.**

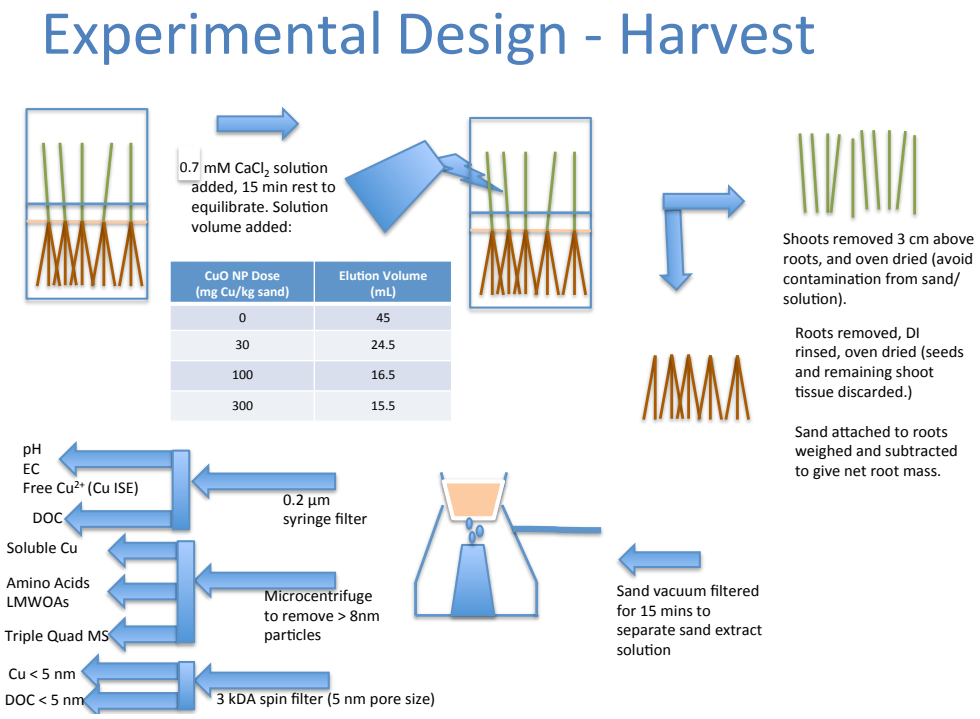

Fig. 0-3. Processing of the plant tissue and water extraction at harvest.

Analysis of plant tissue for metals

Dry weight, digestion of roots and shoots

Fourteen days after germination (4 days on agar and 10 days in the growth boxes), 0.7 mM $Ca(NO_3)_2$ in DI (autoclaved) was added to the Magenta box, and allowed to rest for 15 min, to extract soluble components from the sand. Volumes of 0.7 mM $Ca(NO_3)_2$ indicated in **Fig. 0-3.** After 15 minutes, the plants were carefully removed from the sand matrix (sand loosened with ethanol sterilized spatula then roots teased out of the sand). Roots and shoots were measured in millimeters along the longest of section of each.

Shoots were cut with a razor 3 cm above the level of sand (to ensure no contamination from the sand, and exclusion of potentially CuO NP contaminated coleoptile tissue). Roots were separated from the seeds and 3 cm of remaining shoot, rinsed in DI, before being weighed to obtain fresh weights.

The tissue (roots and shoots) will then be dried overnight at 80 °C, then measured for dry weight. The dry tissue (minimum of 0.09 g) will be digested with 5 mL of concentrated trace metal grade nitric acid and 2 mL 30% hydrogen peroxide (Jones and Case 1990). The digestion will be analyzed for Cu, Zn, Fe, Mn, Ca, Mg, K, Na by inductively coupled plasma- mass spectroscopy (ICP-MS Agilent 7700x).

To further confirm that the wheat is grown under aseptic conditions, 1 root from all boxes of each treatment will be plated onto LB and assessed for microbial growth for an additional 5 days.

Analysis of water extraction

Preparation of water extraction

Each Magenta box with sand and additional Ca solution as above (after 30 min settling time and root removal) is upended carefully into a glass funnel with glass wool inserted, atop a 1000 mL vacuum flask (**Fig. 0-3.**). The glass funnel and glass wool was autoclaved. Inside the flask is a 50 mL sterile plastic vial to capture the solution extracted from the sand. The system is placed under a vacuum for 15 minutes, at which point an approximate volume of solution will be collected according to **Table 0-4.**. The solution is then filtered through a 0.2-μm syringe filter in readiness for analysis.

Analysis

Metals

Total dissolved metals (nano and Cu2+) will be determined by digestion of 0.5 mL syringe filtered solution by trace metal grade nitric acid and hydrogen peroxide using a hotblock (Environmental Express, Model SC154, Charleston SC, USA) from Method 3050 EPA (USEPA 1996) and analyzed using ICP-MS.

For soluble Cu, 1.5 mL of each sand extract solution will be centrifuged using a microcentrifuge (Eppendorf, Centrifuge 5804, Hamburg Germany) at 14,000 x g for 13 minutes, then 1 mL supernatant pipetted off, (to ensure Cu in solution was separated from pelleted CuO NPs) (**Fig. 0-3.**). Based on Stokes Einstein equation this procedure will remove particles greater than 10 nm. All samples will be diluted 1:10 to ensure soluble Cu is in ICP-MS range (reporting range 2.5 – 650 μg Cu/L).

Dissolved Cu will be analyzed by ICP-MS. Free Cu^{2+} will be measured using a Cu ion selective electrode (Orion 96-29 ionplus) (Bravin et al. 2012, Rachou et al. 2007, McLean et al. 2013), using 3 mL of solution.

Amicon-ultra centrifugal filters (3 kDa; Millipore Bilerica, MA, USA) were obtained and calculated to remove ENPs with diameters greater than 1.2 nm. The filters had a 95% recovery of copper ions at 0.5 and 5 mg Cu2+/L. Centrifugal filters were spun for 30 min at 4500 rpm, after being were rinsed three times with DI water immediately prior to use to minimize DOC contamination. Filtrate was spilt into DOC and metals for analysis.

General parameters: pH, EC

pH and electrical conductivity (EC) will be measured in 3 mL of the solution using standard methods (APHA 1995). This 3 mL will be used also for Cu ion selective electrode measurements.

Organics

DOC

DOC will be obtained using combustion with IR detection TOC analyzer (Apollo 9000, Teledyne Tekmar) (Method 5310 B). Samples from pH analysis will be used and preserved with phosphoric acid to pH 2 if required. My preliminary studies with pre-germinated wheat in sand suggest DOC in the range of 100 to 480 mg/L, so dilutions ranging from 1:10 (0 and 30 mg/kg CuO NPs) to 1:100 (100 and 300 mg/kg CuO NPs) to ensure they are in range under the 0.8 -25 mg/L standard curve.

DOC was also distinguished by size via Amicon-ultra centrifugal filters (3 kDa; Millipore Bilerica, MA, USA) removing large proteins and other organics above 3000 amu. Procedure described above under metals. Filtrate was spilt into DOC and metals for analysis.

Amino acids

Procedures for quantifying free amino acids by Aquity ultra performance liquid chromatograph (Waters, Milford MA) have been developed by Dr Randal Lewis' Laboratory (USU) and used previously by our group. Briefly, acetone precipitation will be applied to ensure peptides and intact proteins do not interfere with the analysis. The manufacturer's standard program for amino acid analysis is used for all identification and analysis, along with known standards prior to the run and after each set of samples (Creager et al. 2010).

LMWOAs

Filtered solutions (0.2 μm) will be analyzed to assess LMWOAs and major anions by ion chromatography using a Dionex ICS-3000 equipped with a Dionex IonPac AS11-HC analytical column and guard column and a Dionex ASRS-ULTRA Anion Self-Regenerating Suppressor (Dionex Corp., Sunnyvale, CA). Analyses will be carried out according to the procedure described in Dionex Application Note 123 using a gradient eluent from 3mM to 60 mM KOH produced by a Dionex Eluent Generator (EGGIII KOH). The sample peaks will be compared against standards of lactate, acetate, propionate, iso-butyrate, butyrate, isovalerate, valerate, chloride, nitrate, succinate, malate, sulfate, oxalate, phosphate, citrate, iso-citrate, formate

and gluconate. IC-Time-Of-Flight-Mass-Spectrometry or sample spikes were used if retention time was ambiguous to confirm analytes.

Sugars and proteins

For total sugars, a sulfuric acid method with a glucose standard was used, and UV Vis at 315 nm as per Albalasmeh et al. (2013). Protein concentration was used via BCA Protein Assay kit (Thermo scientific, Rockford, IL) under the 5 - 250 µg/mL method, measured by UV Vis spec at 576 nm. Acetone precipitation was used to minimize interferences.

Phytosiderophores

HPLC grade phytosiderophores were purchased from Toronto Research Chemicals (Toronto, Canada) provided 2' Deoxymugeinic acid. Standards of Cu-complexes will be prepared to verify and quantify Cu-complexes identified in the root exudate (Tsednee et al. 2012). Procedures described by Xuan et al. (2006) using zwitterionic hydrophilic interaction liquid chromatography (ZI-HILIC) to ESI-MS were employed to determine metal-phytosiderophore complexes. Specifically, a zwitterionic 150 mm x 1.0 mm I.D. column and guard column (14 mm x 1.0 mm I.D.) will be purchased from SeQuant (Umea, Sweden) and run under the gradient illustrated in Table 3. Solvent A will be 10 mM ammonium acetate/ACN (10 +90) and Solvent B 30 mM ammonium acetate/ACN (80 + 20), both at pH 7.3. Following each run, the column will be cleaned and equilibrated linearly to 100 % Solvent A for 60 min. Complexes will have shorter retention times than the free siderophores, due to a reduction in charge of the M-phytosiderophore. EDTA will be used to flush

the column to ensure metal-phytosiderophore complexes have not separated in the column and distort results. ESI-MS will be run in negative ionization mode at 4.5 kV with a heated transfer capillary maintained at 350 °C and a tube lens with a voltage of 20 V. An Agilent 1290 ultra HPLC with a 6490 triple quadrupole mass spectrometer will be used for additional determination of Cu- complex configuration.

Table 0-3. Operating conditions for ZI-HILIC column including time and solvent composition

Time (min)	Solvent A	Solvent B
0 – 3	100	0
3 – 33	Linear down to 30%	Linear up to 70%
33 – 40 (isocratic cleanup)	30%	70%

Procedures were developed to ensure siderophore concentrations are sufficient for these analyses, and lyophilisation employed when required.

Formic acid (1%) mobile phase was also used to confirm total DMA in the samples (Schindlegger et al. 2014) via QqQ MS, which was used in geochemical modeling.

Other Metal-organo complexes

Using the procedure detailed for siderophores (Xuan et al. 2006), the LC-ESI-QqQ provided a detailed list of other Cu- complexed organic components.

A complete summary of solution analyses is listed in **Table 0-4.** as determined by schematic in **Fig. 0-3.**

Table 0-4. Volumes of sand extract required for various analyses

	Pretreatment	**CuO NP Dose (mg/kg)**			
		0	**30**	**100**	**300**
EC, pH, Cu ISE	0.2 µm filter	3	3	3	3
DOC	0.2 µm filter	1	1	0.1	0.1
LMWOAs	microcentrifuge	1.5	1.5	1.5	1.5
Amino acids	microcentrifuge	1.5	1.5	1.5	1.5
Total Metals	0.2 µm filter	0.5	0.5	0.5	0.5
< 5 nm Cu	3 kDa spin filter	0.5	0.5	0.5	0.5
< 5nm DOC	3 kDa spin filter	0.5	0.5	0.5	0.5
Dissolved Metals	microcentrifuge	1.5	1.5	1.5	1.5
LC-QqQ-MS	microcentrifuge	3	3	3	3
Sugars	0.2 µm filter	1	1	0.1	0.1
Proteins	0.2 µm filter	0.05	0.05	0.05	0.05
Plating (microbes)		0.05	0.05	0.05	0.05
Total (mL)		14.1	14.1	12.3	12.3
Recovery (mL)		39	25	15	14

Geochemical modeling

The software program MINTEQ (Gustafsson 2014) will be employed to model Cu-complexes in solution. Stability constants not presently in the databases for these models were added based on reported literature values along with values for H^+ complexes, including those for gluconate and DMA.

Statistical Analysis

Statistical analysis using techniques described above will be performed using R (R Core Team 2013) to assess differences in solubility, plant morphology and solution componentry.

Quality Control

Three boxes from each treatment shall be set aside to test for mass balance on Cu sand, as well as water used by the plants (**Fig. 0-2.**). 20 g of wet sand will be dried at 80°C overnight, compared to the original volume of water added at the start of the experiment, and water loss calculated on a per plant basis.

For total Cu mass balance, sand from the experimental Magenta boxes will be thoroughly mixed, a 0.5 g sample taken and digested with Trace Metal Grade Nitric Acid and hydrogen peroxide using a hotblock (Environmental Express, Model SC154, Charleston SC, USA) from Method 3050 EPA (USEPA 1996) and analyzed using ICP-MS. A summation of total Cu in solution, plant tissue and sand will provide a basis for the mass balance calculation.

Appendix E: Data in box plots

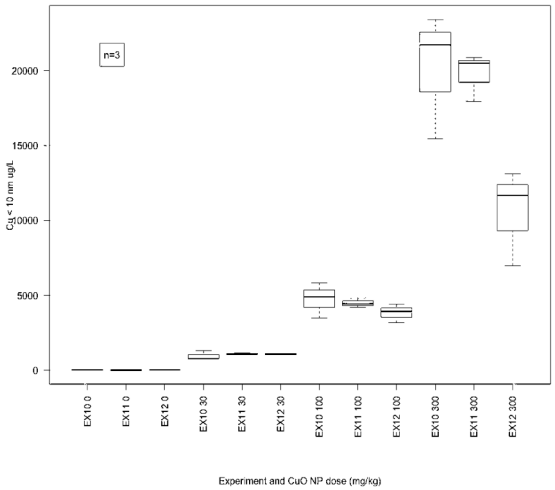
n=3
Cu< 10 nm ug/L
0
5000
10000
15000
20000
EX10 0
EX11 0
EX12 0
EX10 30
EX11 30
EX12 30
EX10 100
EX11 100
EX12 100
EX10 300
EX11 300
EX12 300
Experiment and CuO NP dose (mg/kg)

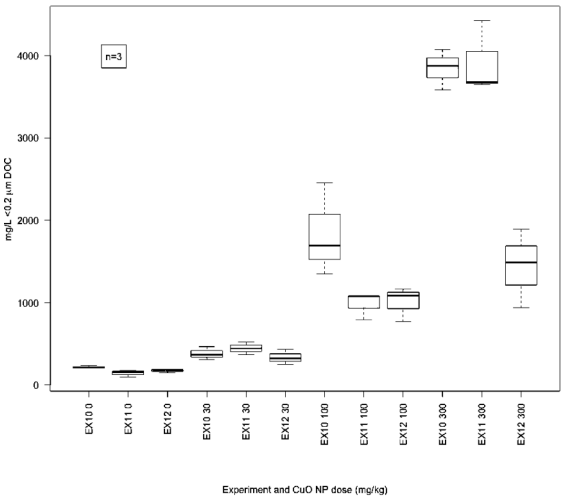
n=3
mg/L <0.2 µm DOC
0
1000
2000
3000
4000
EX10 0
EX11 0
EX12 0
EX10 30
EX11 30
EX12 30
EX10 100
EX11 100
EX12 100
EX10 300
EX11 300
EX12 300
Experiment and CuO NP dose (mg/kg)

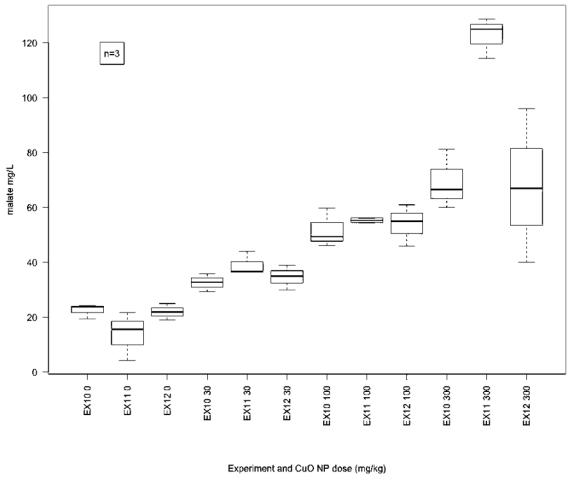
n=3
malate mg/L
0
20
40
60
80
100
120
EX10 0
EX11 0
EX12 0
EX10 30
EX11 30
EX12 30
EX10 100
EX11 100
EX12 100
EX10 300
EX11 300
EX12 300
Experiment and CuO NP dose (mg/kg)

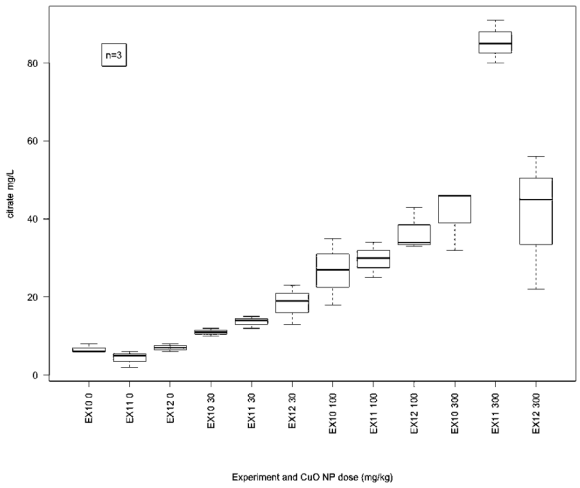
n=3
citrate mg/L
0
20
40
60
80
EX10 0
EX11 0
EX12 0
EX10 30
EX11 30
EX12 30
EX10 100
EX11 100
EX12 100
EX10 300
EX11 300
EX12 300
Experiment and CuO NP dose (mg/kg)

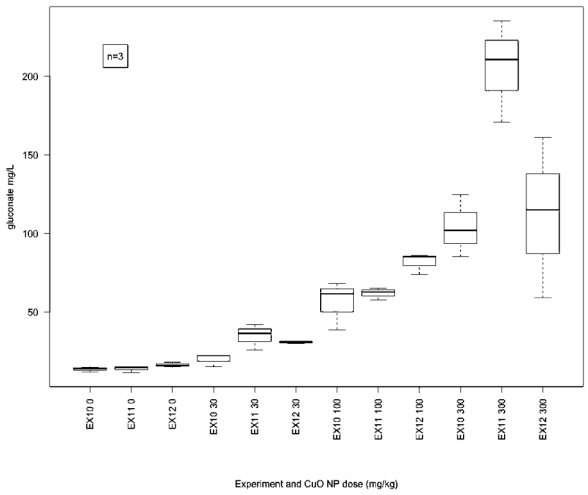

Fig. 0-4. Box plots of datasets for $Cu_{<10}$, DOC, malate, citrate, and gluconate across all studies, grouped by Experiment (10, 11, 12 in chronological order) and CuO NP dose (0, 30, 100, 300) undertaken in R Studio 0.99.489 (R Core Team 2013). Used to assess data spread.

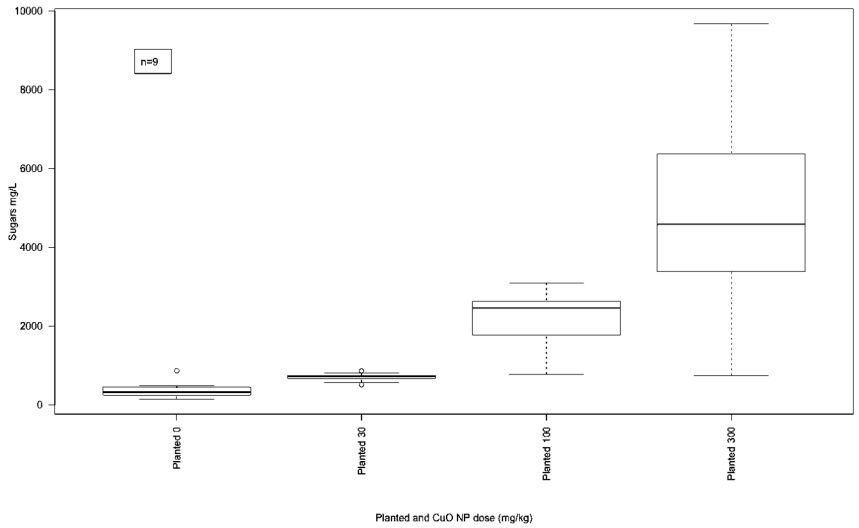

Fig. 0.5. Box plot of Sugars (mg/L) in planted samples across CuO NP doses.

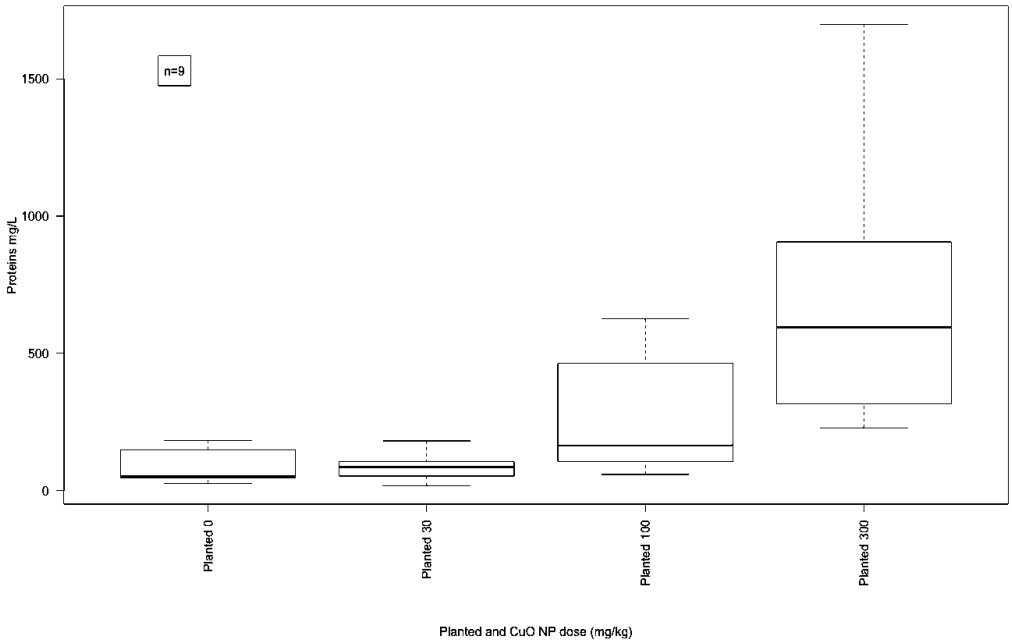

Fig. 0-6. Proteins (mg/L) in planted samples across CuO NP doses.

Appendix F: Full replication of DOC, and Cu dissolution below 10 nm ($Cu_{<10}$)

A randomized blocked design over several months, involving three different experiments at 0, 30, 100 and 300 mg Cu/kg dry sand as CuO NPs provided an indication of biological reproducibility. This investigation did not involve size exclusion apart from centrifugation ($M_{<10}$).

In unplanted treatments, the concentration of soluble Cu (Cu measured by ultracentrifugation or $Cu_{<10}$) was < 0.8 µg/L, 3 ± 2 µg/L (average ±SD), 8 ± 6 µg/L, and 171 ± 172 µg/L with addition of 0, 30 and 100, 300 mg/kg, respectively. There was some experimental variability between studies.

The concentration of soluble Cu was higher by 50 to 100 times in planted compared to their respective unplanted treatment, confirming exposure of CuO NPs to the wheat plant exudates drove solubility. In planted systems Cu solubility increased with CuO NP dose (Fig. 0- a). As before, soluble Cu represented < 1% of the CuO NPs added, so that most Cu remained associated with the solids.

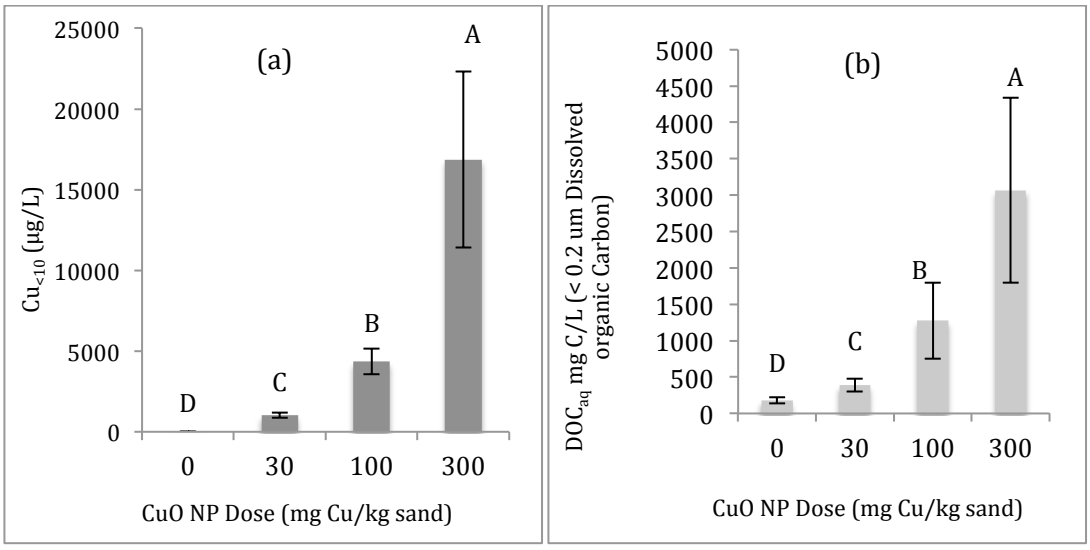

Fig. 0-7. Copper in solution for the planted system measured via microcentrifugation ($Cu_{<10}$) (n = 9) (a). Unplanted samples (not shown) were below detection limit (0.8 µg/L) for the 0 mg/kg treatment, 3 ± 2 µg/L for 30 mg Cu/kg and 8 ± 6 µg/L for 100 mg Cu/kg and 171 ± 172 µg/L with addition of 300 mg/kg. Dissolved organic carbon (DOC) in the planted systems filtered through 0.2 µm (mg C/L) (n = 9) (b). Unplanted DOC (not shown) was not above background sand (< 5 mg/L), showing that DOC was biologically derived. Columns with the same letters are not significantly different (α=0.05) by Tukey's HSD after log transformation. Error bars indicate standard deviation.

Planted treatments had significantly higher DOC compared to all unplanted treatments which were at background DOC (< 5 mg/L), confirming that organic carbon was from the plants including root exudates (Anjum et al. 2015 a; Dakora and Phillips 2002). Furthermore, DOC increased with CuO NP dose in planted samples (Fig. 0- b).

pH is often the principal driving force controlling solubility. pH however was not statistically different across treatments (α = 0.05) comparing planted and unplanted treatments (average 6.87 ± 0.68 SD).

Again, in planted samples, the majority of DOC was comprised of sugars (Fig. 0-8 a), contributing 70% ± 33% of the DOC and proteins (18% ± 13% of DOC) (Fig. 0-8 b). Both sugars and proteins increased with dose of CuO NPs.

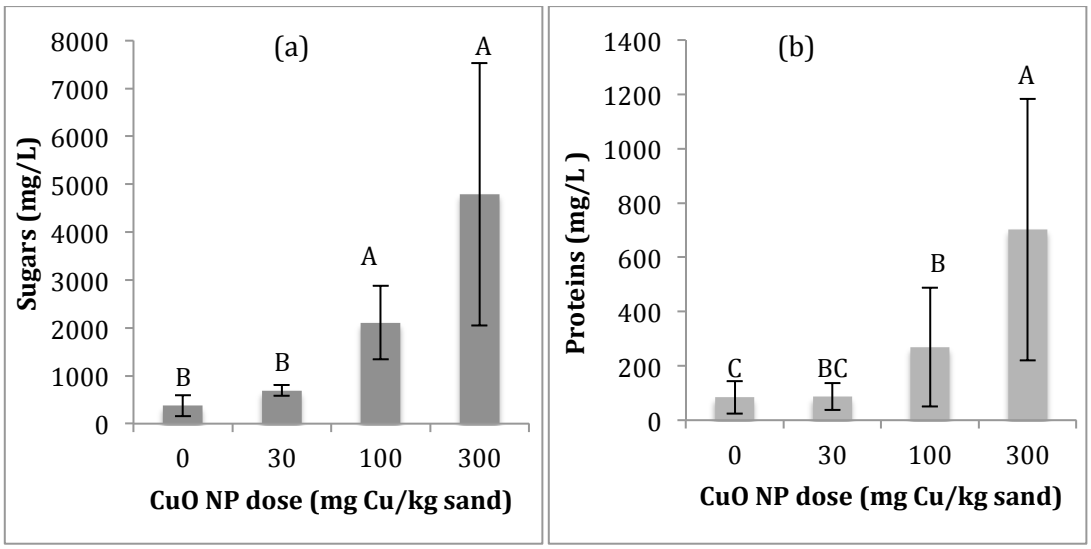

Fig. 0-8. Sugars (a) (mg/L) and proteins (b) (mg/L) from the sand solution in planted samples (n = 9). Columns with the same letters are not significantly different (α=0.05) by Tukey's HSD after log transformation. Error bars indicate standard deviation.

DMA dose dependently increased with CuO NP dose (Fig. 0- a). LMWOAs comprised 7% ± 3% of the DOC overall. Gluconate, malate and citrate were dose dependently higher at each NP dose compared to the control (Fig. 0- b - d).

Amino acids were found in the solution extracted around the wheat roots contributing only 0.4 ± 0.2 % to DOC. A trend of higher exudation of amino acids at 300 mg Cu/kg CuO NP was evident, particularly valine and serine. Of the most prevalent amino acids, arginine had a mean concentration across all NP doses of 0.7 mg/L, leucine 0.8 mg/L, phenylalanine 0.6 mg/L, proline 0.6 mg/L, serine 0.8 mg/L and valine 0.9 mg/L. The concentration of citrate was over 20 times higher than the highest amino acid (Fig. 0- d).

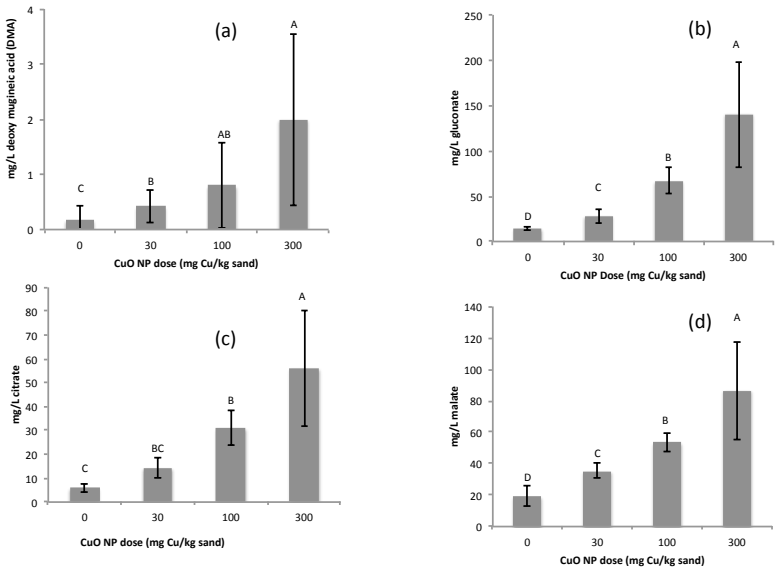

Fig. 0-9. Phytosiderophore DMA (a), LMWOAs gluconate (b), citrate (c), and malate (d) (mg/L) concentrations in sand solution at different CuO NP doses (mg/kg) (n=9). Columns with the same letters are not significantly different (α=0.05) by Tukey's HSD after log transformation. Error bars represent standard deviation.

Appendix G: Derivation of Cu and Fe DMA stability constants

By Joshua Hortin (used with permission)

Problem introduction

2'-deoxymugineic acid (DMA; Fig. 1) is an iron chelator related to mugineic acid (MA) produced by graminaceous plants, especially in iron deficient environments, to enhance the dissolution of iron for plant uptake. We wish to use geochemical speciation modeling to understand how copper and iron ions compete for binding with DMA. The challenge is that deprotonated DMA exists as DMA^{3-}, yet when DMA binds to trivalent ions (such as Fe(III)), it can lose an additional proton from its alcoholic group (Fig. 1). Most geochemical models begins with the fully deprotonated anion and build complexes from there; so should the model use DMA^{3-} or DMA^{4-}? Most metal binding constants are for the general equation metal + DMA^{3-} ↔ metal-DMA, which presents a problem if DMA^{4-} is used. In this paper, two approaches to modeling DMA and metal complexation are made after a discussion of DMA pK_a values: 1) Using DMA^{4-} in the model as the base anion modeling metal complexation as metal + protons + DMA^{4-}, and 2) using DMA^{3-} in the model as the base anion and modeling Fe complexation as metal + hydroxide + DMA^{3-}.

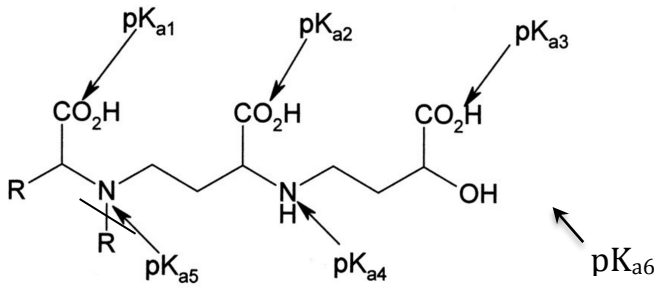

Fig. 1. 2'-deoxymugineic acid structure and assignment of pK_a values; R = CH_2 (von Wiren et al. 2000). pK_{a6} added as noted in Hider et al. (2004).

pK_a values for DMA

DMA technically has 6 possible pK_a values (Fig. 1), but only four to five pKa values are within the typical pH scale. The third, fourth, and fifth pK_a values (assigned to a carboxylic group and the two nitrogen-containing groups) are easily measurable, while the remaining pK_a values are more challenging to measure. The second pK_a value has been measured (Hider et al. 2004) but the first pK_a value could not be measured because the value was too low. The sixth pK_a value has only been estimated by the Taft equation (Murakami et al. 1989) because it exists outside the realm of the typical pH scale (i.e., DMA will never exist as DMA^{4-} within the typical pH scale). Measured and/or estimated pK_a values are scanty and not in good agreement across the literature (Table 1). pK_{a1} and pK_{a6} cannot be measured directly and so estimates must instead be relied upon. pK_{a2} and pK_{a5} show decent agreement within the literature and pK_{a4} shows poor agreement within the literature, while pK_{a3} shows excellent agreement within the literature.

Table 1. Measured and/or estimated (in parentheses) pK_a values for DMA from literature. Blank = not measured/estimated. pK_a values given for the relative general reaction $H^+ + L \leftrightarrow HL$.

pK_a	Murakami et al. (1989)	von Wiren et al. (1999)	von Wiren et al. (2000)	Hider et al. (2004)	Average
1			(2.35)	(<1.5)	1.93
2		2.72	(2.74)	1.94	2.47
3	3.193	3.40		3.42	3.34
4	8.25	7.78		9.12	8.38
5	10.00	9.55		9.66	9.74
6	(17.1)				17.1
Method of	potentiometr	potentiomet	analogous	potentiome	average of

determination	ic titration	ric titration	studies with MA	tric titration	all values given

The best approaches to model DMA seem to be using an average of measured and estimated values, or using those of von Wiren et al. (1999) which are in decent agreement with Murakami et al. (1989) while being more recent. The values of Hider et al. (2004) were measured in response to criticism, and might be avoided because of poor agreement with Murakami et al. (1989) and potential bias in the response. For the model, we select the values of von Wiren et al. (1999) for $pK_{a2\text{-}5}$, the value of Murakami et al. (1989) for pK_{a6} and the average of 1.93 for pK_{a1}.

Approach 1: Using DMA^{4-} as the base anion

To input the pK_a values into MINTEQ v3.1 (Gustaffson 2013), the equations must be rewritten in summation form (Equations 1, 3-7), with DMA fully deprotonated (DMA^{4-}) to begin with. An example is shown in Equations 1-3, and the process is repeated to generate Equations 4-7.

$H^+ + DMA^{4-} \leftrightarrow (H-DMA)^{3-}$	log K = 17.1	Equation 1
$H^+ + (H-DMA)^{3-} \leftrightarrow (2H-DMA)^{2-}$	log K = 9.55	Equation 2
$2H^+ + DMA^{4-} \leftrightarrow (2H-DMA)^{2-}$	log K = 26.65	Equation 3

Equations 1 and 2 are added, so that $(H\text{-}DMA)^{3-}$ cancels on both sides and we are left with the overall equation (Equation 3) utilizing DMA^{4-}. The K values of Equations 1 and 2 are multiplied, and the overall log K value of Equation 3 is 26.65.

The final values of the protonation constants entered into MINTEQ are displayed in Equations 1 and 3-7.

$H^+ + DMA^{4-} \leftrightarrow (H-DMA)^{3-}$	log K = 17.1	Equation 1
$2H^+ + DMA^{4-} \leftrightarrow (2H-DMA)^{2-}$	log K = 26.65	Equation 3
$3H^+ + DMA^{4-} \leftrightarrow (3H-DMA)^{-}$	log K = 34.43	Equation 4
$4H^+ + DMA^{4-} \leftrightarrow (4H-DMA)^{0}$	log K = 37.83	Equation 5
$5H^+ + DMA^{4-} \leftrightarrow (5H-DMA)^{+}$	log K = 40.3	Equation 6
$6H^+ + DMA^{4-} \leftrightarrow (6H-DMA)^{2+}$	log K = 42.23	Equation 7

Next, appropriate values for the equilibrium constants of Cu(II) and Fe(III) with DMA must be found. The notations of metal and ligand equilibrium constants are frequently given in the literature as K_{pqr}, where p = number of metal ions, q = number of ligands, and r = number of protons (or hydroxides if negative), and this notation will be used here. Murakami et al. (1989) found only one complex of Cu(II) and DMA^{3-}, and two complexes for Fe(III) and DMA^{3-}. For Cu(II), there is a 1:1:0 metal:ligand:proton ratio with log K_{110} = 18.7. For Fe(III), there is a 1:1:0 metal:ligand:proton complex with log K_{110} = 18.38 and a 1:1:-1 metal:ligand:proton complex with log K_{11-1} = 16.25, indicating that in an iron-DMA complex, an additional proton may be lost (pK_{a6}).

Murakami et al. (1989) wrote these reactions where the ligand was DMA^{3-} instead of DMA^{4-}, meaning that the value of the first protonation of DMA was implicitly included in these reactions. To convert the reactions to using DMA^{4-}, the proton value for each equilibrium constant would actually increase by one (i.e., K_{111}

instead of K_{110} for the 1:1 complex of Cu(II) and Fe(III) with DMA, and K_{110} for the 1:1:-1 complex of Fe(III) with DMA)). To correct this form for MINTEQ, the first protonation of DMA must be included in these reactions (Equations 1, 8-9).

$Cu^{2+} + (H-DMA)^{3-} \leftrightarrow (Cu-H-DMA)^{-}$	log K = 18.7	Equation 8
$H^{+} + DMA^{4-} \leftrightarrow (H-DMA)^{3-}$	log K = 17.1	Equation 1
$Cu^{2+} + H^{+} + DMA^{4-} \leftrightarrow (Cu-H-DMA)^{-}$	log K = 35.8	Equation 9

By adding Equations 1 and 8, the complex $(H\text{-}DMA)^{3-}$ cancels on both sides and we are left with the overall equation (Equation 9) utilizing DMA^{4-}. The K values of Equations 1 and 7 are multiplied, and the overall log K value of Equation 9 is 35.8. This is the value for the aqueous specie Cu^{2+}-DMA^{4-}-H^{+} entered into MINTEQ.

A similar process may be followed for Fe(III) in the 1:1:1 complex (Equations 1, 10, 12) and the 1:1:0 complex (Equations 1, 11, 13). These two complexes are originally notated as 1:1:0 and 1:1:-1 in Murakami et al. (1989).

$Fe^{3+} + (H-DMA)^{3-} \leftrightarrow (Fe-H-DMA)^{0}$	log K = 18.38	Equation 10
$Fe^{3+} + (H-DMA)^{3-} - H^{+} \leftrightarrow (Fe-DMA-H_{-1})^{-}$	log K = 16.25	Equation 11
$H^{+} + DMA^{4-} \leftrightarrow (H-DMA)^{3-}$	log K = 17.1	Equation 1
$Fe^{3+} + H^{+} + DMA^{4-} \leftrightarrow (Fe-H-DMA)^{0}$	log K = 35.48	Equation 12
$Fe^{3+} + DMA^{4-} \leftrightarrow (Fe-DMA)^{-}$	log K = 33.35	Equation 13

By adding Equations 1 and 10, $(H\text{-}DMA)^{3-}$ cancels on both sides and we are left with the overall equation (Equation 12) utilizing DMA^{4-}. The K values of Equations 1 and 9 are multiplied, and the overall log K value of Equation 12 is 35.48. By adding equations 1 and 11, H^+ and $(H\text{-}DMA)^{3-}$ cancel on both sides and we are left with the overall equation (Equation 13) utilizing DMA^{4-}. The K values of Equations 1 and 10 are multiplied, and the overall log K value of Equation 13 is 33.35. The K values derived from Equations 12 and 13 are the values entered into MINTEQ for the aqueous species Fe^{3+}-DMA^{4-}-H^+ and Fe^{3+}-DMA^{4-}, respectively.

By direct comparison of the equilibrium constants of iron and copper with DMA (Equations 9, 12, and 13), copper seems to bind more strongly to deoxymugineic acids than Fe(III), an observation supported by (Sugiura et al. 1981).

Other authors have reported stability constants for Fe(III) and DMA (Table 2). Again, like the case for the pK_a values, the constants of Hider et al. (2004) seem to be incorrect, compared to their previous work (von Wiren et al. 1999) and the work of Murakami et al. (1989), so the constants of Murakami et al. (1989) are used in the model.

Table 2. Literature stability constants for the Fe(III)-DMA system, after correction for conversion of DMA^{3-} to DMA^{4-}.

Complex, where p = Fe(III), q = DMA^{4-}, r = H^+	Murakami et al. (1989)	von Wiren et al. (1999)	Hider et al. (2004)
1:1:0	33.35		35.34
1:1:1	35.48	35.2	41.96
Method of	potentiometric	spectrophotometric	potentiometric

determination	titration, 1:1 molar metal:ligand ratio	competition, 1:10 metal:ligand ratio	titration, poorly documented

The speciation of DMA^{4-} is shown in Fig. 2. DMA^{4-} (010) does not occur within the normal pH range (0-14). The approximate pK_a values (the point where one species is 50% converted to a neighboring species) align with those given in Table 1.

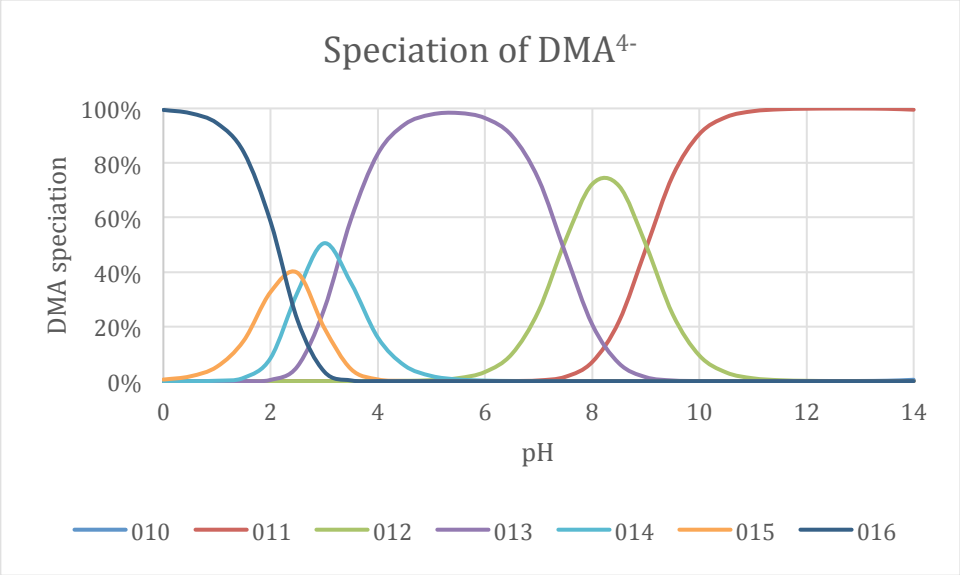

Fig. 2. Speciation of DMA^{4-} with H^+ as a function of pH. pqr notation is metal:ligand:proton ratio.

The speciation of Fe3+ with DMA4- is shown in Fig. 3, compared with the same Fig. from Murakami et al. (1989). It is not a very close match, but the two models do agree that the fully-deprotonated species (110) dominates after pH 4.

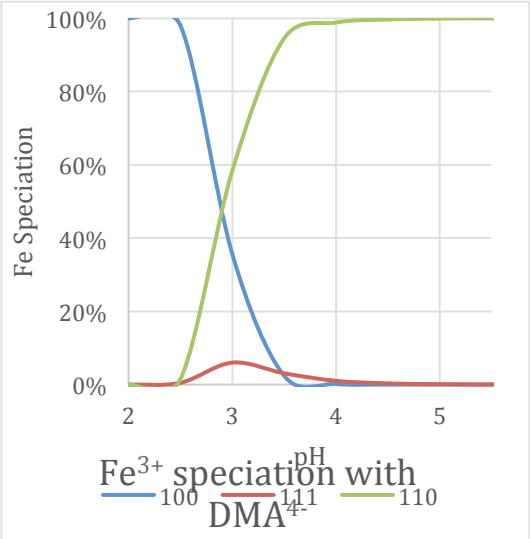

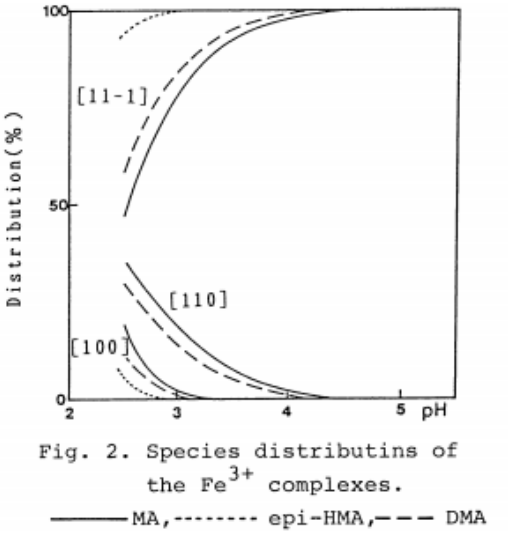

Fig. 3. Left, Fe^{3+} speciation with DMA^{4-} as a function of pH; right, Fe^{3+} speciation with DMA^{4-} as a function of pH as calculated by Murakami et al. (1989). Both models were calculated under the conditions of 25 °C, 0.1 M ionic strength, and a 1:1 metal:ligand ratio. pqr notation is metal:ligand:proton ratio.

Finally, the competition of H^+, Cu^{2+}, and Fe^{3+} for DMA^{4-} is shown in Fig. 4. The copper-DMA complex dominates speciation across the pH range of 3-12.

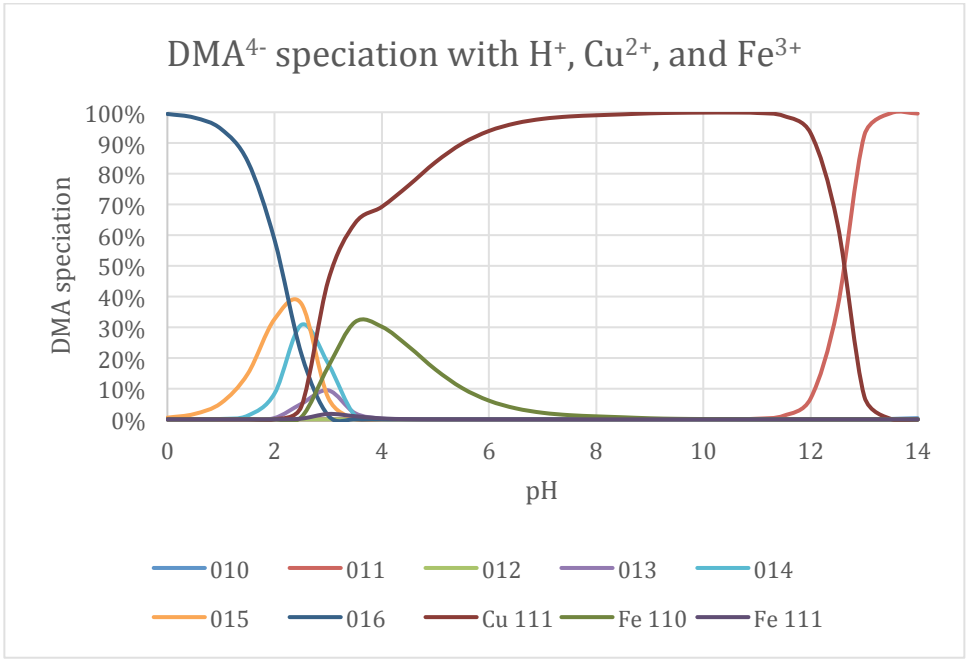

Fig. 4. DMA^{4-} speciation with H^{+}, Cu^{2+}, and Fe^{3+} as a function of pH. Model was calculated under the conditions of 25 °C, 0.1 M ionic strength, and a 1:1:1 Cu:Fe:ligand ratio. pqr notation is metal:ligand:proton ratio.

Approach 2: Using DMA^{3-} as the base anion

When using DMA^{3-} as the base anion, pK_{a6} is no longer necessary. The new protonation stability constants become those shown in Equations 14-18, which are entered into MINTEQ.

$H^+ + DMA^{3-} \leftrightarrow (H-DMA)^{2-}$	log K = 9.55	Equation 14
$2H^+ + DMA^{3-} \leftrightarrow (2H-DMA)^{-}$	log K = 17.33	Equation 15
$3H^+ + DMA^{3-} \leftrightarrow (3H-DMA)^{0}$	log K = 20.73	Equation 16
$4H^+ + DMA^{3-} \leftrightarrow (4H-DMA)^{+}$	log K = 23.45	Equation 17
$5H^+ + DMA^{3-} \leftrightarrow (5H-DMA)^{2+}$	log K = 25.38	Equation 18

The equations for Cu(II) and Fe(III) complexes with DMA^{3-} can now be used as written by Murakami et al. (1989), with a small change to Equation 11 (shown as Equation 11a). This change can be made without change to the log K value because Fe-DMA-H_{-1} is "stoichiometrically indistinguishable from [Fe-DMA-OH], the representation used in most models" (Reichman and Parker 2002).

$Cu^{2+} + DMA^{3-} \leftrightarrow (Cu-DMA)^{-}$	log K = 18.7	Equation 8
$Fe^{3+} + DMA^{3-} \leftrightarrow (Fe-DMA)^{0}$	log K = 18.38	Equation 10

$Fe^{3+} + DMA^{3-} - H^{+} \leftrightarrow (Fe - DMA - H_{-1})^{-}$ log K = 16.25 Equation 11

$Fe^{3+} + DMA^{3-} + OH^{-} \leftrightarrow (Fe - DMA - OH)^{-}$ log K = 16.25 Equation 11a

The speciation of DMA^{4-} is shown in Fig. 5. The approximate pK_a values (the point where one species is 50% converted to a neighboring species) align with those given in Table 1.

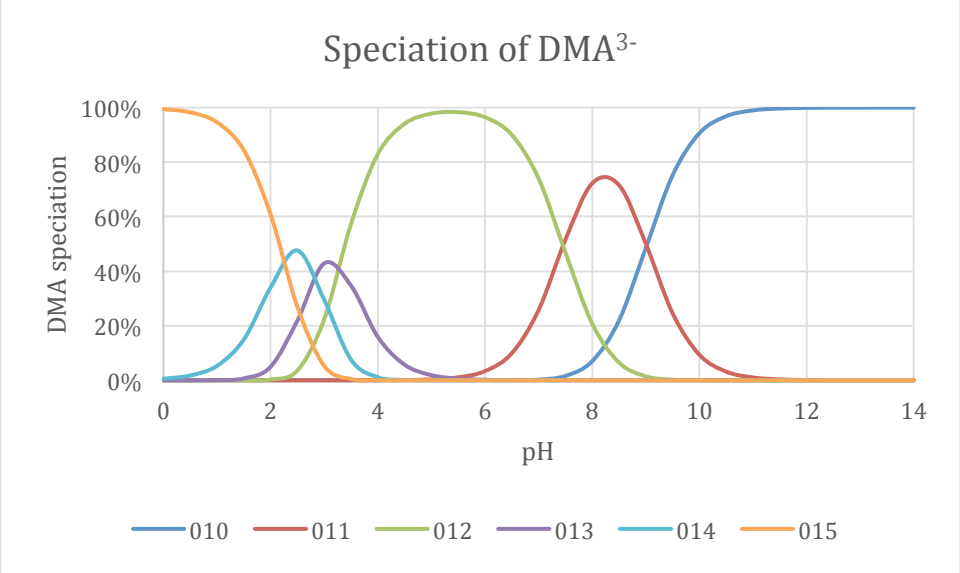

Fig. 5. Speciation of DMA^{3-} with protons as a function of pH. pqr notation is metal:ligand:proton ratio.

The speciation of Fe^{3+} with DMA^{3-} is shown in Fig. 6, compared with the same Fig. from Murakami et al. (1989). It is not a very close match, but the two models do agree that the fully-deprotonated species (110) dominates after pH 4.

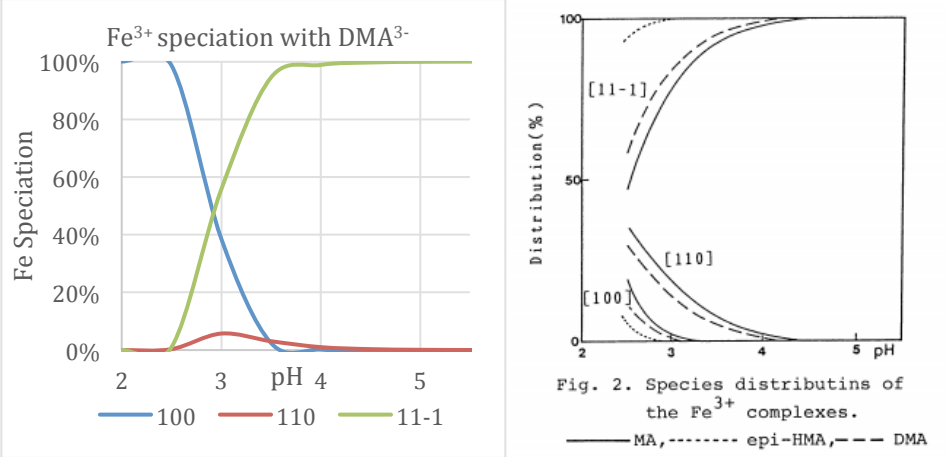

Fig. 6. Left, Fe^{3+} speciation with DMA^{3-} as a function of pH; right, Fe^{3+} speciation with DMA^{3-} as a function of pH as calculated by Murakami et al. (1989). Both models were calculated under the conditions of 25 °C, 0.1 M ionic strength, and a 1:1 metal:ligand ratio. pqr notation is metal:ligand:proton ratio.

Finally, the competition of H^+, Cu^{2+}, and Fe^{3+} for DMA^{3-} is shown in Fig. 7. The copper-DMA complex dominates speciation across the pH range of 3-12.

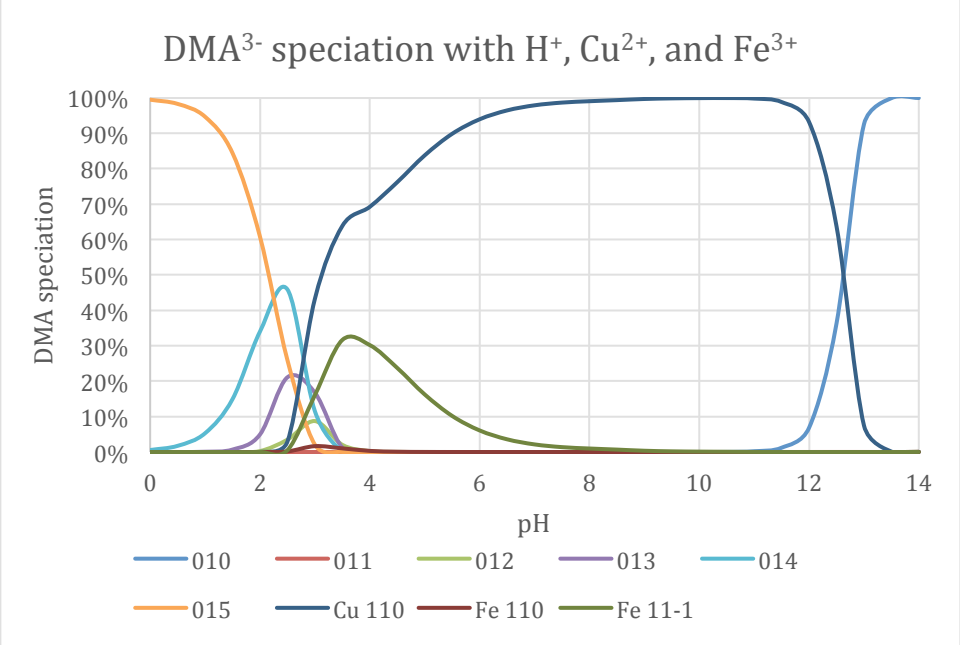

Fig. 7. DMA^{3-} speciation with H^{+}, Cu^{2+}, and Fe^{3+} as a function of pH. Model was calculated under the conditions of 25 °C, 0.1 M ionic strength, and a 1:1:1 Cu:Fe:ligand ratio. pqr notation is metal:ligand:proton ratio.

Comparison of approaches

A comparison of the models was made to determine if one method of modeling was preferable to the other. The input parameters are given in Table 2. The *general equations* are given in Table 2; for the *model-specific* equations, refer to the individual sections.

Table 2. log K values included under approach 1 and 2 to modeling.

General equation	Approach 1	Approach 2
$H^+ + DMA^{4-} \leftrightarrow (H-DMA)^{3-}$	log K = 17.1	not included
$2H^+ + DMA^{4-} \leftrightarrow (2H-DMA)^{2-}$	log K = 26.65	log K = 9.55
$3H^+ + DMA^{4-} \leftrightarrow (3H-DMA)^{-}$	log K = 34.43	log K = 17.33
$4H^+ + DMA^{4-} \leftrightarrow (4H-DMA)^{0}$	log K = 37.83	log K = 20.73
$5H^+ + DMA^{4-} \leftrightarrow (5H-DMA)^{+}$	log K = 40.3	log K = 23.45
$6H^+ + DMA^{4-} \leftrightarrow (6H-DMA)^{2+}$	log K = 42.23	log K = 25.38
$Cu^{2+} + DMA^{3/4-} \leftrightarrow (Cu-DMA)^{-}$	log K = 35.8	log K = 18.7
$Fe^{3+} + DMA^{3/4-} \leftrightarrow (Fe-DMA)^{0}$	log K = 35.48	log K = 18.38
$Fe^{3+} + DMA^{3-} + OH^- \leftrightarrow (Fe-DMA-OH)^{-}$	not included	log K = 16.25
$Fe^{3+} + DMA^{4-} \leftrightarrow (Fe-DMA)^{-}$	log K = 33.35	not included

A comparison of DMA protonation was made across the two models. The models appear very similar, except for slight discrepancies in the green and blue species (the neutral and +1 charges).

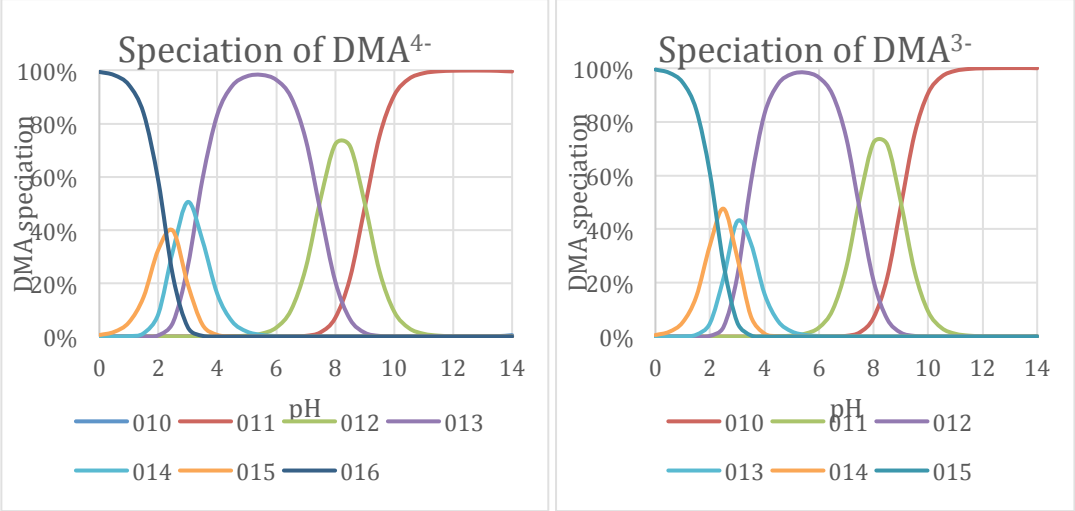

Fig. 8. Right, speciation of DMA^{4-}; left, speciation of DMA^{3-}. Colors have been edited to reflect the species of the same charge (i.e. 011 of DMA^{4-} (orange) is equivalent to 010 of DMA^{3-} (orange)).

A comparison of Fe3+ speciation with DMA is given in Fig. 9. The graphs appear nearly identical.

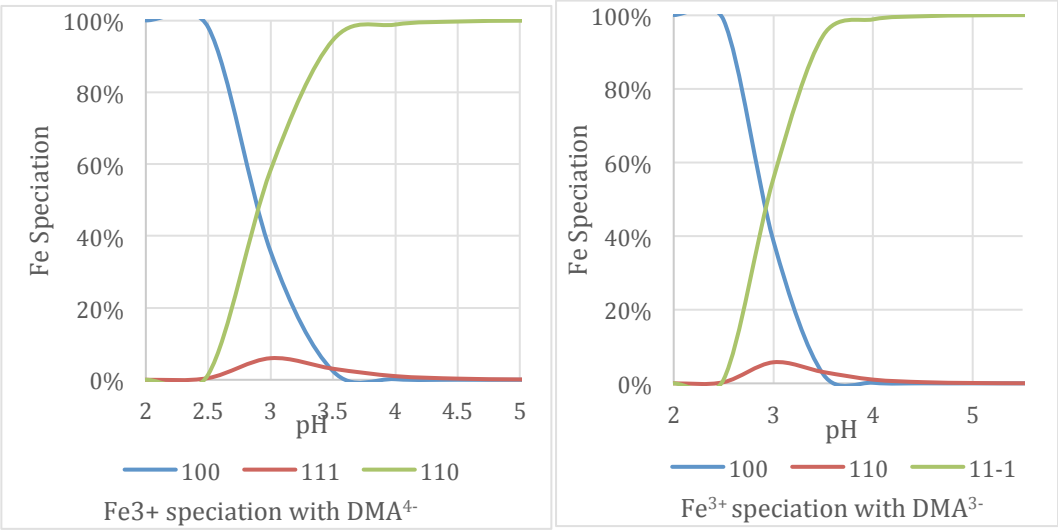

Fig. 9. Right, speciation of Fe^{3+} with DMA^{4-}; left, speciation of Fe^{3+} with DMA^{3-}. Colors have been edited to reflect the species of the same charge (i.e. 111 of DMA^{4-} (orange) is equivalent to 110 of DMA^{3-} (orange)).

A comparison of the competition of H^+, Cu^{2+}, and Fe^{3+} for DMA is shown in Fig. 10. The models appear virtually the same, except for the speciation of DMA with protons at low pH; however between pH 5 and 10 copper appears to dominate the speciation of DMA.

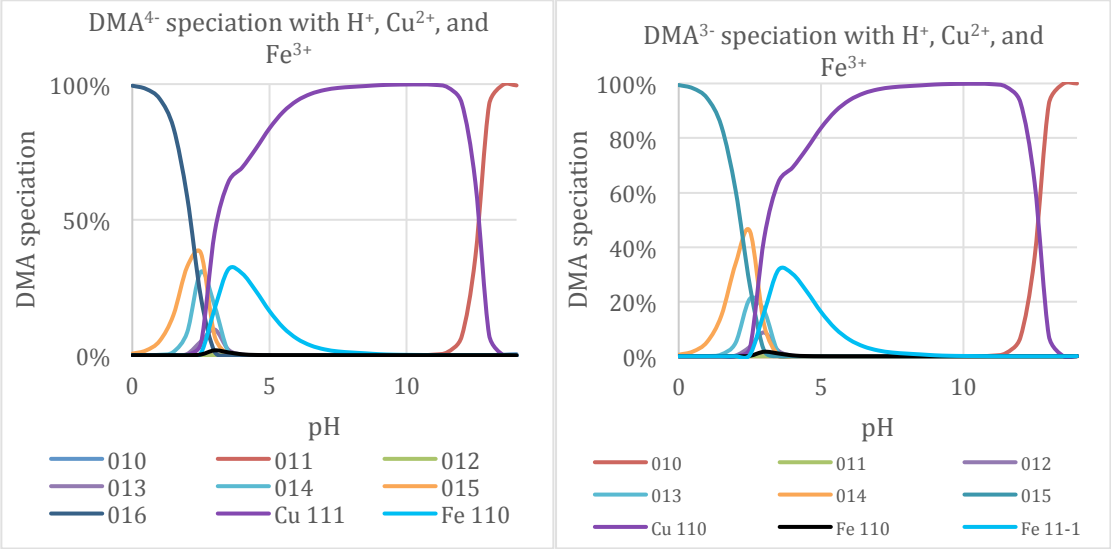

Fig. 7. Left, DMA^{4-} speciation with H^+, Cu^{2+}, and Fe^{3+} as a function of pH; right, DMA^{3-} speciation with H^+, Cu^{2+}, and Fe^{3+} as a function of pH. Colors have been edited to reflect the species of the same charge (i.e. 011 of DMA^{4-} (orange) is equivalent to 010 of DMA^{3-} (orange)).

Conclusion

Besides a small discrepancy in the protonation of DMA between pH 2-4, both models seem to operate well between pH 5-10. It is recommended to use Approach 2 because it requires less overall chemical equation conversions and avoids using estimates for pK_{a6}.

References

Gustaffson, J. P. (2013). "Visual MINTEQ."

Hider, R. C., Yoshimura, E., Khodr, H., and von Wiren, N. (2004). "Competition or complementation: the iron-chelating abilities of nicotianamine and phytosiderophores." *New Phytologist*, 164(2), 204-208.

Murakami, T., Ise, K., Hayakawa, M., Kamei, S., and Takagi, S. I. (1989). "Stabilities of Metal-Complexes of Mugineic Acids and Their Specific Affinities for Iron(Iii)." *Chemistry Letters*(12), 2137-2140.

Reichman, S. M., and Parker, D. R. (2002). "Revisiting the metal-binding chemistry of nicotianamine and 2 '-deoxymugineic acid. Implications for iron nutrition in Strategy II plants." *Plant Physiology*, 129(4), 1435-1438.

Sugiura, Y., Tanaka, H., Mino, Y., Ishida, T., Ota, N., Inoue, M., Nomoto, K., Yoshioka, H., and Takemoto, T. (1981). "Structure, Properties, and Transport Mechanism of Iron(Iii) Complex of Mugineic Acid, a Possible Phytosiderophore." *Journal of the American Chemical Society*, 103(23), 6979-6982.

von Wiren, N., Khodr, H., and Hider, R. C. (2000). "Hydroxylated phytosiderophore species possess an enhanced chelate stability and affinity for iron(III)." *Plant Physiology*, 124(3), 1149-1157.

von Wiren, N., Klair, S., Bansal, S., Briat, J. F., Khodr, H., Shioiri, T., Leigh, R. A., and Hider, R. C. (1999). "Nicotianamine chelates both Fe-III and Fe-II. Implications for metal transport in plants." *Plant Physiology*, 119(3), 1107-1114.